August 2013

The Role of Solution Chemistry and Cell Surface Properties in Mediating Bacterial Transport and Deposition in Porous Media and Interactioin with Nanomaterials

Lixia Wang
University of Wisconsin-Milwaukee

THE ROLE OF SOLUTION CHEMISTRY AND CELL SURFACE PROPERTIES IN MEDIATING BACTERIAL TRANSPORT AND DEPOSITION IN POROUS MEDIA AND INTERACTIOIN WITH NANOMATERIALS

By

Lixia Wang

A Dissertation Submitted in

Partial Fulfillment of the

Requirements for the Degree of

Doctor of Philosophy

in Engineering

at

The University of Wisconsin – Milwaukee

August 2013

ABSTRACT
THE ROLE OF SOLUTION CHEMISTRY AND CELL SURFACE PROPERTIES IN MEDIATING BACTERIAL TRANSPORT AND DEPOSITION IN POROUS MEDIA AND INTERACTION WITH NANOMATERIALS

By

Lixia Wang

The University of Wisconsin – Milwaukee, 2013
Under the Supervision of Professor Jin Li

Groundwater is an important source for drinking water supply. Microbial contaminants have been implicated in two-third of the waterborne disease outbreak. Understanding the fundamental processes, the governing factors and the interfacial interactions that contribute to the deposition of microbial contaminants to porous media will help to elucidate the microbial attachment/transport profile and is highly needed for bioremediation in the environment as well as water purification industry.

In this study, the effects of (1) chemical factors including ionic strength, pH and concentration of phosphate, (2) biological factors including lipopolysaccharide (LPS), biofilm and biofilm extracellular polysaccharide (EPS), and strain type on *E.coli* O157:H7's transport and deposition in saturated sand columns were investigated. The contributions of surface charge, hydrophobicity and steric force to bacterial attachment were quantitatively assessed by calculating extend DLVO theory and steric interaction. Moreover, the role of LPS in protecting bacteria from antibacterial effect of graphene

oxide(GO) was studied. At last, the role of surface functional groups in antibacterial activities of carbon nanotubes was examined.

The overall findings in our study are as follows: (1) The transport of *E.coli* O157:H7 through saturated porous media is enhanced with increasing ionic strength and pH condition; (2) The presence of phosphate in water body encourages the transport of *E.coli* O157:H7 cells through porous media; (3) LPS on the cell surface facilitate *E.coli* O157:H7's transport in sand columns; (4) The retention of *E.coli* O157:H7 in sand is significantly lower than *E.coli* JM109 under various solution chemical conditions; (5) The association of *E.coli* bacteria with biofilm coated on the porous media substantially increase the attachment of cells; (6) XDLVO integrating with steric interaction can qualitatively explain our observations about the retention of *E.coli* O157:H7 on sand surface; (7) The LPS component can protect *E.coli* O157:H7 cells from antibacterial activities of GO sheets; (8) Carbon nanotubes functionalized with amine groups have the highest bacterial removal efficiency. The adsorption of bacteria to the nanomaterials fits to Langmuir isotherm equation and can be expressed by pseudo second order kinetics equation.

TABLE OF CONTENTS

LIST OF FIGURES

LIST OF TABLES

ACKNOWLEDGEMENTS

I would like to express my sincere gratitude to my advisor, Professor Jin Li, for her support and guidance. I truly appreciated her inspiration, encouragement and giving me the opportunity, the trust and freedom to carry out the research and expand my research skills. Her vision towards scientific and industrial challenges opened the research treasure to me. Thanks for everything.

Further, I would like to thank my Ph.D. committee members, Professor Ching-hong Yang, Professor Shangping Xu, Professor Hector Bravo and Professor Qian Liao for their time, valuable discussions and ideas. They gave me much needed advice throughout my project.

I would also like to thank Dr. Chongzheng Na from Notre Dame University and Qiang Yu, Haitao Wang for their help on conducting experiment. Thank Dr. Owen, Dr. Steeber from Biological Science Department and Steven E. Hardcastle from Advanced Analysis Facility lab for their help on using instruments. Thank my coworkers in the lab and all members of Dr.Yang's lab, Dr. Xu's lab and Dr. Liao's lab for putting up with me for the past six years. Thank my friends Fei Zhang and Wei Huang. Also, I am very grateful for the help from Betty Warras to keep me on track with all the correct forms and deadlines. This work was funded by National Science Foundation.

Lastly, I would like to thank my family, my husband Yonghong and my son Derek and Ryan for their love and their support all along my Ph.D. study.

Chapter 1 Introduction

1. 1 Groundwater contamination

The U.S. Environmental Protection Agency reports that 90% of the world's water is contaminated in some way [1]. Groundwater is an important source for drinking water supply. Worldwide, more than 1.5 billion people use groundwater as their only source of drinking water [2]. In the United States, groundwater provides 25% to 40% of all drinking water [3]. Meanwhile, the illness cases caused by water contamination remain substantial in the last decade [4]. Each year, groundwater contamination is responsible for an estimated 750,000 to 5.9 million illnesses and 1400-9400 deaths in the US [5].

Microbial contaminants have been implicated in two-third of the waterborne disease outbreak [6]. Bacterial strains such as *Cryptosporidium oocysts, Enterococcus faecalis, Salmonella typhimurium, Yersinia enterocolitica, Bacillus subtilis, Erwinia chrysanthemi* and *Pseudomonas aeruginosa* [7-11] are the major cause of illnesses through waterborne contamination. In 1993, the city of Milwaukee's drinking water supply infiltration system was contaminated by *Cryptosporidium oocysts*, which infected 403,000 residents and caused at least 104 deaths [6]. In 1999, a waterborne outbreak of *E.coli* O157:H7 infection at the Washington County Fair in New York State resulted in 921 cases infection, including 11 cases of hemolytic uremic syndrome and two deaths [12]. In 1993, another contamination of community water supply system by *Salmonella typhimurium* in Gideon, Mo., led to more than 650 persons illness and 7 deaths [13].

Understanding the fundamental processes, the governing factors and the interfacial interactions that contribute to the deposition of microbial contaminants to porous media will also help to elucidate the microbial attachment/transport profile and is highly needed for bioremediation in the subsurface environment as well as water purification in the industry.

1.2 The pathogenic bacteria-- *Escherichia coli* O157:H7

In the past several years, *Escherichia coli* O157:H7 has caught people's attention due to its frequent outbreaks. Many of its outbreaks were associated with contaminated undercooked ground beef, lettuce, radish sprout, and unpasteurized apple juice [14]. Water-borne transmission of *E.coli* O157:H7 was becoming an important infection pathway in recent years. Thirty-one percent *E.coli* O157:H7 outbreaks were reported to be waterborne during 1982-2002 [15, 16]. The Center for Disease Control and Prevention (CDC) estimated that *E.coli* O157:H7 caused ~73,000 illnesses, ~2200 hospitalizations and ~61 deaths each year in the United States and drinking water was responsible for ~15% of the reported infections [16, 17].

E.coli O157:H7 belongs to *Escherichia coli (E.coli)* and falls within the family *Enterobacteriaceae*. *E.coli* colonizes the infant gastro-intestinal tract within hours after birth and remains dominant in the human colonic flora. Even though most of the *E.coli* members are non-pathogenic, several *E.coli* strains have acquired specific virulence factors and caused a variety of infections in humans and animals, typically *E.coli* O157:H7. In the name of *E.coli O157:H7*, O denotes the type of somatic and H specifies the flagellar type. O antigen defines a serogroup, and the combination of O and H antigens defines the "serotype" of an isolate.

Infection of *E.coli* O157:H7 can cause fatal diseases such as hemorrhagic diarrhea and hemolytic uremic syndrome (HUS) [16, 18]. The infection is especially severe to children under 5 years old and elderly people [19]. *E.coli* O157:H7 was first recognized as a pathogen in 1982 during an outbreak investigation of hemorrhagic colitis. Drinking water outbreak of *E.coli* O157:H7 was first reported in 1989, when people became sick after drinking contaminated water in rural Missouri [20]. A waterborne outbreak at the Washington County Fair in New York State in August 1999 resulted in 921 cases of *E.coli* O157:H7 infection, including 11 cases of hemolytic uremic syndrome and two deaths [12]. Well supplying undisinfected water to several vendors of beverages and ice was likely contaminated by manure. Outbreaks *of E.coli* O157:H7 in Wyoming [21] and Canada [22] were also reported to be associated with public drinking water system. Drinking water source associated outbreaks of *E.coli* O157:H7 were also reported in Asia [23], Europe [24] and Africa [25]. The *E.coli* O157:H7 outbreaks linked to the consumption of contaminated groundwater highlight the importance of understanding the transport of *E.coli* O157:H7 within the soil-groundwater system [26-28].

The contamination sources of *E.coli* O157:H7 primarily come from animal manure, such as cattle [26, 29-31]. Survey results showed that *E.coli* O157:H7 was commonly detected in cattle manure and its density could reach as high as 10^5 CFU g^{-1} [32-37]. Additionally, it was found that *E.coli* O157:H7 in cattle manure could survive for as long as 21 months [38-40]. Human may be at risk of infection long after an environment being initially contaminated. When manure from cattle farms is applied to agricultural fields by both conventional and organic crop producers as a fertilizer, *E.coli* O157:H7 cells can

leach out, infiltrate through the soil zone and subsequently contaminate the underlying groundwater [28, 41]

1.3 Factors affecting bacterial deposition in porous media

When bacteria approaching to a medium, firstly, physical and/or chemical interactions will take place for its adhesion between the planktonic cell and the medium's surface, and this process is estimated to be several hours [42]; secondly, biological process such as cell growth or phenotype adaptation will develop after incubation period. Bacterial transport or deposition in porous media could be affected by physical, chemical and biological factors.

1.3.1 Physical factors

The influence of straining that removes colloids from porous media was reported to be significant when the ratio of colloids to median grain size is greater than 0.0083 [43, 44]. When straining did not play a major factor of colloid removal, colloid size, grain size distribution [45], pore space geometry [46], medium surface heterogeneities [47] and substrate surface roughness [48, 49] were all reported for their influences on colloids deposition in porous media.

In addition to the factors of medium, the environmental physical factors, such as temperature, fluid velocity, and time, were also tested for their impact on bacterial deposition/transport through porous media. However, their effect to bacterial deposition remains divergent. For instance, to temperature, some researchers found it has a positive effect on bacterial deposition [50]; while Kim et. al. observed that it did not cause a significant difference for bacterial deposition rate coefficient on quartz grains as latex

colloids do among temperature range from 4-25ºC [51]. According to Guber et. al., fluid velocity has a negative effect to the nonmotile cells retention onto soil columns [52], while it enhances the motile cells escaping when reducing fluid velocity at low fluid velocity [53]. For the contact time, cell attaching to the sand in artificial ground cold environment was tested remaining no significant altered for several weeks [50, 54, 55]; yet starvation for 18h displayed was examined to decrease adhesion in other studies [50, 54, 55]. These contadictory findings on the impacts of environmental physical factors on bacterial retention indicate combined effects of these physical factors with cell surface chemistry or biological factors.

When considering bacterial transport and retention in porous media under unfavorable conditions, hydrodynamic drag was hypothesized to lead to the rolling movement of cells along grain surface and contributing to the non-monotonic distribution (down- gradient center) retention profiles of microsphere or bacteria through porous media column. It was also suggested to drive re-entrainment of secondary minimum associated microspheres in porous media under unfavorable conditions [56, 57].

1.3.2 Chemical factors

Ionic strength, electrolyte ion valence and pH conditions of solution are the three main factors influencing bacterial interaction with sand surface [51, 58-60] and the effects of them on bacterial deposition have been evaluated by many researchers, however, the findings were quite inconsistent. For instance, increasing ionic strength (IS) would in theory increase bacterial retention on negatively charged subsurface sediments because of the compression of the electrostatic double layer of counterions that balance the surface charge of bacteria and the sediment [10, 58]. Nevertheless, a distinct trend

was discovered by Kim et. al. for strain *E.coli* O157:H7. They found that there is no effect of IS (1, 10,100mM) on cell deposition at pH of 5.8. At pH of 8.4 and 9.2, the bacterial deposition behavior was inversely proportional to IS (1-100mM) [61]. Similarly, increasing pH would theoretically decrease bacterial deposition resulting in more negatively charged surface [10]. However, some researchers found that bacterial attachment was unaffected by pH(5.0-9.0) [58]. Electrolyte with divalent cations (such as Ca^{2+}) could play a "bridge" role and interact non-specifically with cell surface charged functional groups and a greater rate of deposition of bacteria in porous media [51], but the effect of negatively charged multi-valence ions to bacteria or viruses transport or retention in subsurface was opposite [9]. LPS containing saccharides with phosphate also results in low bacterial attachment efficiencies [62]. In addition, some researchers found that the presence of humic substances in solution inhibits bacteria's adhesion to sand [63-65].

Surface potential (zeta potential) [66-68], hydrophobicity [69, 70]are two major factors for mediating interactions between surfaces. Solution chemistry had an influence on bacterial interaction with sand surface because of the change of surface charges and/or hydrophobicity [71].

1.3.3 Biological factors

When multiple bacterial strains were studied for their transport behavior, various deposition profiles were observed [8, 51, 62, 65, 72]. Bacterial strain-specific shapes, sizes [73], surface functional groups such as lipopolysaccharide (LPS) [74-77], outer membrane protein [7, 78, 79], extracellular polysaccharide(EPS) [76, 80-86], fimbriae(pili) [87, 88] and flagella [59, 89] might contribute to the differences. Cell

concentration[53] together with bacterial growth conditions [90, 91] can also affect bacterial deposition behaviors by influencing their surface properties. For instance, Ryu et al. found that an EPS-overproducing mutant *of E.coli* O157:H7 strain ATCC 43895 had significantly lower numbers attaching to stainless steel coupons compared to its wild type strain [92]. Kim et. al. treated the cells with proteinase K and cleaved the surface protein, smaller amount of the cells were retained in the column as compared to the untreated ones, indicating that the extracellular protein of *E.coli* O157:H7 cells enhance the cell retention [78]. Salerno et al. coated microspheres with protein and conducted the column experiments packed with glass beads, and they found that the attachment rate efficiencies of protein covalently coated microspheres were increased significantly [93].

LPS is an important component of bacterial outer membrane. They are anchored in the outer membrane of bacterial cells and from inside to outside, are composed of the hydrophobic lipid A (the component that interacts with the inner leaflet of the outer membrane), an inner and an outer core, and the repeating units of O-antigen for smooth strains [94]. The core region of the LPS consists of negatively charged groups, such as phosphates and carboxylic groups, which usually give the LPS its negative charge [95]. The outer polysaccharide part of the LPS is the O-antigen, which consists of 20-70 repeating units of three to five sugars and can protrude up to 30 or more nm into the cell surroundings. LPS occupies 75% of the surface of the bacterium, and *E.coli* is estimated to have 10^6 molecules per cell [96].

William et. al. found that the adhesion of LPS mutants of *Pseudomonas fluorescens* to quartz sand in columns increased [74]. On the contrary, Lai removed the LPS composition from *E.coli* JM109 and discovered that the adhesion affinity between the

bacterial cells and the AFM tip decreased. They also observed that the bacterial retention to glass or in packed beds to quartz sand decreased after LPS removal [95]. Walker compared the deposition of *E.coli* K12 (intact LPS with O-antigen), D21(LPS with core) and D21f2(LPS truncated mutant with lipid A only) to packed-bed column but did not find a correlation between either the length or the charge characteristics of the LPS molecule and the deposition kinetics [97]. Ong studied the interactions between lawns of *E.coli* and model surfaces with the use of atomic force microscopy (AFM) and concluded that the presence of LPS caused steric repulsion with mica surface and that its truncation resulted in an attraction between the two materials [98].The composition of LPS also plays a role in mediating bacterial adhesion behavior. Foppen examined 54 *E.coli* strains for the effect of surface properties of the outer membrane on the attachment efficiencies to saturated quartz sand and concluded that low attachment efficiencies were statistically associated with LPS containing saccharides with phosphate and/or carboxyl groups [62].

1.3.4 Coupled effects

When particles were eluted by free or low ionic strength solution (usually 1mM), the attached cells were not completely recovered. This suggests the coupled effects of chemical conditions and physical pore space geometry [46]. The particles not washed out were believed firstly retained at the secondary minimum and then rolling along the interface by the hydrodynamic drag, finally they were trapped in hydrodynamically disconnected regions. Moreover, the chemical factors such as pH, ionic strength or surface charge were suggested to affect soil structure (aggregating behavior of colloid particles) and the effective pore size distribution [46].

Fontes et. al. [99] were ranking the importance of physical factors(grain size and cell size) and chemical factors (ionic strength) on their influence to transport of microorganisms through porous media in well-controlled clean quartz sand and concluded that grain size was the most important factor controlling transport of bacteria. Cell size and ionic strength were less important affecting bacterial transport comparing to grain size. In field studies, Dong et. al. [100] has compared the relative importance of physical and chemical heterogeneity for controlling the transport of an adhesion-deficient bacterial strain in an intact sediment cores. Grain size was determined to be the primarily factor and chemical heterogeneity caused by adsorbed organic carbon matters was less important.

There is a classic two rate-limiting steps assumption for describing colloid deposition through porous media. [101] First, transport of colloidal particles to matrix surfaces by Brownian diffusion, interception, or gravitational sedimentation in colloid-matrix collisions and then second, attachment of colloidal particles to the matrix surfaces. According to their theory, the transport step depends primarily on physical factors such as size and density of colloidal particles, accessible surface area for colloid deposition, pore structure, and flow velocity. The kinetics of the attachment step largely depends on solution and surface chemistry because colloid attachment is controlled by interparticle forces between colloidal particles and matrix surfaces. In other words, short distance forces such as van der waals force, electrostatic force, which depends on surface properties of the bacterial cell, substratum surfaces as well as the intervening medium, will only begin to act once bacteria cells overcome the interaction barrier and get close to the medium surface [102].

1.4 Colloids filtration theory

The transport of colloidal particles through granular porous media can be described by accounting for particle advection, hydrodynamic dispersion, and deposition. Under steady state saturated flow conditions where the blocking and ripening effect are not significant and particle releasing is negligible, the concentration of fluid-phase particles, C(x,t) and retained particles, S(x,t), at column depth x and time t can be described by a one-dimensional advection-dispersion equation with a first-order kinetic deposition term.

$$\frac{\partial C}{\partial t} + \frac{\rho_b}{\epsilon}\frac{\partial S}{\partial t} = D\frac{\partial^2 C}{\partial x^2} - v\frac{\partial C}{\partial x} \qquad (1)$$

$$\frac{\rho_b}{\epsilon}\frac{\partial S}{\partial t} = kC \qquad (2)$$

Here, v is the interstitial particle velocity, D is the hydrodynamic dispersion coefficient, ϵ is the bed porosity, ρ_b is the porous medium bulk density and k is the particle deposition rate coefficient, /min.

k can be determined with the following equation:

$$k = -\frac{U}{\epsilon L} ln(\frac{C}{C_0}) \qquad (3)$$

Here, C/C_0 is the normalized breakthrough concentration relevant to "clean bed" conditions, U is the approach(superficial) fluid velocity, cm/min, and L is the length of the packed bed, cm. k can also be acquired through the single-collector removal efficiency, η_0 via the following expression[103]:

$$k = \frac{3(1-\epsilon)v}{2d_c}\alpha\eta_0 \qquad (4)$$

where d_c is the diameter of the collector grains, α is empirical attachment (collision) efficiency.

Under steady state, the influence of hydrodynamic dispersion is negligible. Thus, for a continuous particle injection at concentration C_0 (at x=0) and time period t_0, the solutions to eqs 1 and 2 for a column initially free of particles are

$$C(x) = C_0 \exp\left(-\frac{k}{v}x\right) \qquad (5)$$

$$S(x) = \frac{t_0\epsilon k}{\rho_b}C(x) = \frac{t_0\epsilon k C_0}{\rho_b}\exp\left(-\frac{k}{v}x\right) \quad (6)$$

Equation 5 is the classical colloid filtration model and can be used for modeling the transport of colloids or microorganisms in saturated porous media.

1.5 Extended DLVO theory

Once the bacterium is transferred to the solid surface by diffusion, convection, or active transfer, the interfacial interactions between a bacterium and a surface are thought to be governed by the classical DLVO (Dejarguin-Landau-Verwey-Overbeek) energy. Its quantitative expression, which is comprised of an electrodynamic or van der Waals component (Φ_A) and an electrostatic component (Φ_R), has been considered as the fundamental model for colloid interfacial interaction [104].

$$\Phi_{TOT} = \Phi_A + \Phi_R \qquad (7)$$

$$\Phi_A = -\frac{Aa_b}{6h} \qquad (8)$$

Where A is the Hamaker constant, h is the separation distance between the cell and the substratum, a_b is the radius of the cell. The cells are assumed to be spherical.

The electrostatic interaction comes from the Coulomb interaction between charged surfaces. It is related to the surface potential ψ, the distance between the cell and the surface d and the Debye length κ.

$$\Phi_R \propto \psi^2 e^{-\kappa d} \qquad (9)$$

$$\kappa = \sqrt{\frac{2000e^2 N_A c}{\varepsilon\varepsilon_0 kT}} \qquad (10)$$

Where N_A is Avogadro's constant, c is the concentration of the ions of the electrolyte (mol/L),ε, the dielectric constant of the solution, ε_0 is the dielectric permittivity of free space, k is the Boltzmann constant and e is the electronic charge, T is the absolute temperature.

A thermodynamic approach to calculate the Gibbs adhesion energy for the bacterial adhesion using the Dupre equation is as following [105]:

$$\Delta G^{adh} = \gamma_{BS} - \gamma_{BL} - \gamma_{SL} \quad (11)$$

Where $\gamma_{BS}, \gamma_{BL} and\ \gamma_{SL}$ are respectively the interfacial energy of the bacterium-substratum, bacterium-liquid and substratum- liquid interfaces. Adhesion is favored if the free energy per unit area,ΔG^{adh}, is negative.

In the DLVO theory, the interaction energy is distance-dependent whereas in the thermodynamic approach the formation of a new cell- substratum interface is calculated. If adhesion occurs in the secondary minimum and a new cell- substratum interface is not formed, the thermodynamic theory is not applicable.

Marshall et. al.[106] in 1971 first used DLVO theory to qualitatively explain bacterial adhesion among different concentrations of electrolyte. However, reported deviations [48, 66, 78, 107-110] results from the theory for the interfacial interactions brought up the need to further investigate the interaction energy profiles. Van Oss [111]and colleagues have extended DLVO theory by accounting for Lewis acid-base interactions, which is essential for describing polar media interfacial interactions.

$$\Delta G^{adh} = \Delta G^{VDW} + \Delta G^{EDL} + \Delta G^{AB} \quad (12)$$

Different from the rigid particles, bacterial surfaces are soft and dynamic. To predict the interactions between polymer containing surfaces, many researchers value the contributions of steric force. As an example, Jacob Israelachvili [112] believes that the steric- polymer force is one the most important forces between lipid bilayers and biological membranes.

DeGennes [113] quantified the steric interactions between polymer surfaces by considering the contributions of the forces 1) the osmotic pressure inside each brush; and 2) the elastic restoring forces which tend to thin out the brush and the expression is as follows:

$$P = \frac{kT}{s^3}\left[\left(\frac{2L}{D}\right)^{\frac{9}{4}} - \left(\frac{D}{2L}\right)^{\frac{3}{4}}\right] \quad \text{For } D < 2L \qquad (13)$$

Where *P* is the pressure between the two parallel surfaces, *D* is the average distance between attachment points, *L* is the thickness of brush layer and *s* is the average distance between anchoring sites. The first term in the bracket is the osmotic term; the second one is elastic term.

1.6 The objectives of my study

In this study, the effects of chemical factors including ionic strength, pH and solution constituents on O157 transport will be investigated in saturated sand columns. The role of cell surface lipopolysaccharide (LPS) in mediating the pathogen cells transport will also be documented. The bacteria's deposition profiles will be investigated in biofilm coated sand column to evaluate the role of biofilm and EPS to its retention onto biofilm coated sand column. As a comparison to *E.coli* O157:H7, the transport of a nonpathogenic strain *E.coli* JM109 will be performed under the same experimental conditions. To evaluate the transport pattern, extend DLVO theory including hydrophobicity and steric interaction will be calculated. Surface charge and hydrophobicity together with steric force will be assessed for their contributions to the attachment. Moreover, the protection of LPS from antibacterial effect of graphene oxide will be studied. At last, the importance of surface functional groups in enhancing bacterial removal rates of carbon nanotubes will be discussed with three surface functionalized nanotubes.

Chapter 2. The influence of phosphate on the transport of *E.coli* O157:H7 in sand column

Phosphate is a ubiquitous chemical species that can be found in minerals, soils, human bodies and water. Phosphate is also a key ingredient used in numerous domestic and industrial applications, e.g., detergents, metal surface coating, fertilizers, and drinking water distribution pipe corrosion control. The addition of phosphate to water mains has been shown to improve the water quality by reducing the occurrence of coliform bacteria and inhibit biofilm growth despite the fact that phosphate serves as an essential nutrient for microorganisms [114]. Several studies investigating the role of phosphate in bacterial interaction with iron coated sand [115] and iron oxyhydroxide particles [114] have attributed the reduced bacterial adhesion to charge modification of the grain surface from positive to negative by adsorbed phosphate ions. In soil solution and, particularly in agricultural soil that receives manure and/or chemical fertilizers, phosphate concentrations can reach mM levels [116-121]. As phosphate was reported to enhance the transport of bacterial cells (e.g., *Pseudomonas fluorescens*) and virus within natural porous media [122, 123], little is known about its impacts on the transport of *E.coli* O157:H7. The main goal of this research was to examine the effect of phosphate on the transport of *E.coli* O157:H7 with quartz sand packed columns. In addition, the release of *E.coli* O157:H7 cells attached to sand surfaces was evaluated when phosphate concentration in the mobile aqueous phase was elevated.

2.1. Materials and Methods

2.1.1 Preparation of bacteria suspension

E.coli O157:H7 strain EDL933 stx1 and stx2 double mutant was obtained from Dr. C-H Yang's lab in Biological Sciences at the University of Wisconsin, Milwaukee and used in this experiment. Preserved cells stored in 20% glycerol at -80 °C was streaked onto Luria-Bertani (LB) agar plates supplemented with 20 μg/mL chlorampfenicol, 50μg/mL kanamycin and 150 μg/mL rifampin and the plate was incubated at 37 °C overnight. One single colony was picked by a sterile needle and transferred into culture tubes that contained 10 ml sterile LB broth amended with antibiotics of similar concentrations. Following 6-hour incubation at 37°C, 0.5 mL of the starter culture was added to a flask that contained 250 mL sterile LB broth amended with antibiotics, which was incubated at 37°C with 200 rpm shaking for 18 h. The bacterial cells were harvested through centrifugation (3000 *g*, 10 min, 4°C) and the pellets were rinsed twice using appropriate electrolyte solutions to remove the growth media. Cell concentration was then adjusted to ~3×10^7cells/mL and the suspension was ready for column transport experiments. The cell surface macromolecules were left unaltered in the suspension used in the column transport experiments. The motility of the bacteria did not change after the double mutation.

2.1.2 Electrolyte solutions

Six different types of electrolyte solutions were used in the experiment. The total ionic strength of the electrolyte solutions was either 10 mM or 100 mM (adjusted using NaCl). Under each ionic strength condition, the phosphate concentrations varied as 0 mM (no phosphate), 0.1mM (77μM Na_2HPO_4, 23 μM NaH_2PO_4) and 1 mM (770μM Na_2HPO_4, 230 μM NaH_2PO_4), respectively. Because the presence of phosphate changed

water pH to ~7.2, the pH of the solutions that contained no phosphate was raised to 7.2 using 0.1 mM $NaHCO_3$.

2.1.3 Column transport experiments

High purity quartz sand (US Silica) with a size range of 0.354-0.420 mm was used in the column transport experiments. The porosity of the sand was 0.344. The sieved sand was treated alternately with hot, concentrated nitric acid and diluted NaOH solutions to remove surface iron oxide/hydroxide coatings and organic materials, as well as fine particles that were attached to sand surfaces, respectively. Following each cleaning step, the sand was thoroughly rinsed with deionized water. The clean sand was dried in an oven at 55 °C and then stored in high-density polyethylene (HDPE) containers until use.

Duplicate glass chromatography columns (Kontes) measuring 15 cm in length and 2.5 cm in diameter were wet packed using the clean quartz sand. The packed columns were equilibrated with more than 20 pore volumes of background electrolyte solution. Peristaltic pumps (Cole-Parmer MasterFlex) were used to regulate the flow and the specific discharge was maintained at 0.31 cm/min. Following the equilibrium step, bacterial suspensions were injected into the columns and the injection lasted 60 min (~3 pore volumes). The column effluent was connected to flow-through quartz cells and the concentration of the bacterial cells was monitored every 30 s using a spectrophotometer (Shimadzu UV-1700) at a wavelength of 220 nm [124, 125]. Upon the termination of cell suspension injection, the columns were flushed with background electrolyte solution until the absorbance of the effluent returned to zero.

It was previously shown that, for the relatively uniform sand used in this research, the effect of dispersion on the transport of colloid-sized particles was negligible [126]. The kinetics of the deposition of *E.coli* O157:H7 cells within the saturated sand packs under clean-bed conditions can be estimated through calculating the deposition rate coefficient, k_d (min^{-1}), from the early cell breakthrough concentrations in the effluent [127, 128]:

$$k_d = -\frac{U}{\varepsilon \cdot L} \ln\left(\frac{C}{C_0}\right) \qquad (2.1)$$

Where ε is the porosity of the sand (cm^3/cm^3), U is the specific discharge (cm/min), L is the length of the column (cm) and C/C_0 is the normalized breakthrough concentration relevant to clean-bed conditions, which was obtained from average bacterial breakthrough concentrations between 1.8-2.0 pore volumes [127, 129].

Experiments were also performed to investigate the potential release of *E.coli* O157:H7 cells due to increased phosphate concentration in the mobile aqueous phase. For this purpose, column transport experiments were firstly conducted using a solution that had an ionic strength of 100 mM but did not contain any phosphate. Once the columns were flushed, a solution that had similar ionic strength and pH (i.e., 100 mM and 7.2) but contained 0.1 mM phosphate was injected into the columns. Concentrations of released bacterial cells in the effluent were recorded through measuring the absorbance at a wavelength of 220 nm (Shimadzu UV-1700). When the released cells were flushed out from the columns (i.e., the absorbance of the effluent returned to background values), a 100 mM solution that contained 1 mM phosphate was then injected into the columns. The release experiments were stopped after the pulse release of the bacterial cells was completed.

2.1.4 XDLVO interaction between *E.coli* O157:H7 cells and quartz sand

The transport of bacterial cells within saturated porous media is governed by the energy interactions between bacterial cells and the surface of solid matrix (e.g., sands). According to the extended Derjaguin-Landau-Verwey-Overbeek (XDLVO) theory, the forces include the Lifshitz−van der Waals (LW) interactions and the electrostatic double layer (EDL) repulsion, the Lewis acid-base (AB) (i.e., hydrophobic) interaction [57, 130, 131]:

$$\Phi^{\mathrm{Total}} = \Phi^{\mathrm{LW}} + \Phi^{\mathrm{EDL}} + \Phi^{\mathrm{AB}} \qquad (2.2)$$

The LW, EDL and AB interaction energies (Φ^{LW}, Φ^{EDL} and Φ^{AB}) can be calculated using the following equations [42, 66, 98, 108, 109, 132-134]:

$$\Phi^{\mathrm{LW}} = -\frac{A\,a_b}{6h} \quad (2.3)$$

$$A = 24\pi h_0^2 \left(\sqrt{\gamma_b^{LW}} - \sqrt{\gamma_w^{LW}}\right)\left(\sqrt{\gamma_s^{LW}} - \sqrt{\gamma_w^{LW}}\right) \quad (2.4)$$

$$\Phi^{\mathrm{EDL}} = \pi\varepsilon_0\varepsilon_w a_b \left\{2\psi_b\psi_s\, ln\left[\frac{1+\exp(-\kappa h)}{1-\exp(-\kappa h)}\right] + (\psi_b^2 + \psi_s^2) ln[1 - \exp(-2\kappa h)]\right\} \quad (2.5)$$

$$\Phi^{\mathrm{AB}} = 2\pi a_b \lambda_w \Delta G_{h_0}^{AB} \exp\left(\frac{h_0 - h}{\lambda_w}\right) \quad (2.6)$$

$$\Delta G_{h_0}^{AB} = 2\left[\sqrt{\gamma_w^+}\left(\sqrt{\gamma_b^-} + \sqrt{\gamma_s^-} - \sqrt{\gamma_w^-}\right) + \sqrt{\gamma_w^-}\left(\sqrt{\gamma_b^+} + \sqrt{\gamma_s^+} - \sqrt{\gamma_w^+}\right) - \sqrt{\gamma_b^-\gamma_s^+} - \sqrt{\gamma_b^+\gamma_s^-}\right] \quad (2.7)$$

where A represents the Hamaker constant; a_b is the equivalent radius of the bacterial cells; h is the separation distance between the bacterium and sand surface; h_0 represents the minimum equilibrium distance between the cell and sand surface and equals to 0.157 nm; γ^{LW}, γ^+ and γ^- are the LW, electron-accepting and electron-donating

interfacial tension parameters, respectively; ε_0 and ε_w are the dielectric permittivity of vacuum and water, respectively; κ is the inverse of Derby length; ψ_b and ψ_s are the surface potentials of the bacterial cells and sand, respectively; λ_w (= 0.6 nm) is the characteristic decay length of AB interactions in water; and $\Delta G_{h_0}^{AB}$ represents the hydrophobicity interaction free energies per unit area corresponding to h_0. For the interfacial tension parameters (i.e., γ^{LW}, γ^+or γ^-), the subscripts of *b*, *w* and *s* represent bacteria, water and sand, respectively. For water, the values of γ^{LW}, γ^+or γ^- are 21.8, 25.5 and 25.5 mJ m^{-2}, respectively [111]. Values of γ^{LW} (39.2 mJ m^{-2}), γ^+ (1.4 mJ m^{-2})or γ^- (47.8 mJ m^{-2}) for quartz were determined in Morrow et al. [66] and were used in this research. Values of γ^{LW}, γ^+or γ^- for *E.coli* O157:H7 cells were determined by measuring the contact angles (θ) using three different probe liquids with known surface tension parameters [111]:

$$\gamma_i^L (1+\cos\theta)=2\sqrt{\gamma_i^{LW}\gamma^{LW}}+2\sqrt{\gamma_i^+\gamma^-}+2\sqrt{\gamma_i^-\gamma^+} \quad (2.8)$$

where the subscript *i* represents water (γ^L=72.8, γ^{LW}=21.8 and γ^+=γ^- = 25.5 mJ m^{-2}), glycerol (γ^L=64.0, γ^{LW}=34.0, γ^+= 3.92 and γ^-=57.4 mJ m^{-2}) or diiodomethane (γ^L=50.8, γ^{LW}=50.8 and γ^+=γ^- = 0 mJ m^{-2}) [111]. The contact angles were acquired with a Rame-Hart goniometer using bacterial lawns produced by filtering cells onto porous membrane [98].

2.1.5 Steric interaction between *E.coli* O157:H7 cells and quartz sand

In biological systems, the classic DLVO model often could not fully explain bacterial transport and deposition behavior observed in experiments due to the presence of extracelluar macromolecules on bacterial surface [40-43]. The steric repulsion between

two parallel surfaces similarly coated by macromolecules is described by the deGennes equation [112, 135]:

$$P = \frac{kT}{s^3}\left[\left(\frac{2L}{D}\right)^{\frac{9}{4}} - \left(\frac{D}{2L}\right)^{\frac{3}{4}}\right] \quad \text{For } D < 2L \qquad (2.9)$$

Where P is the pressure between the two parallel surfaces, D is the separation distance, L is the thickness of brush layer and s is the average distance between anchoring sites. For *E.coli* O157:H7, of the value of D is ~30 nm [136] and the values of s is ~2.2nm[137].

If one plate has the brush and the other plate is bare, 2D should substitute D and the pressure should be divided by 2 [138]:

$$P = \frac{1}{2}\frac{kT}{s^3}\left[\left(\frac{L}{D}\right)^{\frac{9}{4}} - \left(\frac{D}{L}\right)^{\frac{3}{4}}\right] \quad \text{For } D < L \qquad (2.10)$$

Integration using Derjaguin's approximation we have the steric force expression for a sphere-plate system [112, 135]:

$$F = 2\pi R\frac{1}{2}\frac{kT}{s^3}\int_D^L\left[\left(\frac{L}{x}\right)^{\frac{9}{4}} - \left(\frac{x}{L}\right)^{\frac{3}{4}}\right]dx = \frac{4L}{35}\pi R\frac{kT}{s^3}\left[5\left(\frac{D}{L}\right)^{\frac{7}{4}} + 7\left(\frac{L}{D}\right)^{\frac{5}{4}} - 12\right] \qquad (2.11)$$

The integration of F gives the steric interaction energy (Φ^{Steric}) for a sphere – plate system

$$\Phi^{Steric} = \int_D^L F(x)dx = \frac{4}{385D}\pi R\frac{kT}{s^3}\left[-20D^3\left(\frac{D}{L}\right)^{\frac{3}{4}} \mp 308L^3\left(\frac{D}{L}\right)^{\frac{3}{4}} \pm 420DL^2 \mp 132D^2L\right]$$

(2.12)

2.1.6 *E.coli* O157:H7 cell characterization

Zeta potential values of bacterial cells and sands were used in the place of surface potentials in equation (5) [133]. Cell suspensions were prepared in a similar fashion as the column transport experiments and the quartz sands were pulverized and colloid-sized quartz particles were suspended in the electrolyte solutions. The electroporetic mobility of the bacterial cells and colloidal quartz sand under each solution was then measured using a ZetaPALS analyzer (Brookhaven Instruments Corporation). Smoluchowski equation was used to convert electrophoretic motility values into zeta potentials. To measure cell sizes, photos of *E.coli* O157:H7 cells suspended various solutions were obtained using a Nikon Eclipse 50i microscope, which was equipped with a Photometric coolsnap ES digital camera and MetaMorph software. The length and width of the cells were then determined using the ImageJ software and the equivalent radii of the cells were calculated as $\sqrt{\frac{L_C \times W_C}{\pi}}$, where L_C and W_C represent the length and width of the cell, respectively [54].

2.2. Results and Discussion

2.2.1 Transport of *E.coli* O157:H7 within sand packs

Results from the column transport experiments showed that higher percentages of *E.coli* O157:H7 cells could travel through the sand columns when the concentration of phosphate was progressively increased from 0 to 1 mM, indicating that phosphate could promote the transport of *E.coli* O157:H7 (Figure 1). At a constant ionic strength of 10 mM, 55.3% (±1.6%), 32.2% (±0.3%) and 23.0% (±0.8%) of the *E.coli* O157:H7 cells were immobilized within the sand packs for phosphate concentrations of 0, 0.1 and 1

mM, respectively. Accordingly, the deposition rate coefficient (k_d) decreased from 0.054 (±0.003) min^{-1} to 0.019 (±0.0007) min^{-1} when phosphate concentration increased from 0 to 1 mM (Figure 2). Similar trend was observed when the ionic strength was maintained at 100 mM. The fraction of immobilized *E.coli* O157:H7 cells decreased from 33.0% (±1.7%) to 12.1% (±1.4%), and the deposition rate coefficient decreased from 0.025 (±0.0007) min^{-1} to 0.0005 (±0.0001) min^{-1} when phosphate concentration increased from 0 to 1 mM. The clear increase in breakthrough is difficult to dispute even in the absence of a mass balance.

It was reported that under high pH (>8.4) conditions, the retention of *E.coli* O157:H7 cells within quartz sand decreased with increasing ionic strength [61]. Consistent with the previous finding, results from this research showed that the deposition of *E.coli* O157:H7 cells reduced with increasing ionic strength under a pH of 7.2, regardless of phosphate concentrations (Figures 1 and 2). For instance, under the absence of phosphate, the deposition rate coefficients were 0.054 (±0.003) min^{-1} and 0.025 (±0.0007) min^{-1} for 10 and 100 mM of ionic strength, respectively.

2.2.2 The deposition rate coefficients k_d

The equation (2.1) represents a simplified model that has neglected processes such as dispersion and detachment. It was previously shown (based on tracer test data) that for the relatively uniform sand used in this research, the hydraulic dispersion coefficient is around 0.1 cm^2/hour [126]. The Peclet number (Lv/D) is thus around ~8000, suggesting that the neglect of dispersion is justified. The cell breakthrough curves also displayed negligible tailing, suggesting that cell detachment can be reasonably neglected. This is further confirmed by our simulation results (see figure 3). We noticed that because the

effluent concentrations of bacterial cells in the experiments (particularly for the 10 mM experiments) increased slightly with time, a more complex, second-order Langmuir type of model could potentially provide an improved description for the breakthrough concentrations over the whole time course of the experiments. It is also true that when the quantity of attached bacteria is low (i.e., under clean-bed conditions), the second order model can be reasonably approximated by the first-order model. Therefore as far as the clean-bed deposition rate coefficients are concerned, they can be determined using the first-order model as long as the initial values of C/C_0 (i.e., values of C/C_0 under clean-bed conditions) are selected. In this research, we followed many previous publications and selected the early C/C_0 values to calculate k_d [125, 139, 140]. To confirm this, we also fitted the second-order Langmuir-type model (without considering cell detachment) to our breakthrough data using a Levenberg-Marquardt algorithm and the best-fit values of deposition rate coefficients were obtained (This inverse simulation technique is similar to that used by HYDRUS-1D or CXTFIT, please refer to [126] for details about the fitting process). The R^2 values were always greater than 0.97 for all the simulations. A excellent 1:1 match between deposition rate coefficients estimated using the second-order model and the first-order model (employed in this research, equation (2.1)) was observed (see Figure 3). Thus the values of k_d calculated using equation (2.1) can faithfully reflect the differences in the transport behavior of the *E. coli* O157:H7 cells under our experimental conditions, and equation (2.1) is appropriate to estimate the clean-bed deposition rate coefficients.

2.2.3 XDLVO Interaction Energy Profiles

The measured contact angles of water, glycerol and diiodomethane on *E.coli* O157:H7 lawns were 22.1º (±0.1 º), 27.0º (±1.8º) and 63.0º (±0.7º), respectively. The values of γ^{LW}, γ^{+}or γ^{-} for *E.coli* O157:H7 cells were calculated as 26.9, 47.6 and 4.82 mJ m^{-2}, respectively. Using the values previously determined for quartz in Morrow et al. [66], the Hamaker constant (equation (2.4)) for the bacterium-water-quartz system was estimated as 1.522×10^{-21} J. The estimated value of $\Delta G_{h_0}^{AB}$ was 24.94 mJ/m^2, suggesting repulsive AB interactions between *E.coli* O157:H7 cells and quartz sands immersed in water.

The equivalent cell radius was around 0.85 μm and showed little variation with changes ionic strength and phosphate concentrations (Figure 4A). The zeta potential of both the *E.coli* O157:H7 cells and quartz sand was negative (Figure 4B). In general, the zeta potential of sands were ~30 mV less negative when ionic strength increased from 10 mM to 100 mM due to the compression of electric double layer. The zeta potential of the *E.coli* O157:H7 cells was close to neutral and, in contrast to the trend observed for quartz sand, an increase in ionic strength led to a slight decrease in the zeta potential of the bacterial cells (Figure 4B). For both quartz sand and bacterial cells, phosphate led to decreased zeta potential values. This could be related to adsorption of phosphate onto the surface of quartz sand (e.g., through the bonding between phosphorus and oxygen at the surface of quartz) and bacterial cells, which could increase the negative surface charges under the pH conditions employed in this research [141].

The calculated XDLVO energy interaction profiles are shown in Figure 5. Under an ionic strength of 10 mM, there was no repulsive energy barrier for cell attachment to sand surface when phosphate was absent (Figure 5A). Energy barriers were present when

phosphate concentrations were either 0.1 mM or 1 mM. The energy barrier values were 0.86 kT (0.1 mM phosphate) and 1.33 kT (1 mM phosphate), respectively, where *k* is Boltzmann constant and T is absolute temperature in Kelvin. Similarly, when ionic strength was 100 mM, the energy barrier changed from absent for no phosphate to ~53 kT for both 0.1 mM and 1 mM phosphate (Figure 5B). The energy barriers, although small, could hinder the attachment of *E.coli* O157:H7 cells to the surface of quartz sands and thus changed a system that would otherwise be favorable for deposition, and made it unfavorable for deposition. This trend was consistent with results from the column transport experiments, which suggested that phosphate increased the transport of *E.coli* O157:H7 cells. Additionally, the magnitude of the energy barriers was generally higher for the 100 mM ionic strength conditions than the 10 mM ionic strength conditions. This was consistent to the observation that the transport of *E.coli* O157:H7 cells within the sand packs increased with ionic strength (Figures 1 and 2).

The total XDLVO energy interaction profiles reflect the summation of the LW, EDL and AB interactions. Inspection of the LW and AB components of the overall interaction energy showed that they were independent on water chemistry parameters and remained the same for all conditions. Ionic strength, however, had significant impact on the zeta potential values of both the bacterial cells and the sands (Figure 4B). As the sand zeta potential became less negative when ionic strength increased from 10 to 100mM, the zeta potential of *E.coli* O157:H7 cells became more negative. In response to the changes in the zeta potential values, the calculated EDL interactions between bacterial cells and quartz sand under 100 mM ionic strength conditions were more repulsive than the EDL interactions under 10 mM ionic strength conditions.

2.2.4 Release of immobilized *E.coli* O157:H7 cells

Results from that column transport experiments using a solution that had an ionic strength of 100 mM and contained no phosphate showed that ~33% of the bacterial cells were immobilized within the sand packs (Figure 1B). Upon the completion of the experiments, solutions with similar ionic strength but progressively higher phosphate concentrations (0.1 mM and then 1 mM) were sequentially injected into the columns to examine the release of the immobilized *E.coli* O157:H7 cells. The results showed that the increase in phosphate concentration in the mobile aqueous phase led to release of previously retained *E.coli* O157:H7 cells (Figure 1B). Maximum cell concentrations in the first and second release pulses reached ~16% and ~9% of influent concentration. Integration of the release pulses showed that the total quantity of released cells for the first and second pulses was equivalent to 2.5% (±0.5) and 1.4% (±0.5) of the total amount of bacterial cells that were injected into the columns, respectively. When combined, ~12% of the immobilized bacterial cells were flushed out during the two-stage phosphate perturbation experiments.

According to the XDLVO theory, when repulsive barrier (and thus secondary energy minimum) is absent in the energy interaction profile of bacterial cells and sands, the primary energy minimum is primarily responsible for cell deposition, which is considered as irreversible [133]. The observed release of immobilized *E.coli* O157:H7 was thus contrary to the XDLVO energy interaction profiles, which suggested the presence of energy barrier and secondary minimum (100 mM, no phosphate). The energy interaction profiles shown in Figure 5, however, were calculated using the average cell zeta potential values. Considering the variations in the measured cell zeta potential values (Figure 4B),

repulsive interaction barrier and secondary energy minimum could be present in the interaction energy profiles of a fraction bacterial cells and sand surfaces. Cell deposition within the secondary energy minimum could thus occur. For these cells, perturbations in water chemistry (i.e., phosphate concentration) could lead to their release. This was consistent to the observation that only a fraction (~12%) of the immobilized bacterial cells was released. For the fraction of *E.coli* O157:H7 cells that did deposit into the primarily minimum, the increase in phosphate concentration actually made the release less likely because, as suggested in Hahn et al. [142], the energy barrier for cell release increased. Our results also highlighted the vital importance that the energy interaction within 5 nm from the surface plays in cell deposition and release [142].

According to the colloid filtration theory [103, 106], the clean-bed deposition rate coefficient can be expressed as a function of the product of the collector efficiency (η) and collision efficiency (α). As the collector efficiency (η) can be estimated from correlation equation reported in the literature [103], the collision efficiency (α) can then be estimated from the experimentally determined deposition rate coefficient and collector efficiency[103]. The calculated values of α were all less than 1, suggesting that the deposition condition was not completely favorable (Table 1). This was also consistent to our observation that the retention of *E.coli* O157:H7 was reversible even if the XDLVO theory predicted the absence of energy barrier. In addition, the observed trend that values of α decreased with phosphate concentrations (Table 1).

2.2.5 Steric Interactions

As shown in the previous section, the XDLVO theory and our experimental observation did not always agree with each other (e.g., although XDLVO predicted no

energy barrier, the deposition of *E.coli* O157:H7 was reversible under the 100 mM, no phosphate condition). Steric interactions due to the presence of extracelluar macromolecules on bacterial surface were reported to be partly responsible for the discrepancies between model and experimental results [46].

The model results (Figure 6) indicate that the steric interaction between *E.coli* O157:H7 surface and quartz sand was significantly higher than the XDLVO forces at comparable distances. This was qualitatively consistent to our observation that the retention of *E.coli* O157:H7 was reversible when XDLVO theory predicts the absence of energy barrier. Additionally, it was hypothesized that the conformational changes caused by the deprotonation of bacterial surface lipopolysaccharides (LPS) carboxylic and phosphoric functional groups allowed for greater penetration of the counter ions into the polymer layer, which in turn decreased the attachment of *E.coli* O157:H7 cells onto the surface of quartz sand [61]. Elevated phosphate concentrations may have caused conformational changes of the bacterial extracellular polymers and consequently more repulsive steric interactions between the cell and quartz sand. More experimental investigations are needed to further examine the relationship between phosphate and the conformation of *E.coli* O157:H7 surface macromolecules as well as the associated impacts on the steric interactions.

2.2.6 Environmental implications

Cattle manure represents a major source of *E.coli* O157:H7 [26, 29-31]. Manure produced in cattle farms is commonly applied to the agricultural fields as a fertilizer. The *E.coli* O157:H7 cells that are introduced into the soil through this process could be leached out and contaminate the underlying groundwater. Findings from this research

suggest that phosphate, a key ingredient used in numerous domestic and industrial applications, e.g., detergents, metal surface coating, fertilizers, and drinking water distribution pipe corrosion control, could potentially change a system that would otherwise be favorable for *E.coli* O157:H7 cells deposition, and makes it unfavorable for deposition. Considering that groundwater is the primary source of drinking water, particularly in rural areas, the enhanced mobility of *E.coli* O157:H7 cells could translate into greater public health risks. Phosphate concentrations in the soil can also change as a result of fertilizer (including manure) application, plant uptake, rainfall, irrigation and plant evatranspiration. Our results indicated that increase in phosphate concentration could lead to the pulse-type release of previously immobilized *E.coli* O157:H7 cells. This release represents another mechanism that can result in the wider spread of *E.coli* O157:H7 cells within the soil-groundwater system. Our results also provided insights into mechanisms contributing to the reduced occurrence of coliform bacteria and biofilm inhibition in drinking water distribution systems through the addition of phosphate.

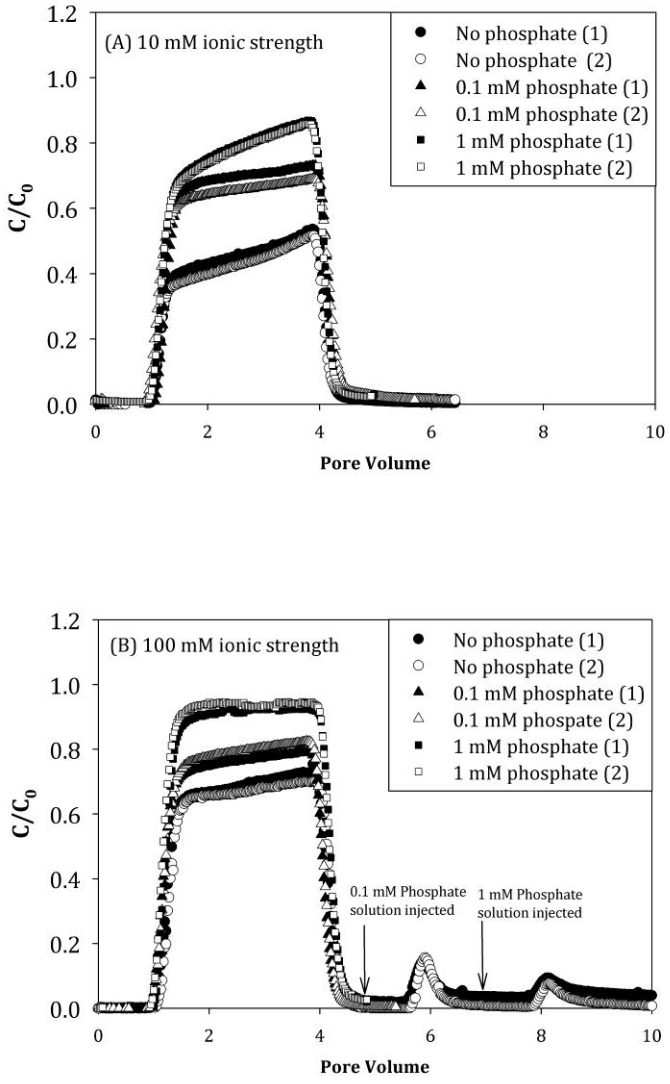

Figure 1. Breakthrough concentrations of *E.coli* O157:H7. The ionic strength of the solution was (A) 10 mM and (B) 100 mM, respectively. Concentrations of phosphate were 0, 0.1 and 1 mM. In (B), the release of immobilized *E.coli* O157:H7 cells was investigated through injecting solutions which had similar ionic strength (100 mM) but progressively higher phosphate concentrations.

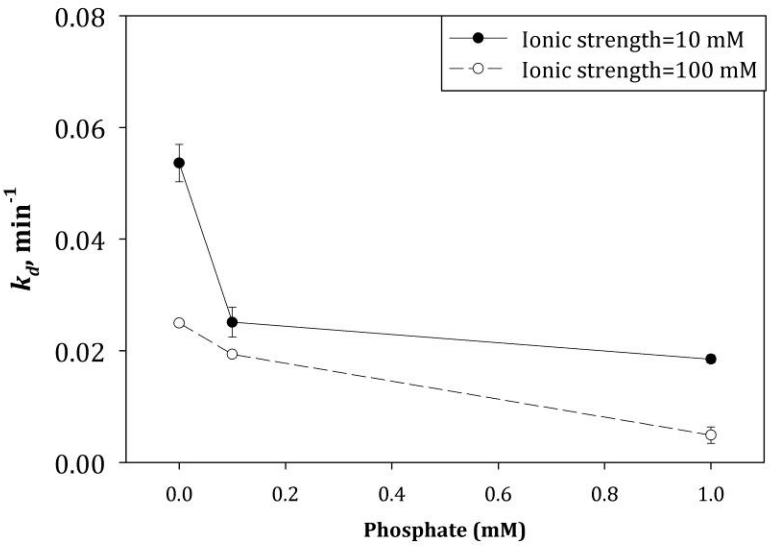

Figure 2. Deposition rate coefficient, k_d (min^{-1}), as a function of ionic strength and phosphate concentration. Error bars represent standard deviation of duplicate experiments.

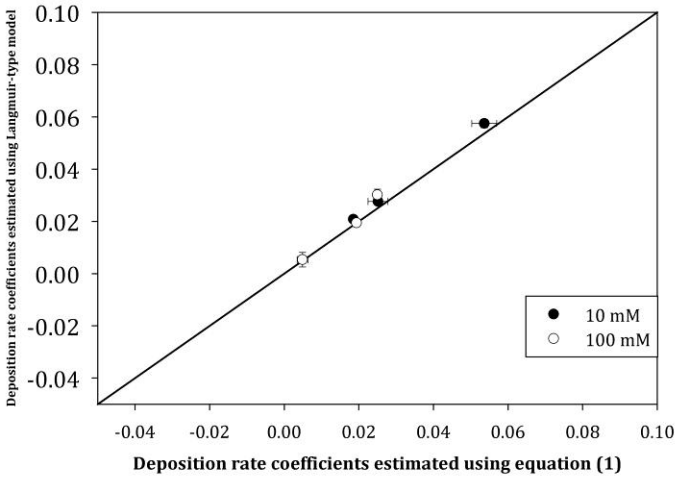

Figure 3. Comparison of values of k_d calculated using the second-order model and the first-order model. Error bars represent standard deviation.

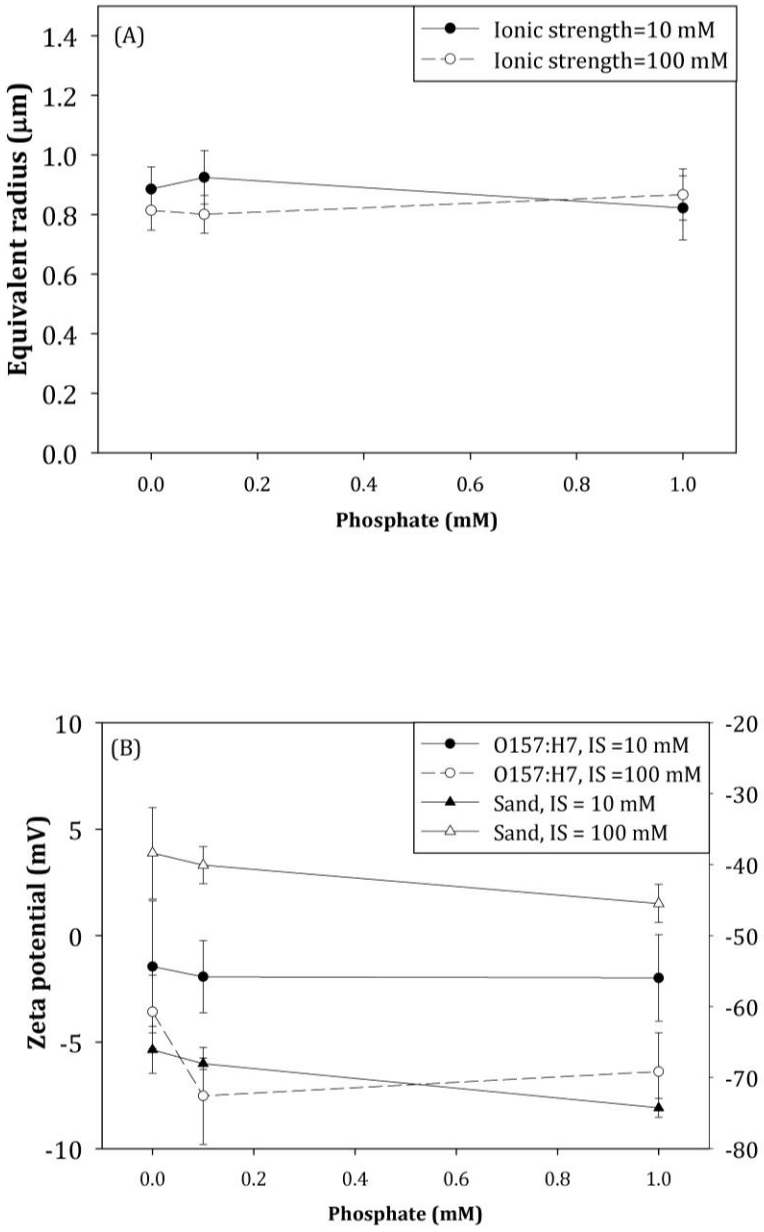

Figure 4. (A) Equivalent radius of *E.coli* O157:H7 cells suspended in various electrolyte solutions. (B) Zeta potential of bacterial cells (left axis) and quartz sands (right axis) under different ionic strength and phosphate concentration conditions. Note that the zeta potential values of bacterial cells and quartz sands were plotted at different scales.

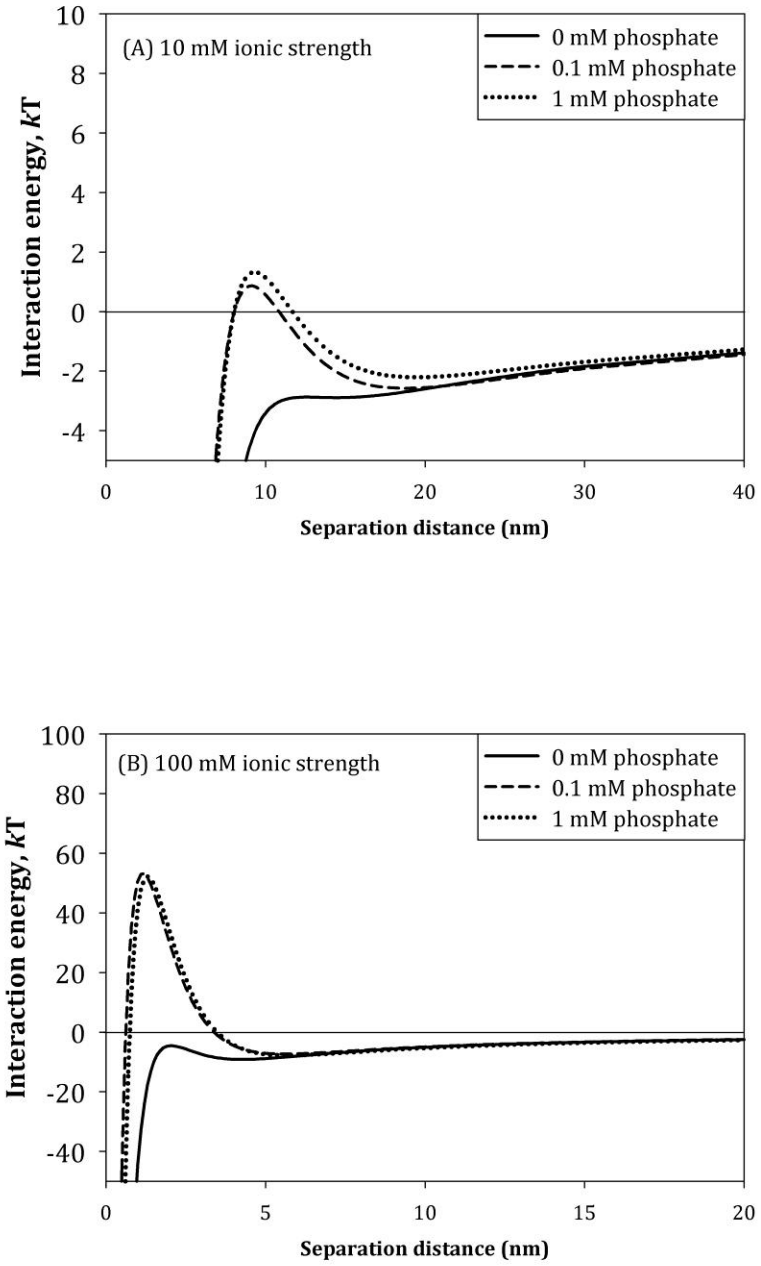

Figure 5. XDLVO energy interaction profiles between *E.coli* O157:H7 cells and surface of quartz sands. The energy interactions were expressed in *k*T, where *k* is Boltzmann constant and T is absolute temperature in Kelvin.

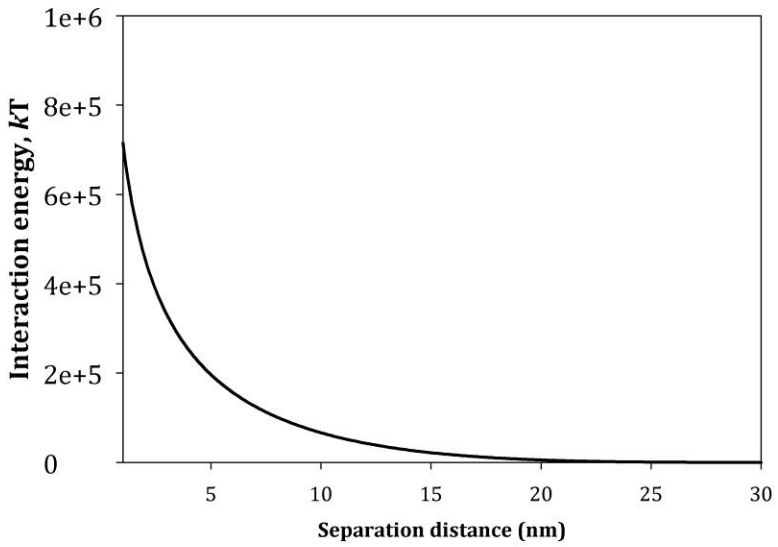

Figure 6. Steric interaction energy profile between *E.coli* O157:H7 cells and surface of quartz sands. The energy interaction was expressed in *k*T, where *k* is Boltzmann constant and T is absolute temperature in Kelvin.

Table 1. Values of collision efficiency (α) for the *E.coli* O157:H7 cells under various chemistry conditions.

Phosphate concentration	η		α	
	10 mM	100 mM	10 mM	100 mM
0 mM	0.4541	0.4771	0.314	0.139
0.1 mM	0.4434	0.4818	0.150	0.110
1 mM	0.4742	0.4597	0.104	0.029

Chapter 3 The role of LPS on the transport and deposition of *E.coli* O157:H7 in sand column

The significance of Enterohemorrhagic *Escherichia coli* (EHEC) O157 as a public health concern has been recognized since 1982 [143], when an outbreak of hemorrhagic colitis (severe bloody diarrhea) was traced to the consumption of poorly cooked ground beef in a fast food restaurant chain in the U.S. According to a CDC estimate[144], serotype O157:H7 is responsible for 73,000 cases of infection and 60 deaths in the U.S. each year. Between 1982 and 2002, a total of 350 *E.coli* O157:H7 outbreaks were reported in the U.S. and the majority of the outbreaks involved death[15]. While previous studies[145, 146] have pinpointed the association between waterborne outbreaks and the use of contaminated recreational waters, recent outbreaks [29, 30, 147]have been linked to the consumption of contaminated groundwater as a result of certain agricultural practices, e.g., the widespread use of animal manure and wastewater without adequate disinfection to eliminate bacterial pathogens prior to plant fertilization and irrigation, and heavy rainfall can cause the transport of bacteria to deeper layers of the soil by leaching[148, 149]. For example, 25.5% of water samples from drinking water system were positive with *E.coli* O157 in South Africa[150]. *E.coli* O157:H7 can be viable in underground condition for as long as 21 months. [38, 151, 152] A better understanding of the factors that affect the fate and transport of *E.coli* O157:H7 in soil and groundwater systems will help to evaluate the risk of drinking water contamination associated with those agricultural practices.

The environmental factors in the attachment/deposition behavior of *E.coli* O157:H7 onto substrate surface have been studied comprehensively including ionic strength, pH, divalent ions [61, 153], temperature [129] and so on. The surface macromolecules were observed to play an important role in mediating bacterial transport behavior and many studies were conducted [154, 155]. In the enterobacteriaceae, LPS occupies 75% of the surface of the bacterium [96] and it is considered as characteristic and essential for Gram-negative bacteria[156]. LPS are implicated in cell adherence to biotic and abiotic materials[157] [158] [74] [159] [97, 160]. However, divergent conclusions on the effect of LPS to bacterial attachment/deposition to substrate were acquired and it might be dependent on bacterial strain or experimental conditions. To our knowledge, the influence of LPS to bacteria strain *E.coli* O157:H7's transport and deposition in porous media has not been investigated.

LPS is composed of lipid A, a core region, and the repeating units of O-antigen (Figure 7) [94]. Lipid A is a phosphorylated glucosamine disaccharide connected with long-chain fatty acids, these hydrophobic fatty acid chains anchor the LPS in the cell wall. The core region of the LPS consists of negatively charged groups, such as phosphates and carboxylic groups, which usually give the LPS its negative charge [95]. The core region can be further subdivided into two regions based on the structure, the inner and outer core. The inner core contains 3-deoxy-D-manno-oct-2-ulosonc acid(KDO) and L-glycero-D-manno-heptopyranose(Hep). The lipid A and inner core were highly conserved, yet the structure of the outer core varies, which has 5 different chemotypes. The core of *E.coli* O157:H7 belongs to R3 type [161, 162], which is composed of heptose and KDO together with glucose, galactose and galactosamine. The

outer polysaccharide part of the LPS is the O-antigen, which consists of 20-40 repeating units of three to five sugars and can protrude up to 30 or more nm into the cell surroundings.

RfaC is the enzyme responsible for transferring the first heptose sugar onto the KDO moiety of the lipopolysaccharide inner core. A mutation in *rfaC* results in the strain heptoseless and contains KDO as its only core sugar. A mutation in *waaL* causes the lack of the O antigen in the LPS layer. O-antigen is an important indicator for determining if an isolated *E.coli* strain is pathogenic. *E.coli* serotype O157 is pathogenic and can cause severe symptoms of dysentery. The lipid A is widely conserved among *E.coli* while O-antigens are more diverse. There are more than 180 types of O- antigens of *E.coli* strains which have been chemically characterized.

In this study, the O antigen truncated mutant (*ΔwaaL*) and a core mutant with both O antigen and heptose missing (*ΔrfaC*) of *E.coli* O157:H7 were used(Figure 7) . Cells size, zeta potential and hydrophobicity were characterized. The transport of the three companions was conducted in quartz sand columns. XDLVO theory combining with steric interaction was applied for mathematically understanding the interaction between the strain and sand surface.

3.1. Materials and methods

3.1.1 Bacteria and solution chemistry

E.coli O157:H7 EDL933 wild type, Δ*waa L* (O-antigen deficient) and Δ*rfaC* (outercore and O-antigen deficient) were used in this study. Bacteria stored in -80°C freezer were grown overnight in Luria-Bertani (LB) agar plate (10g/liter Bacto tryptone,

5 g/ liter Bacto yeast extract, 5 g/liter NaCl) broth or agar(1.5[wt/vol] agar). When required, antibiotics were added as follows: 150μg/mL of rifampin and 50μg/mL of kanamycin. One single colony was picked by sterilized needle and transferred into 10ml Luria-Bertani broth in the presence of the appropriate antibiotics. Cells were precultured at 200 rpm at 37°C for 6 h, inoculated to fresh medium at the ratio of 1:50. After 18 h incubation with oscillation, cells were collected by centrifugation at 3000 × g, 4°C, for 10min. The supernatant was decanted and the pellet was resuspended in electrolyte. This centrifugation procedure was repeated twice to completely decant growth media. The cell density was adjusted to OD of 0.3±0.01 at wave length of 220 nm for column experiment. The correspondence cells concentration was 3×10^7 cells/ml.

Two pH (5.6 and 8.4) and three ionic strength (10,100, and 300mM) conditions were applied in the experiment. PH of 5.6 electrolytes comprised NaCl ions only, and pH of 8.4 electrolytes was adjusted with 0.1mM $NaHCO_3$.

3.1.2 Porous media

Quartz sand was purchased from US Silica Company. Sand was size-fractionated with stainless steel sieves, and fractions in 0.707-0.841mm range and a mean diameter of 0.774mm were used in the column experiments. The sand was first treated to remove metal and organic matters from surface. Briefly, the sand was boiled in nitric acid (70%) (Fisher) for 48h. After that, it was washed in deionized water (Barnstead Inc.) and immersed in 0.1M NaOH for 24h. Finally, it was rinsed with deionized water thoroughly. The acid-base cleaning step was repeated one time to completely clean the sand. Then the sand was dried in an oven at 55 °C for 2 days and stored in covered Pyrex beakers until use.

3.1.3 Bacterial column transport experiment

Bacterial transport experiments were carried out in glass chromatography columns packed with clean quartz sand. Columns (Kontes) with 15 cm height and 2.5 cm inner diameters were used. Columns were wet packed by tap filling method to maintain a gravimetrically porosity at 0.344. Before each experiment, the columns were pumped (Masterflex) more than 20 pore volumes of background electrolyte to equilibrate the porous media environment. Bacterial cells suspension was then pumped through the column for 60 min (approximately 3 pore volumes) followed by the same background electrolyte for 60 min. The approaching velocity during the column experiments was at 0.51 cm s^{-1}.

The absorbance of the effluent from sand column was measured onsite with a UV/vis spectrophotometer (Model1600, Shimadzu) and the cell concentration was converted using a calibration curve. The wave length of 220nm was used.

3.1.4 Hydrophobicity (Contact angle) measurement

The hydrophobicity of bacteria and sand was determined by measuring their contact angles with three liquids, water (γ^{L}=72.8, γ^{LW}=21.8 and $\gamma^{+}=\gamma^{-}$=25.5 mJ m^{-2}) , glycerol(γ^{L}=64.0, γ^{LW}=34.0 and γ^{+}= 3.92 and γ^{-}=57.4 mJ m^{-2}) and diiodomethane (γ^{L}=50.8, γ^{LW}=50.8 and $\gamma^{+}=\gamma^{-}$=0.0 mJ m^{-2}) [70]. Bacterial lawn was produced by filtering through membrane and the contact angle was detected by Rame- Hart goniometer. Basically, the filter membrane covered with bacterial lawn after filtering was placed in a petri dish to keep it from drying out. In 10 minutes, the membrane was mounted onto the platform of the goniometer and 3 µl of the test liquid was vertically dropped by pipette onto the membrane. When the drops reached the stable status, the

images were captured and the contact angle between the drops and the bacterial lawn surface from both the left side and right side were recorded. The average value was taken as one measurement data and was written as θ. Triplicate tests were performed for each strain and 3-4 drops were measured for each liquid. The values of γ^{LW}, γ^{+} and γ^{-}, which were used for calculating the free energy of the bacterium, were calculated using the following equations: $\gamma_i^L(1+cos\theta) = 2\sqrt{\gamma_i^{LW}\gamma^{LW}} + 2\sqrt{\gamma_i^{+}\gamma^{-}} + 2\sqrt{\gamma_i^{-}\gamma^{+}}$. where the subscript i represents water, glycerol or diiodomethane [70].

3.1.5 Zeta potential measurement

The zeta potential of bacteria sand was measured by using a ZetaPAL analyzer (Brookhaven Instruments Corporation, Holtsville, NY). Cells were diluted to 10^6cells/ml for each measurement. Measurements were conducted in duplicate, and 10 runs were chosen for each sample. Smoluchowski equation was used to convert the electrophoretic motilities to zeta potentials.

3.1.6 Cell size measurement

The size of bacterial cells (expressed as equivalent radius that equals to the square root of the product of width and length divided by the constant π) was measured by taking photos using a Nikon Eclipse 50i microscope which was equipped with a Photometric coolsnap ES digital camera. At least 50 cells were measured for one condition.

3.1.7 Cell deposition expression

k_d was used to determine the deposition rate of *E.coli* O157:H7. It was estimated using the steady state breakthrough concentrations of the cells applied to the following equation

$$k_d = -\frac{U}{\varepsilon \cdot L} \ln\left(\frac{C}{C_0}\right) \qquad (3.1)$$

ε is the bed porosity,0.344, U is the approach velocity, L is the length of the column(15cm) and C/C_0 is the normalized breakthrough concentration and was obtained from each bacteria breakthrough curve by averaging the values measured between 1.8-2.0 pore volume.

3.1.8 XDLVO calculation

The transport of bacterial cells within saturated porous media is governed by the energy interactions between bacterial cells and the surface of solid matrix (e.g., sands). According to the extended Derjaguin-Landau-Verwey-Overbeek (XDLVO) theory, the energy interactions between bacterial cells and quartz sand immersed in water include the Lifshitz−van der Waals (LW) interactions, the electrostatic double layer (EDL) interaction as well as the Lewis acid-base (AB) (i.e., hydrophobic) interaction.

Steric interaction between cell suface and medium surface has been considered as an important factor which could play a role in mediating the deposition of bacteria to surface and it contains two components--osmotic and physical pressure expressed by the deGennes equation for two parallel surfaces

The energy form has been deduced and applied to the XDLVO equation to quantify the total interaction energy profile.

$$\Phi^{\mathrm{Total}} = \Phi^{\mathrm{LW}} + \Phi^{\mathrm{EDL}} + \Phi^{\mathrm{AB}} + \Phi^{Steric} \quad (3.2)$$

The LW, EDL, AB and steric interaction energies (Φ^{LW}, Φ^{EDL} , Φ^{AB} and Φ^{Steric}) can be calculated using the equations described in Chapter 2.

3.2 Results and Discussion

3.2.1 Cell size, zeta potential and hydrophobicity

The ionic strength and pH has a negligible effect onto bacterial cells size(data not shown). On the contrary, the mutation has resulted in cells size change in both length and width direction, hence the equivalent size. After measuring the length and width of the cells and doing the conversion, the equivalent radius for WT, Δ*waaL* and Δ*rfaC* were respectively1.19±0.08μm and 1.49±0.14 μm and 1.69±0.08μm.

The wild type strain has near neutral zeta potentials (~-1 mV) from 10~300mM IS (Table 2). The two LPS mutants were more negatively charged under both pH conditions. At IS of 10mM and pH of 8.4, the zeta potential of Δ*waaL* and Δ*rfaC* were respectively -29.50mV and -43.80mV. Increasing ionic strength resulted the zeta potential of the two mutant strains less negative and Δ*rfaC* was influenced more than Δ*waaL*. For instance, the zeta potentials of Δ*waaL* and Δ*rfaC* were respectively increased ~ 9.9mV and ~24.2mV to both ~ -19.6mV at IS of 100mM, and the zeta potentials of Δ*waaL* and Δ*rfaC* were further increased ~3.8mV and ~5.7mV to -15.80mV and -13.92mV at IS of 300mM, respectively. The exposure of phosphate groups at the cell's surface might be responsible for the more negative surface charge of *ΔrfaC* mutant and more sensitive to the ionic strength change than Δ*waaL* and wild type strain. The zeta

potential of sand was more negative than the bacterial cells and became less negative with increasing IS.

pH negatively impacted the zeta potentials of both bacteria and sand. That is, elevated pH value resulted in more negative zeta potentials of the bacterial and sand's surface. According to our contact angle experiments, the LPS mutants became more hydrophobic (Table. 2). Our observation of zeta potential and contact angle of the mutants was consistent with study of Burks [75] and Ong's [98], which had used isogenic LPS truncated mutant D21f2 and wild type D21 and JM109 as the test strains.

3.2.2 Transport of *E.coli* O157:H7 within sand packs

Results from the column transport experiments showed that LPS truncated strains had lower breakthrough curves than wild type at ionic strength of 100 and 300mM, indicating that deletion of LPS increased the deposition of cells to sand at high IS (Figure 8). For instance, at IS of 100mM, the percentage of bacterial cells that transport through columns were respectively 93.2% (±1.3%), 81.1%(±0.6%) and 59.3% (±0.3%)%) for wild type, Δ*waaL* mutant and Δ*rfaC* mutant. Accordingly, the deposition rate coefficient (k_d) was 0.006±0.002 sec^{-1}, 0.041±0.001 sec^{-1}, 0.091±0.002 sec^{-1} for wild type, Δ*waaL* and Δ*rfaC* mutants, respectively. Interestingly, at low IS of 10mM, the mutation did not have significant influence on bacterial transport and deposition in sand columns, 97.4%(±3.4%) wild type cells traveled through sand columns and 96.5%(±2.1%) and 95.2%(±2.4%) for Δ*waaL* mutant and Δ*rfaC* mutant, respectively. Accordingly, the deposition rate coefficient (k_d) was 0.001±0.002sec^{-1}, 0.002±0.001 sec^{-1} and 0.003±0.001 sec^{-1} at 10mM IS (Figure 9).

Increasing ionic strength will significantly increase the deposition of the two LPS mutants onto sand packs. At IS of 10mM, the percentage of cells that traveled through sand packs were 96.5%(±2.1%) and 95.2%(±2.4%), respectively, for the *E.coli* O157:H7 Δ*waaL* mutant and Δ*rfaC* mutant, respectively. At IS of 300mM, the percentage of bacteria remained in the effluent was reduced to 66.1%(±1.6%) and 39.7%(±0.5%) for Δ*waaL* mutant and Δ*rfaC* mutant, respectively. However, increasing ionic strength did not have influence as significant as the mutants for the transport of wild type, which has 97.4%(±3.4%) cells passed through columns at 10mM and 93.0%(±1.6%) at 300mM IS.

The higher breakthrough curves of the three *E.coli* strains (Figure 8) at pH of 8.4 comparing to pH of 5.6 indicated elevated pH value increased bacterial transport.

3.2.3 Interaction Energy Profiles

The LPS equilibrium length of *E.coli* O157:H7 is 30±13nm [136]. The combination of the lipid A plus inner, and outer cores was 4.4nm and the length of lipid A itself is 2.4 nm [163]. The truncation of LPS leads to change of LPS length, and thus steric interaction between cells and sand surface.

The interaction energy profiles with incorporation of steric interaction for the three LPS isogenic strains versus distance were plotted in figure 10. The energy barriers of the three strains were all high ($>10^5$ *kT*) and less likely to be overcome. The deposition of cells was then attributed to happen mainly at the secondary minimum[133]. For interaction energy profile of wild type, the secondary minimum was at around -5 *kT* and separation distance of 30nm, the secondary minimum did not show significant shifting towards ionic strength. This is in consistent with the column results that the deposition

rate of wild type was low and had little variation under all ionic strength conditions. For Δ*rfaC* mutants, the energy profiles of the secondary minimum were -5*kT*,-23*kT* and -35*kT* at separation distance of 25nm, 6nm and 5nm for 10mM, 100mM and 300mM ionic strength, respectively. Consistently, the column results showed that Δ*rfaC* mutants had higher deposition rate than wild type at high IS and the deposition rate was significantly influenced by ionic strength. The interaction energy profiles with incorporation of steric interaction for the three LPS isogenic strains showed qualitatively consistent with the macro-scale results in term of deposition of cells onto sand surface.

3.3 Discussion

Penagonda [157] phenol-chemically extracted lipopolysaccharide of *Escherichia coli* k-12, and the cells exhibit stronger interaction with silica sand. Williams also [74] observed the LPS mutants of *Pseudomonas fluorescens*' retention in quartz sand columns was greater than the parent strain. On the contrary, Lail and Camesano removed the LPS molecules from *E.coli* JM109 with chemical method and found that bacterial retention to glass or in packed beds to quartz sand decreased. In an addition, Velegol and Logan [49], Burks [164] and Walker[97] found that there was no correlation between the length of the LPS and the collision efficiencies or deposition rate of bacterial cells.

The variations in finding the role of LPS in bacterial adhesion might be due to experimental conditions and surface complexities of bacterial strains. In considering this, isogenic mutants were constructed and compared for the effects of LPS in bacterial transport and deposition through sand columns. With the isogenic LPS mutation, cells became more negative charged on the surface and more hydrophobic comparing to the parent cells, which is consistent with the observations using other strains [75, 98].

The LPS mutation increased the deposition of *E.coli* O157:H7 to quartz sand over IS of 10-300mM under both tested pH conditions. Based on XDLVO theory, the change in surface potential and hydrophobicity for LPS mutants would discourage the attractive interaction with sand and hence would result in reduced cells deposition profile. The deviated results from the theory suggest additional interaction force(s) may come into play.

Camesano [160] found the higher repulsion force between the LPS intact cells and the AFM tip than EDTA- treated cells. Ong [98] [110] incorporated steric and hydrophobic interactions into DLVO model which thus explained the enhanced repulsion force for *E.coli* D21 to polystyrene comparing to its LPS truncated compartment *E.coli* D21f2. Lu[165] recently used SFA to measure the force between the different LPS length molecules and solid surfaces and found the correlation between LPS length and bacterial adhesion. In our study, when we incorporate steric interaction to the XDLVO equations, the interaction energy profiles were then qualitatively consistent with the deposition of the three LPS isogenic strains onto sand surface.

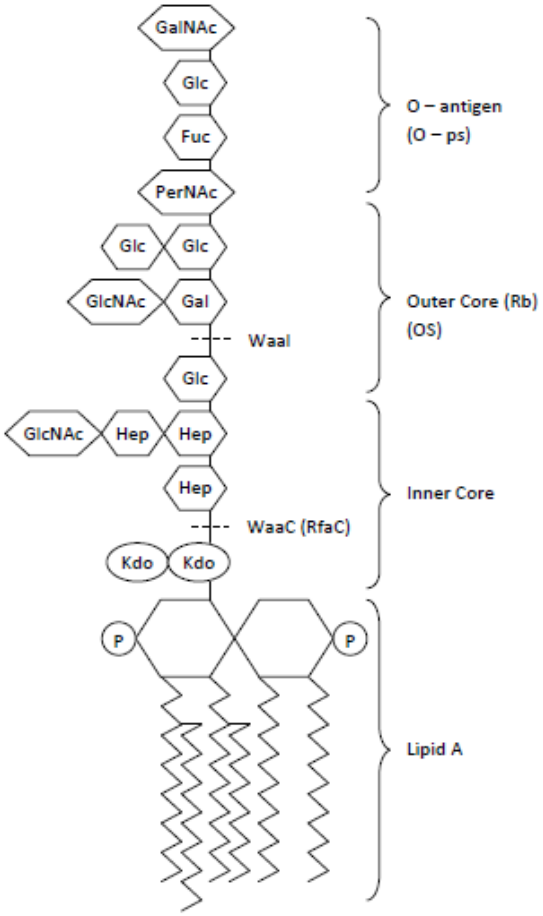

Figure 7. Sketch of *E.coli* O157:H7 LPS structure and its LPS mutants

Table 2. Zeta potentials of the three strains, wild type, Δ*waaL* and Δ*rfaC* in three ionic strength conditions (10, 100 and 300mM) and two pH conditions (5.6 and 8.4)

Cell type	**Zeta potential at pH=5.6(mV)**			**Zeta potential at pH=8.4(mV)**			**Contact angle measurements**		
	10	100	300	10	100	300	θ_{water}	$\theta_{Glycerol}$	θ_{DI}
WT	0.5±2.5	1.0±0.1	5.7±1.	-1.0±2.5	0.2±3.9	0.4±5.0	11.8±2.0	18.0±2.0	35.6±0.8
ΔwaaL	29.9±2.4	-15.3±2.8	-11.06±1.7	-29.5±1.4	-19.6±2.4	-15.8±3.7	28.1±1.2	25.0±2.0	48.7±0.6
Δ rfaC	-37.4±1.0	-18.1±1.9	-9.0±2.2	-43.8±1.5	-19.6±2.3	-13.9±1.2	47.0±2.4	32.3±2.2	54.8±2.0
sand	-59.8±1.0	-32.1±2.2	-25.1±3.4	-77.7±1.5	-41.5±2.3	-21.7±1.2	14.2±0.8	8.5±0.8	34.5±1.1

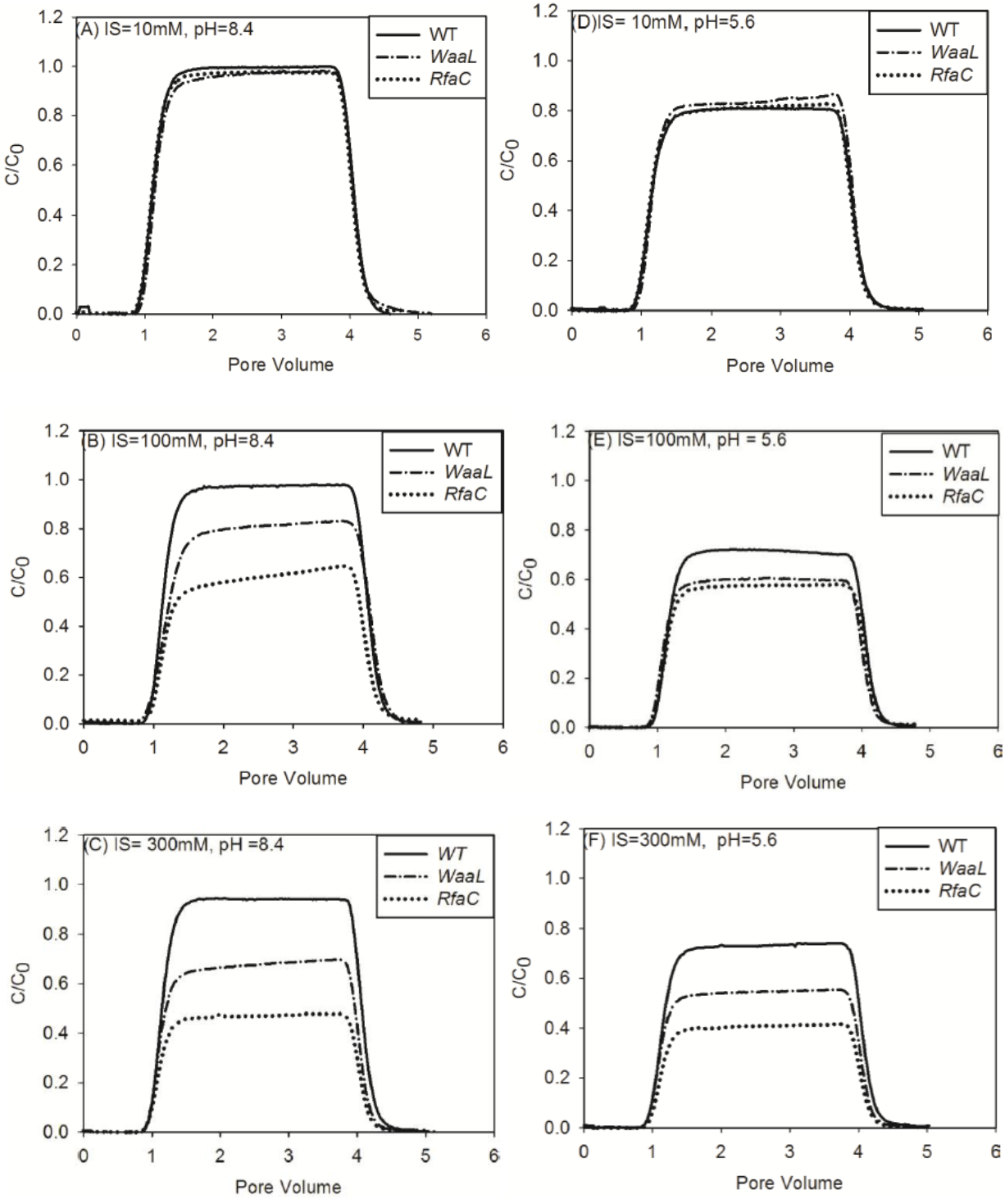

Figure 8. Breakthrough curves of the three strains under 10,100,300mM ionic strength NaCl at pH= 8.4(A,B,C) and 5.6 (D,E,F)

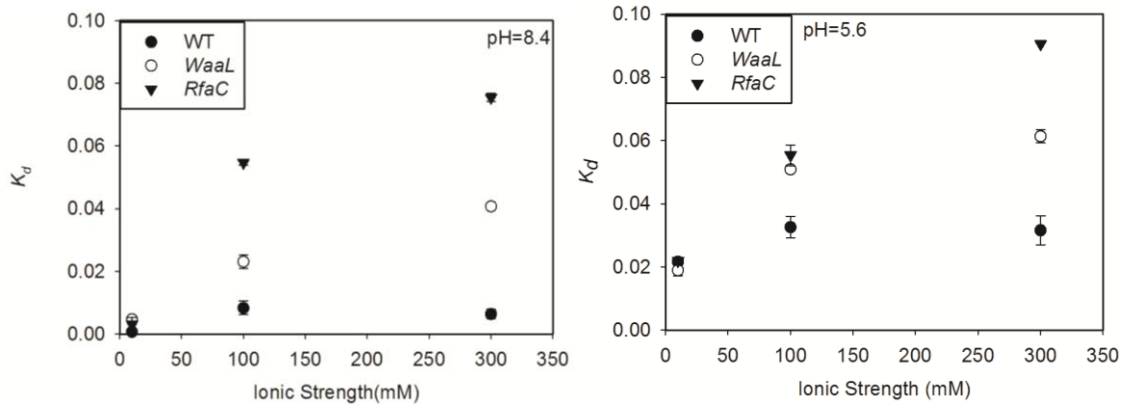

Figure 9. The k_d of the three strains under 10,100,300mM ionic strength NaCl at pH=5.6 and 8.4

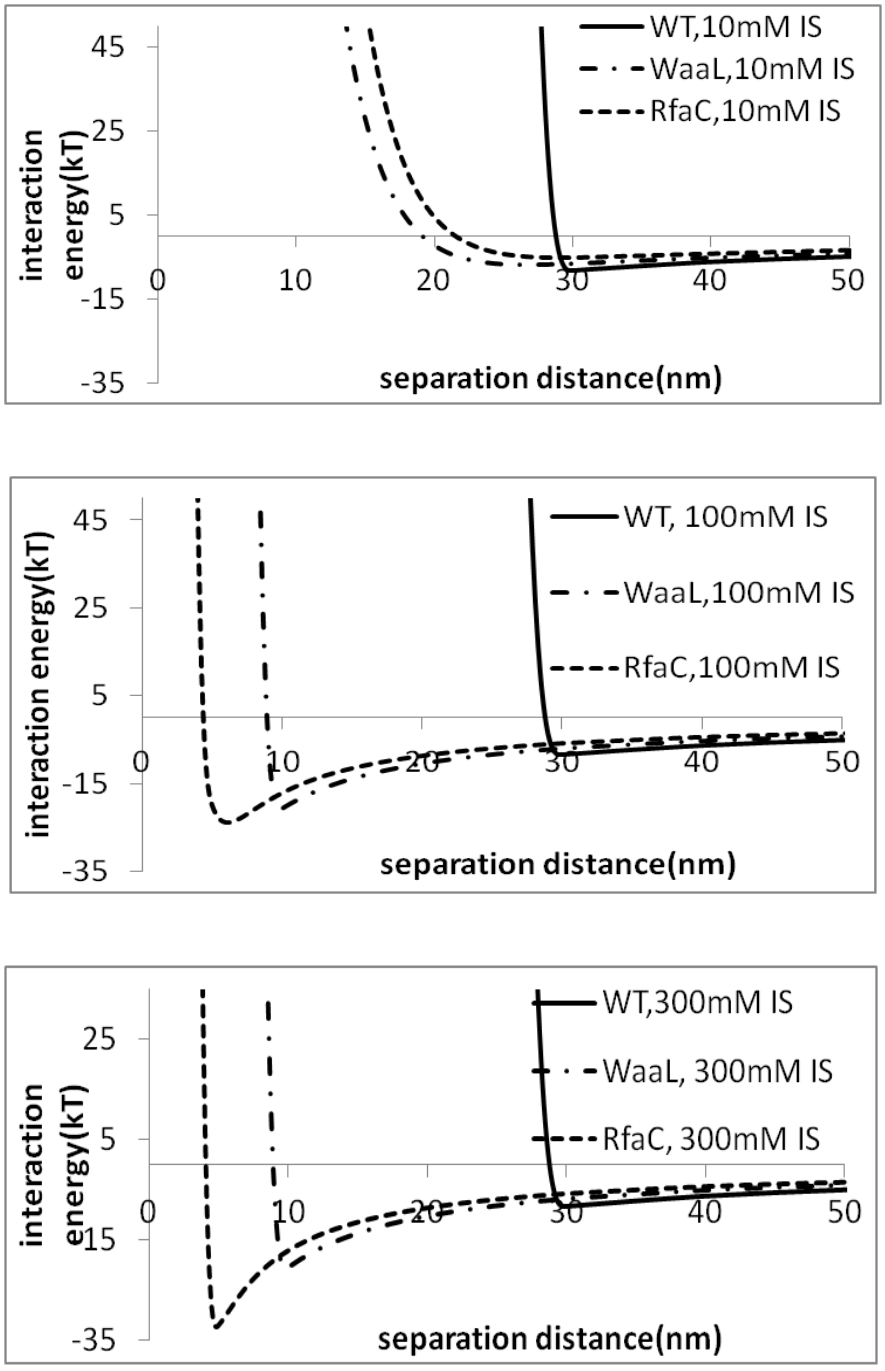

Figure 10. XDLVO interaction energy + steric interaction energy for *E.coli* O157:H7 EDL933 wild type, *ΔwaaL* and *ΔrfaC* strains at IS=10mM, 100mM and 300mM

Chapter 4 The role of strain type and biofilm on *Escherichia coli* transport and retention through porous media

In this study, the transport and retention of two *E.coli* strains, O157:H7 and JM109, in quartz sand were investigated to better understand the transport of *E.coli* bacteria under various environmental conditions. *E.coli* JM109 is a laboratory strain that has been used as a surrogate to study the fate and transport of pathogenic *E.coli* in soil and groundwater [166-170]. Our study focused on the effect of solution chemistry, physical flow conditions, and bacterial surface macromolecules on the attachment of both *E.coli* strains to sand surface.

In addition, the interaction between *E.coli* bacteria and *P. aeruginosa* biofilm was also investigated. *P. aeruginosa* has been widely used as a model microorganism to study the structure and function of biofilm because of its ability to form uniform biofilms and secrete various extracellular products. In our study, biofilms of *P.aeruginosa* PAO1 and PDO300 strains with different EPS production capability were coated onto packed glass beads columns. The biofilm of PDO300 and PAO1 differ in three ways: 1) the PDO300 has a higher biomass and EPS concentration than PAO1; 2) PDO300 biofilm contains mannuronic acid and guluronic acid monomers, while PAO1 biofilm's main composition is neutral sugars; and 3) the architecture of the PDO300 biofilm differs from that of the PAO1biofilm with a higher roughness and more water channels. The transport and deposition of *E.coli* JM109 and *E.coli* O157:H7 were tested and compared with PAO1 and PDO300 biofilm-coated porous media.

4.1 Materials and Methods

4.1.1 Bacterial Cells Preparation

The two *E.coli* strains used in this study are *E.coli* O157:H7 EDL933 nontoxic mutant- stx1 and stx2 double mutant, and *E.coli* JM109. Both strains were provided by Prof. Ching-Hong Yang in the Department of Biological Sciences at the University of Wisconsin-Milwaukee. The preserved cells stored in 20 % glycerol at -80 °C were streaked onto Luria-Bertani (LB) agar plates. The agar plates for growing *E.coli* O157:H7 were supplemented with 20 μg/mL chloramphenicol, 30 μg/mL kanamycin, and 150 μg/mL rifampicin. The agar plates for growing *E.coli* JM109 were supplemented with 50 μg/mL nalidixic acid. *E.coli* O157:H7 mutant lacking Stx1 and Stx2 was generated by allelic exchange which is resistant to chlorampfenicol, kanamycin, and rifampicin [171]. JM109 is resistant to nalidixic acid [172]. Stock solutions with 34, 100, and 50 mg/ml of chlorampfenicol, kanamycin, and rifampicin were prepared by dissolving them in ethanol, water, and methanol respectively. A 30 mg/ml stock solution of nalidixic acid was prepared by dissolving it in 1M NaOH. These antibiotic stocks were further amended into media to make the final concentrations described above. Both strains were incubated at 37 °C overnight. One single colony was picked with a sterile needle and transferred into 10 mL sterile LB broth amended with antibiotics. After 6-hr pre-culture at 37 °C, the bacterial cells were transferred to a fresh LB broth with a volume ratio of 1:200 and incubated at 37 °C and 200 rpm for 18 hrs. The bacterial cells were then centrifuged at 3000 g, 4 °C for 10 min and the pellets were rinsed twice using 10mM or 100mM phosphate buffered saline (PBS) solutions to remove the growth media. The 100mM PBS solution was made with 0.662g/L Na_2HPO_4, 0.192g/L $NaH_2PO_4 \cdot H_2O$, 5.136g/L NaCl [173] and a 10-fold dilution with ultrapure water was used to make the 10mM PBS. The

pH of the electrolytes remained at ~7.2. The cell concentration was adjusted to ~3×10^7 cells/mL using a spectrophotometer (Shimadzu UV-1700) by measuring the absorbance of the cell suspensions at a wavelength of 220 nm [124, 125] prior to the column transport experiments.

4.1.2 Column Transport Experiment

Duplicate glass chromatography columns (Kontes) 15 cm in length and 2.5 cm in diameter were wet packed with clean quartz sands. The sands were washed as previously described. The packed columns were equilibrated with more than 20 pore volumes (~600mL) of background electrolyte solution. Peristaltic pumps (Cole Parmer) were used to regulate the flow and the specific discharge was maintained at 0.31 cm/min. Following the equilibrium step, bacterial suspensions were injected into the columns, and the injections lasted for 60 min (~3 pore volumes). The column effluent was monitored using a UV spectrophotometer (Shimadzu) at a wavelength of 220 nm. Upon termination of the cell suspension injection, the columns were flushed with bacterial free electrolyte solution until the absorbance of the effluent returned to zero.

The classical filtration theory (CFT) was used to model bacterial transport and retention in the packed columns. The kinetics of bacterial cell deposition in the saturated sand columns was quantified by calculating the deposition rate coefficient, k_d (min^{-1}) from cell breakthrough concentrations in the effluent [127, 128]:

$$k_d = -\frac{U}{\varepsilon \cdot L} \ln\left(\frac{C}{C_0}\right) \qquad (4.1)$$

Where ε is the porosity of the sand (cm^3/cm^3), it was 0.344 in this study. U is the specific discharge (cm/min), L is the length of the column (cm) and C/C_0 is the normalized breakthrough concentration relevant to clean-bed conditions, which was obtained from average bacterial breakthrough concentrations between 1.8-2.0 pore volumes [127, 129].

The particle distribution S(X), i.e. the number of deposited bacteria per mass of the granular collector, was calculated using the following equation:

$$S(X) = \frac{t_0 \cdot \varepsilon \cdot k_d \cdot C_0}{\rho_b} \exp\left(-\frac{k_d \cdot X \cdot \varepsilon}{U}\right) \quad (4.2)$$

Where X is the bacterial travel distance, ρ_b is the porous medium bulk density, and t_0 is the duration of continuous particle injection.

4.1.3 Zeta Potential Test

The electrophoretic mobility of bacterial cells was measured using a ZetaPALS analyzer (Brookhaven Instruments). The Smoluchowski equation ($\zeta = \frac{\mu\eta}{\varepsilon_{0\varepsilon_r}}$), where η is the viscosity of the electrolyte solution, ε_r and ε_0 are the relative permittivity of the electrolyte solution and a vacuum, was used to convert electrophoretic motility values into zeta potentials [174].

Quartz sands were pulverized and colloid-sized quartz particles were suspended in electrolyte solutions for the zeta potential test.

4.1.4 Hydrophobicity Test

The hydrophobicity of bacterial cells was measured using the microbial adhesion to hydrocarbons (MATH) test. Five mL of n-dodecane was added to 5 mL of cell

suspension and the mixture was vortexed (Fisher Scientific) for 15 sec. After leaving the mixture for 1 hr at room temperature, the optical density of the cells in the water phase was measured at 600 nm. The percentage of the cells partitioned to the oil phase was calculated.

4.1.5.LPS Analysis

The LPS of *E.coli* O157:H7 and *E.coli* JM109 was isolated and analyzed following the method described by Sheng et. al.[175] with slight modification. Briefly, 20 ml of LB overnight grown cells with an OD_{600} of 1.0 were washed with 25mL of 1× PBS for three times. The pellets were then resuspended in 1.0 ml PBS and inoculated at 60 °C for 30 min. The suspension was centrifuged at 11,750 g for 30 min. 100 μL of the supernatant was mixed with 100 μL of glycine sample buffer (Biorad Laboratories.) containing 2-β- mercaptoethanol (2 %) and the mixture was boiled for 10 min. Protease K was added to a final concentration of 0.4 mg/ml. The sample was then incubated at 60 °C for 60 min and centrifuged at 16,000 g for 30 min. LPS was analyzed by glycine- sodium dodecyl sulfate (SDS)-polyacrylamide gel electrophoresis (PAGE) method[176]. Silver stain technique [177] was used to visualize the LPS bands.

4.1.6 Biofilm Development

Cylindrical polycarbonate plastic (25 cm long, 2.5 cm internal diameter) columns were used for biofilm development experiment. Biofilms of *P. aeruginosa* wild-type strain (PAO1) and its isogenic mucoid alginate-overproducing strain with a mucA22 mutation (PDO300) were introduced to the packed bed columns. To establish the biofilm, 150ml bacterial suspension with approximately 10^8 CFU/mL PAO1 or PDO300 cells were continuously pumped upward through the columns at a flow rate of 3.0 mL/min for

12 h. Synthetic wastewater then replaced the cells solution and the columns were operated continuously for five days. The synthetic wastewater consisted of 25mg/L K_2CO_3, 25mg/L K_2HPO_4, 10mg/L KH_2PO_4, 11.25 mg/L $MgSO_4 \times 7H_2O$, 13.75 mg/L $CaCl_2 \times 2H_2O$, 0.125 mg/L $FeCl_3 \times 6H_2O$, 0.0112 mg/L $MnSO_4 \times H_2O$, 0.0007 mg/L $CuSO_4$, 0.0004 mg/L $Na_2MoO_4 \times 2H_2O$ and 0.012 mg/L $ZnSO_4 \times 7H_2O$. The chemical oxygen demand (COD) of the wastewater was 150 mg/L and the pH was 7.2-7.6. The flow rate was kept unchanged, but the flow injection direction was switched every 12 hours. The biofilm was grown at room temperature (20-25 °C) in the dark. The development of *P. Aeruginosa* biofilm was monitored daily by measuring the suspended bacterial concentration in the column effluent. The bacterial concentration in the column effluent reached 10^{10} CFU/mL in the first two days of inoculation. After five days, the bacterial concentration in the column effluent remained steady at 10^5-10^6 CFU/mL.

4.1.7 Transport Model

The transport of bacterial cells within saturated porous media is governed by the energy interactions between bacterial cells and the surface of solid matrix (e.g., sand). According to the extended Derjaguin-Landau-Verwey-Overbeek (XDLVO) theory, the forces include the Lifshitz−van der Waals (LW) interactions and the electrostatic double layer (EDL) repulsion, the Lewis acid-base (AB) (i.e., hydrophobic) interaction [57, 130, 131]:

$$\Phi^{\mathrm{Total}} = \Phi^{\mathrm{LW}} + \Phi^{\mathrm{EDL}} + \Phi^{\mathrm{AB}} \qquad (4.3)$$

The LW, EDL, and AB interaction energies (Φ^{LW}, Φ^{EDL} and Φ^{AB}) can be calculated using the equations described in Chapter 2.

4.2 Results and discussion

4.2.1 Zeta Potentials, Hydrophobicity and LPS profiles of *E.coli* O157 and *E.coli* JM109

The zeta potential of *E.coli* O157:H7 was slightly negative (-1.9±0.6mV) at 10mM and the cell surface became more negatively charged (-7.5±1.5mV) when the ionic strength was increased to 100mM (Table 3). The measured zeta potentials of *E.coli* O157:H7 were consistent with results reported in the literature [8, 72, 178]. This increase in *E.coli* O157:H7 surface negative charge under higher ionic strength was contrary to common believe that increasing ionic strength would lead to electric double layer compression and reduced cell surface zeta potential. The surface zeta potentials of *E.coli* JM109 were -38.3 ±2.4mV at 10mM and -17.7±2.3mV at 100mM which is consistent with the theory.

The bacterial surface hydrophobicity was measured using the microbial adhesion to hydrocarbons (MATH) test. The MATH test calculates the percentage of the cells partitioned to the oil phase and a higher percentage suggests a higher hydrophobicity. As shown in Table 3, the hydrophobicity of *E.coli* O157:H7increased from 56.9% to 71.3% when the ionic strength was increased from 10mV to 100mV. The cell surface hydrophobicity did not change significantly for *E.coli* JM109 with the ionic strength increase. The surface of *E.coli* O157:H7 was more hydrophobic than *E.coli* JM109 under both low and high ionic strength conditions. This implied the presence of distinct macromolecule groups at the surface of *E.coli* O157:H7 and JM109. Analysis of the LPS profiles of *E.coli* O157:H7 and *E.coli* JM109 shown the two strain had very different laddered bands (Figure 11). Many high-molecular weight laddered bands which

represented the O-polysaccharide side chains in *E.coli* O157:H7 strains were missing in the JM109 LPS lane. The SDS-PAGE band of *E.coli* O157:H7 strain was consistent with Sheng et al.'s observations [175]. The band difference implies that the two bacterial strains have distinct LPS chemical composition.

4.2.2 Breakthrough Curves of *E.coli* O157:H7 and *E.coli* JM109

As shown in Figure 12, the effluent bacterial cell concentration was significantly higher for *E.coli* O157:H7 than JM109 under both ionic strength conditions. The average C/C_0 for *E.coli* O157:H7 was around 65±3% in 10mM solution and was 78±3% in 100mM solution. In contrast, the C/C_0 was only 5±2% and 3±1% for JM109 under the same conditions. Correspondingly, the k_d value of *E.coli* O157:H7 was less than JM109 under both conditions (Figure 13).When the ionic strength was increased from 10 mM to 100 mM, the deposition rate of *E.coli* O157:H7 decreased slightly from 0.025±0.003 to 0.018±0.002, while the deposition rate of JM109 increased from 0.170±0.001 to 0.226±0.003 when the ionic strength increased. The observed deposition behavior of JM109 is in accordance with the classical DLVO theory. When the electric double layer was compressed, the electrostatic repulsion force was reduced and the sum of the van der waals forces and electrostatic forces increase; however, *E.coli* O157:H7 showed an opposite trend towards ionic strength variation, which could not be explained by classical DLVO theory. Additional interaction forces such as acid-base interaction force or steric interaction force could play a role.

4.2.3 Computed XDLVO profiles of *E.coli* O157:H7 and *E.coli* JM109

The acid-base interaction which describes the polar media interfacial interactions is the dominant force at short separation distance [179, 180]. XDLVO theory

incorporating the acid-base interaction was able to successfully predict the bacterial deposition behavior in previous studies [66, 181]. As shown in Figure 14, the calculated XDLVO profiles were qualitatively in agreement with the observed deposition rates of bacteria in various chemical conditions. For instance, the interaction energy barrier of of *E.coli* O157:H7 at 100 mM (~51kT) was higher than at 10 mM IS (~1kT), which is consistent with the column results showing lower deposition rates of cells happens at 100 mM comparing to 10 mM PBS. Since the hydrophobicity of *E.coli* O157:H7 increased with higher ionic strength, it might have played a role in the reduced deposition rate of *E.coli* O157:H7 at higher ionic strength. For strain *E.coli* JM109, the computed energy barrier was much lower in 100 mM IS (~200kT) and the secondary minimum was deeper (~-23kT at 5nm) than in 10 mM solutions which had energy barrier of ~2400kT and the secondary minimum of ~5kT at 25nm. The high energy barrier of *E.coli* JM109 suggests that majority of cells deposit on the surface of the grains at the secondary energy minimum [133]. The column results of *E.coli* JM109 also agreed with the XDLVO profiles in that bacterial cells had higher deposition rates at 100mM IS condition. When comparing the energy profiles of the two strains, although generally *E.coli* O157:H7 had much lower energy barriers than *E.coli* JM109, the deposition rates of *E.coli* O157:H7 was significantly less than *E.coli* JM109(Figure 13). This contradictory finding might be due to the different deposition mechanisms of the two strains. While the deposition of *E.coli* JM109 was attributed to mainly retain at the secondary minimum, there might be another factor involving *E.coli* O157:H7 cells retention. *E.coli* O157:H7 was observed to possess long lipopolysaccharide(LPS) for around 30±13nm in length covering the cell surface[160], which might result in steric force [61] between cells and the grain surface

and render cells deposition at the secondary energy minimum. Thus the retention *E.coli* O157:H7 cells most likely happen when cells overcome the energy barrier. We also conducted LPS composition analysis for further validating the difference between the two strains(Figure 11).

4.2.4 Impact of Biofilms and Biofilm EPS

Figure 15 shows the bacterial breakthrough curves of *E.coli* O157:H7 and *E.coli* JM109 through columns with and without biofilms. In general, biofilm coating increased the deposition of the cells for both strains and the lowest deposition profiles were found under clean-column condition (no biofilm). Approximately 80-90 % of injected bacterial cells went through the clean column and were detected in the effluent. *P. aeruginosa* biofilms EPS composition, however, had a limited role in influencing *E.coli* O157:H7 cell deposition onto sand surface. The k_d for *E.coli* O157:H7 cells in PAO1 and PDO300 biofilm-coated columns were 0.044±0.005 and 0.040±0.006, respectively. Similarly to *E.coli* O157:H7, a higher number of *E.coli* JM109 cells were retained in the PAO1and PDO300 biofilm-coated columns compared with the clean-column condition. However, PDO300 biofilms had a minimum impact on the adhesion of JM109.

In Figure 16, the retained bacterial concentration was plotted as a function of their transport distance from the column inlet. For *E.coli* O157:H7, the deposition of the cells decreased with travel distance in clean columns and the bacterial deposition profile generally agrees with the CFT prediction. In the presence of PAO1 and PDO300 biofilms, the majority of the O157:H7 bacteria retained close to column inlet (distance of 0 nm); and the retention of the cells decreased along the path nonmonotonically. The cells retention reached to the lowest point when passing through about 4/5 of column,

after that, it had a noticeable increase at the tailing. For JM109, higher numbers of cells were also detected near the inlet of the columns; however, the retained bacterial profile was different from *E.coli* O157:H7. It decreased log-linearly with increasing transport distance for all three columns but the decreasing pace among the three columns was different. Under the clean-column condition, the retention profile decreased in good accordance with CFT prediction and had the lowest slope among the three conditions. In the PAO1 biofilm-coated column, the slope of log-linear profile deviate from and was steeper than CFT line, suggesting that majority of cell retention occurring at the column inlet. PDO300 biofilm coating had a milder impact on the deviation of JM109 cells retention through columns than PAO1 biofilm. Over all, the discrepancies of both strains retention profiles from CFT prediction were significant in biofilm coated columns and the deviations were in varied forms. Many other researchers have discovered bacterial or microsphere deviations from CFT in the forms such as hyperexponential decreases[182] or nonmonotonica variations[56, 57, 131] in deposition along travel distance, and factors such as straining, hydrodynamic drag or re-entrainment were hypothesized to play a role. In this study, *Pseudomonas aeruginosa* PAO1 and PDO300 biofilm matrix on the surface of the clean sands might have physiologically changed the hydrodynamic conditions within the columns and the composition difference in the EPS would also affect the passage of cells through pores.

4.3 Conclusions

E.coli O157:H7 is a pathogenic strain that has caused several waterborne outbreaks worldwide, and the transport and retention pattern of O157 in soil and groundwater is highly important in predicting their environment risk. The O157 strain has

a near neutral surface charge, which differs significantly from other *E.coli* strains. The column transport experiments performed in this study show that *E.coli* O157:H7 can travel underground for a longer distance than normal *E.coli* strains, indicating that *E.coli* strains may not be the best substitutes for monitoring O157's transport in groundwater.

The association of bacteria with biofilm coated on the porous media can substantially increase the attachment of cells in the subsurface environment. Under our experimental conditions, the pathogenic serotype *E.coli* O157:H7 exhibited different adhesion behavior than the laboratory strain *E.coli* JM109. Similar numbers of *E .coli* O157:H7 cells were retained in the PAO1 biofilm-coated columns and the PDO300 biofilm-coated columns; while higher numbers of *E.coli* JM109 cells were retained in the PAO1 biofilm columns than in the PDO300 columns. Additional research is needed to further explain the deviation of experimental results from CFT and XDLVO prediction and to better understand bacterial transport in soil and groundwater.

Table 3. Zeta potential and hydrophobicity of *E.coli* O157 and JM109 in 10mM and 100mM PBS

	Zeta Potential(mV)			Hydrophobicity (MATH,%)	
	O157	JM109	Sand	O157	JM109
10mM PBS	-1.9±0.6	-38.3±2.4	-70.3±1.1	56.9±3.0	41.0±1.0
100mM PBS	-7.5±1.5	-17.7±2.3	-37.0±2.2	71.3±1.3	40.0±5.0

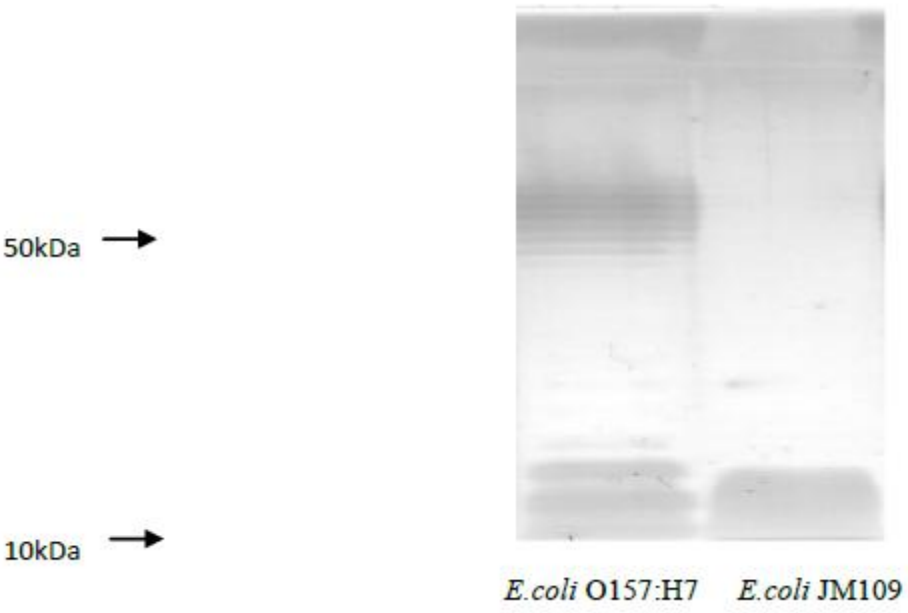

Figure 11. LPS analysis of *E.coli* O157:H7 and *E.coli* JM109. LPS samples from equal numbers of bacterial cells were loaded in the lanes, separated by Glycine-SDS-PAGE on a 14% acrylamide gel, and visualized by silver staining.

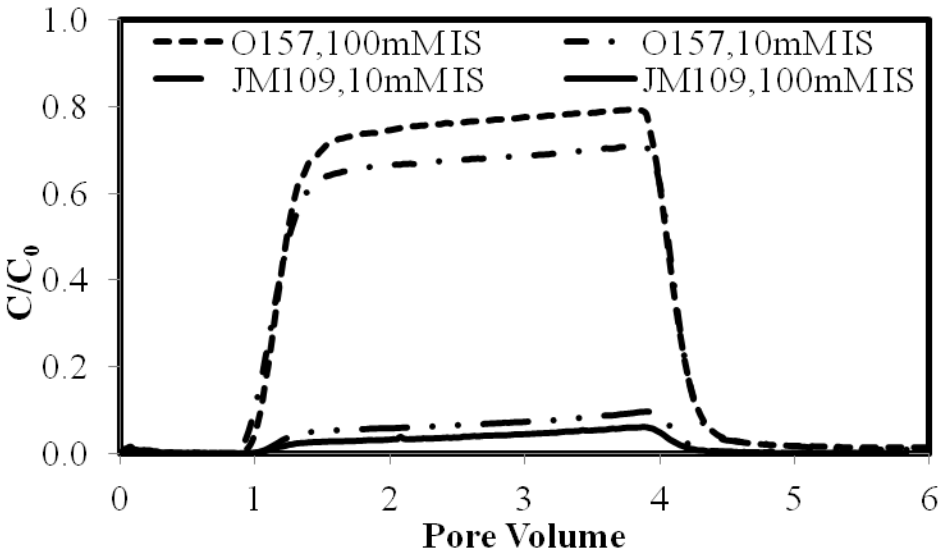

Figure 12. Breakthrough concentrations of *E.coli* O157:H7 and JM109 in saturated porous sands under ionic strength conditions of 10mM and 100mM PBS. pH=7.2. Error bars present standard deviation of duplicated experiments.

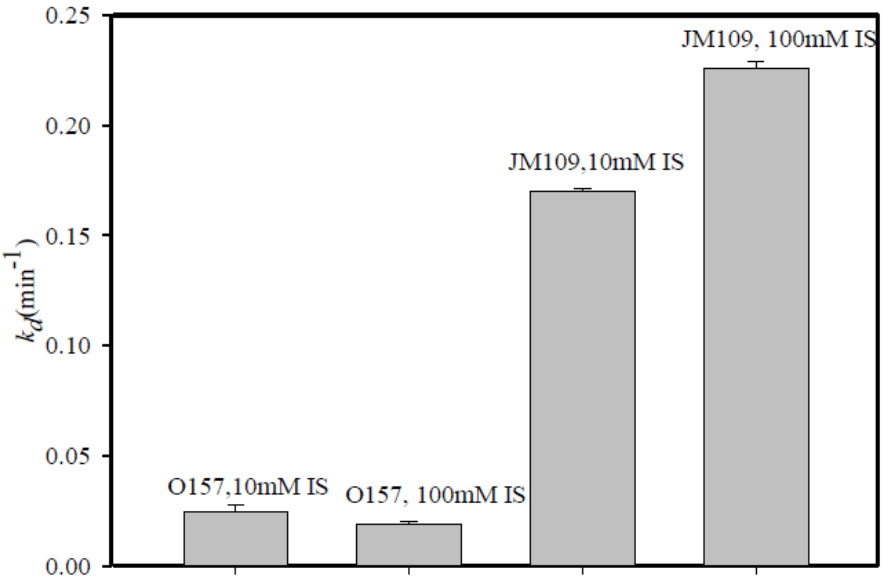

Figure 13. Deposition rate coefficients (k_d) for *E.coli* strains under ionic strength conditions of 10mM and 100mM PBS. The values of k_d were calculated using Eq.4.1. Error bars present standard deviation of duplicated experiments.

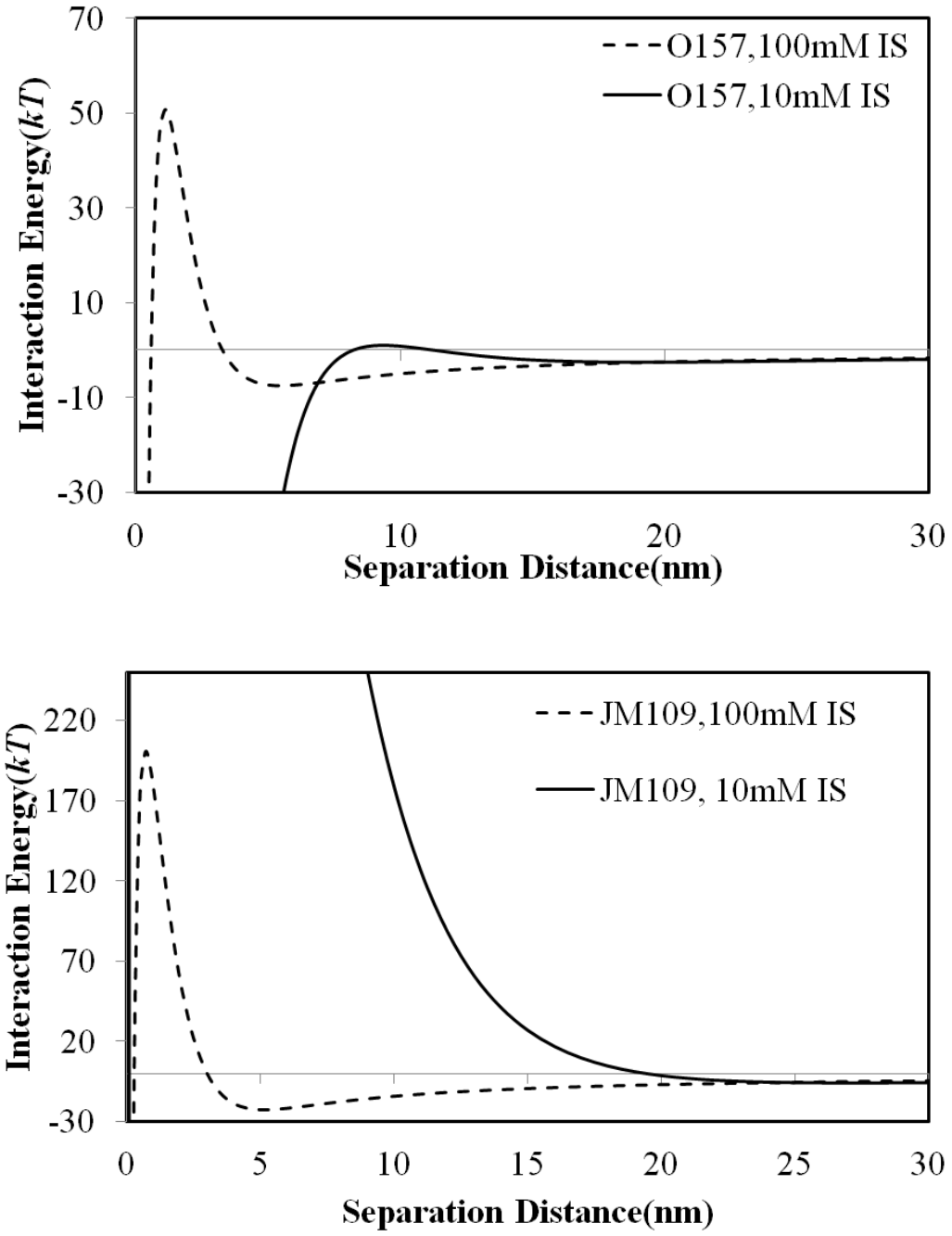

Figure 14. Computed XDLVO profiles of *E.coli* O157:H7 and JM109.

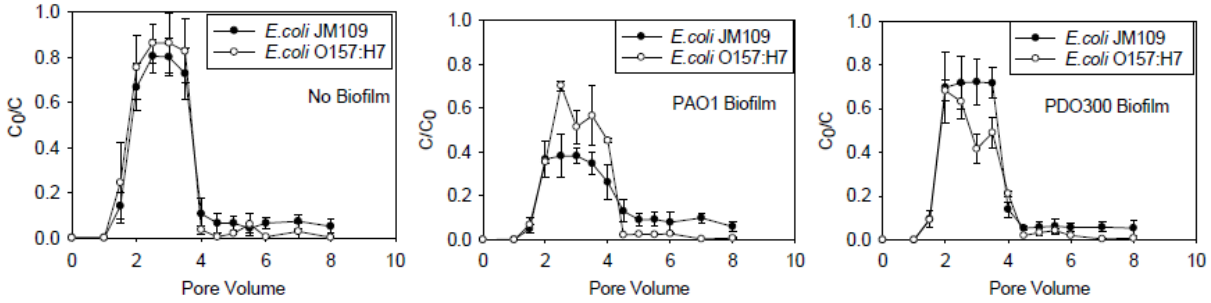

Figure 15. Breakthrough curves of *E.coli* O157:H7 and JM109 in clean, *P. aeruginosa* PAO1 biofilm-coated and PDO300 biofilm-coated columns.

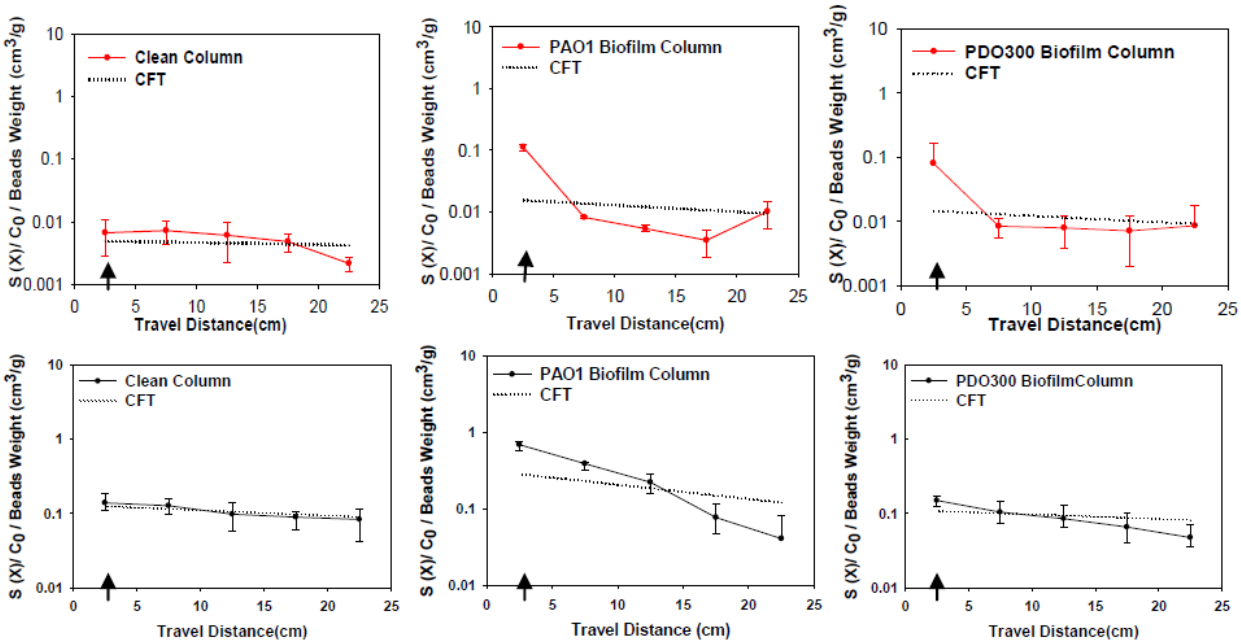

Figure 16. Measured retained bacteria concentration profiles of *E.coli* O157:H7 (top row), JM109 (bottom row), and the CFT predict (in dotted line) in clean bed, *P. aeruginosa* PAO1 biofilm-coated and PDO300 biofilm-coated columns. Arrowhead pointed to the inlet of bacteria solution.

Chapter 5 The role of LPS in protecting cells from antibacterial activity of graphene oxide to *E.coli* O157:H7

Graphene oxide(GO) is a modification of graphene monolayer. It has carboxylic groups at its edges and phenol hydroxyl and epoxide groups on its basal plane[183], which enables its water soluble capability and its hydrophicility characteristics besides excellent properties as graphene, such as high thermal stability, high mechanical strength, biocompatibility and often low cost[184]. They were believed to have great potentials in applications of health and environmental related aspects such as nanomedicine, nanosensors, nanoelectronics [185]. However, their impact on environment e.g. antibacterial activity, needs to be thoroughly evaluated[186]. Currently, researches about the antibacterial activity of GO to bacteria remain contradictory. For instance, Fan et. al.[184] found that almost 99% of the *E.coli* cells were destroyed after two hours in contact with a 85 μg/mL solution of GO at 37 °C. Oppositely, Bunker in Ohio, concluded that GO does not have any antimicrobial properties but instead encourages the proliferation of bacteria and mammalian cells on its surface [187]. The opposite results implied the complication of GO's antibacterial activities. Some researchers suggest the antibacterial effect of GO to bacterial cells were dependent on the surface properties of bacterial cells. For instance, Akhavan[188] deposited GO to stainless steel and found that this GO coated material damaged gram-positive bacteria significantly severer than gram-negative bacteria. These two types of bacteria are different in surface compositions in that gram-negative bacteria have outer membrane but gram-positive bacteria do not. This finding suggests that outer membrane might play an important role in protecting bacterial cells from antibacterial activities of GO.

LPS is a major characteristics component of bacterial outer membrane[189], it occupies 75% of the surface of the bacterium in the enterobacteriaceae [96]. It composes lipid A, core component and O-antigen[96] for smooth strains and the LPS lengths ranges from 17 ±10 to 37 ± 9 nm for strains with O-antigen[160]. *E.coli* O157:H7 has been studied extensively for its virulence and transport pattern because of its epidemic background around the world[190-192]. In this study, the antibacterial activities of GO sheets to *E.coli* O157:H7 wild type (WT) and its LPS truncated mutant(*ΔrfaC*) were tested and compared for evaluating the LPS's protection role.

5.1 Materials and Methods

Graphene oxide(GO) sheets were purchased from Cheaptubes Inc. (Brattleboro, VT). They were generally single-layered and lateral size between 300 to 800 nm according to manufacturer data [186]. Upon receiving, the particles were sonically dispersed in 0.9% NaCl (~154mM). The pH of the GO suspensions was ~6.0.

Bacterial cells solution was prepared as described in previously chapter. To conduct the test, 0.3 ml and 1.5 ml well mixed 500mg/L GO was introduced into tubes that contains 30ml of ~3×10^7cells/ml bacterial solution. The final concentration of GO sheets was 5mg/L and 25mg/L, respectively. The mixed samples were immediately placed onto an ambient shaker horizontally at 100 rpm/sec and started the contact time. The sample solution was collected at time of 0min, 30min, 60min,90min, 120min and 180min. Flow cytometry method was used to quantify the live cells concentration of the solution. Cell viability was determined using the Live/Dead BacLight Viability Kit (Invitrogen), which specifically assayed the integrity of cell membrane.

Briefly, 0.5ml of the mixed sample was stained using 1uL of the staining reagent and the mixture was incubated at room temperature for 15min. All (both live and dead) cells were stained by the SYTO9 component of the reagent and produced green fluorescence (optimal excitation/emission wavelengths: 480/500 nm), and dead cells, which possesses damaged bacterial membranes, can only be stained by propidium iodide and produced a red fluorescence (optimal excitation/emission wavelengths: 493/635 nm; Gant et al. 1993). Fluorescence data for the *E.coli* cells were acquired using a FACS flow cytometer (Becton Dickinson). The number of live and dead cells was then determined from the fluorescence readings. The cell viability was calculated as the ratio of live and total (live+ dead) cells.

5.2 Results

5.2.1 GO sheets antibacterial activities

The figure 17 shows the live cells ratio of *E.coli* O157:H7 WT and *ΔrfaC* strain over time. The antibacterial impact of GO sheets to these two strains was significantly different. The live cells ratio of WT strain incubated with 0mg/L GO, 5 mg/L GO and 25mg/L GO were remained at 80±4%, 83±6% and 72±6% after 3 hours of contact, respectively. As a comparison, the live cells ratio of *ΔrfaC* under the same test conditions were reduced to 76±3%, 15±4%, and 4±2%, respectively. In another words, majority of WT strain remained alive after 3 hours incubation while most bacterial cells of *ΔrfaC* strain lost their viability. Interestingly, the live cells ratio in control samples also decreased over time and the death rate of the two strains was comparable, which was 20% cell death rate for WT strain and 24% cell death rate for *ΔrfaC* strain in the first 3 hours. Considering the cell death rate in control samples, the viability loss of WT due to

GO sheets was 0 for 5mg/L GO concentration and 8% for 25mg/L GO concentration. In comparison, 68% of *ΔrfaC* strain lost their viability because of GO sheets at 5mg/GO and 80% at 25mg/L GO concentration.

The antibacterial activity of GO to the two strains was also time-dependent. The ratio of live cells of the two strains decreased approximately linearly with time. The slope of the simulated line indicated the decreasing rate of the live cells along time and it is dependent on the strain and GO sheets concentration. For WT strain, the slope is -0.002 for 5mg/L and -0.003 for 25mg/L. For *ΔrfaC* strain, the slope of the simulated line is -0.004 for 5mg/L. However, at 25mg/L GO concentration, the live cells ratio of *ΔrfaC* sharply decreased to 6.75% in the first 1 hour, which indicated most of the antibacterial activities happened within 1 hour under this condition, and then the live cells ratio slowly decreased to around 3% in the next 2 hours.

As we have found in Chapter 3 and also consistent with other researchers findings, the *ΔrfaC* strain , which LPS chain was truncated, had greater attachment efficiency to quartz sand comparing to WT [75] [193]. Qualitatively speaking, according to the finding in Chapter 3, despite the discourage of the increased cells surface negative charges as well as hydrophobicity [76] on *ΔrfaC* cells, they will still have higher attachment efficiency than WT to the negatively charged and hydrophilic GO sheets through the extended DLVO theory [183] because of the reduced steric force between the cells and the GO sheets. The correlationship of higher attachment efficiency and higher cells death rate of *ΔrfaC* strain suggested a pathway of GO inactivating bacterial cells, that is, when cells attaching to GO sheets, the GO sheets will cause the loss of cells viability through chemical effect such as cellular oxidative stress or blocking their active sites on

membranes. This hypothesis is in consistent with Liu's findings, who has observed that bacterial cells were wrapped by GO sheets and blocked bacterial proliferating [183, 188].

5.2.2 Adsorption kinetic study

A pseudo second order was used for studying the cells adsorption kinetic behaviour to GO[194]

$$\frac{t}{q_t} = \frac{1}{k_2 q_e^2} + \frac{1}{q_e} t \qquad (5.1)$$

where qe is the amount of bacteria sorbed after 3 hrs contact, k_2 is the rate constant of second order adsorption. This model is more likely to predict the behaviour over the whole range of adsorption.

The adsorption kinetics of *E.coli* on GO sheets can be interpreted well with pseudo second order kinetics equation with R^2 value around 1 (Figure 18). Consistently, the rate constant k_2 of WT was lower than *ΔrfaC* under both 5mg/L GO and 25mg/L GO conditions (Table 4), which indicated the slow adsorption rate of WT cells on GO sheets. However, *ΔrfaC* strain has lower q_e value than WT strain under the two conditions, which means less amount of adsorbed cells per ug GO sheets and contradictory to its high attachment efficiency. As far as we know, both "physical and chemical" factors were suggested contributing to the antibacterial activity of GO while discussing its antibacterial mechanisms. Besides of the chemical stress, membrane stress induced by intensive physical interactions between cells and sharp edges GO nanosheets was proposed, which will result in physical damages on cell membranes and release of intracellular contents, for instance, RNA[184, 188]. The smaller amount of adsorbed cells of *ΔrfaC* strain on the other hand verified the function of GO sheets membrane stress,

that is, GO sheets physically damage cell membranes and remain low level cells concentration for *ΔrfaC* strain.

5.3 Conclusion

LPS is an important component of cell surface in that it not only conveys cells metabolic activities and mediate cells deposition in porous media, but also plays a role in protecting cells from damaging from nanoparticles such as GO sheets. In this study, the antibacterial effect of GO sheets to *E.coli* O157:H7 wild type cells and LPS truncated mutant-*ΔrfaC* strain was compared. GO sheets had a minimal antibacterial effect to *E.coli* O157:H7 wild type cells but inactivated 80% of *ΔrfaC* cells under 25mg/L in 3 hours contacting. Both chemical stress and membrane stress were proposed for the GO sheets' inactivation mechanisms. The steric interaction incurred by the LPS component on wild type strains surface resulted less attachment efficiency of WT cells thus protect them from inactivation of GO sheets.

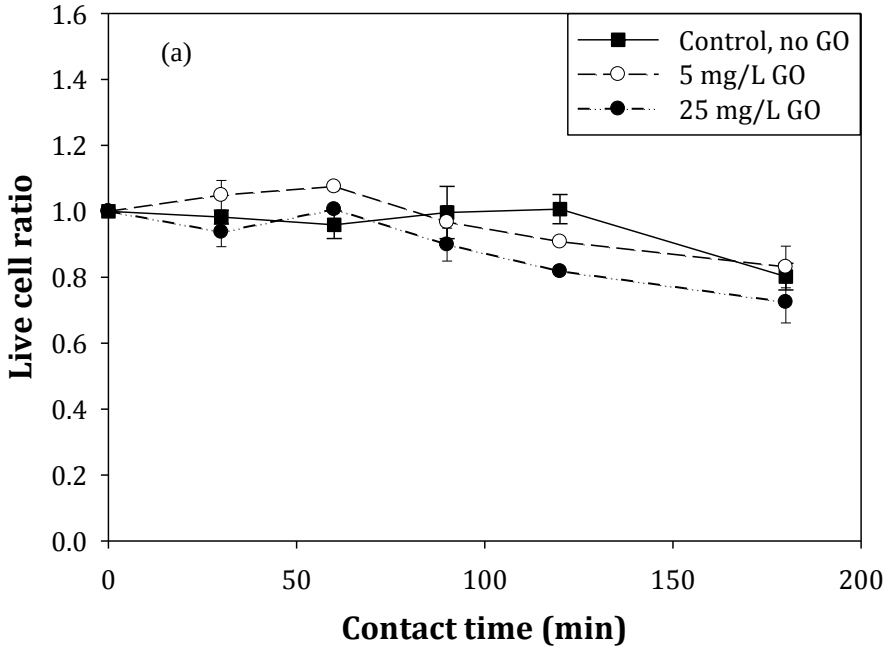

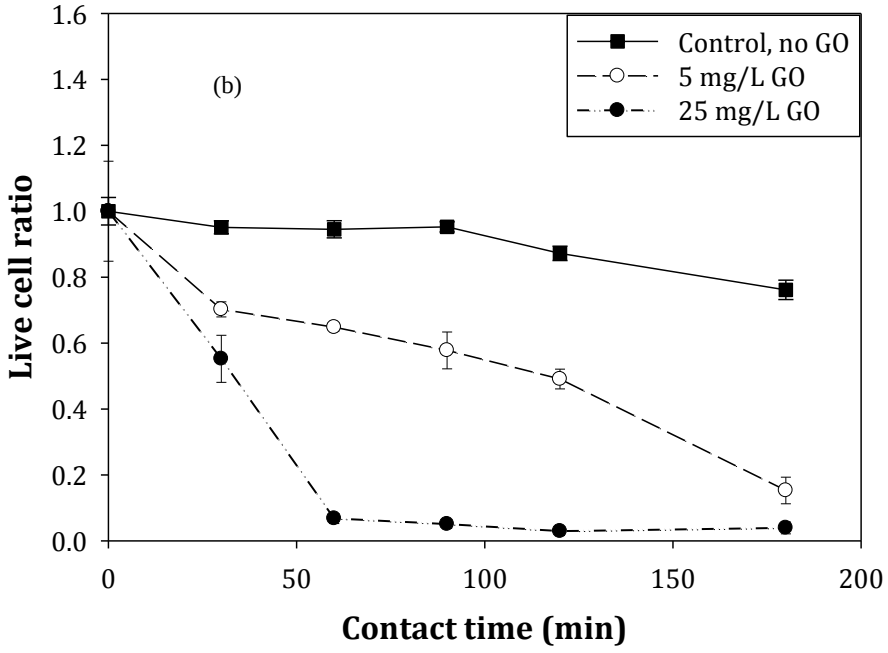

Figure 17. Live cells ratio over time after contacting with GO sheets (a) *E.coli* O157:H7 WT, (b) *E.coli* O157:H7 *ΔrfaC* strain

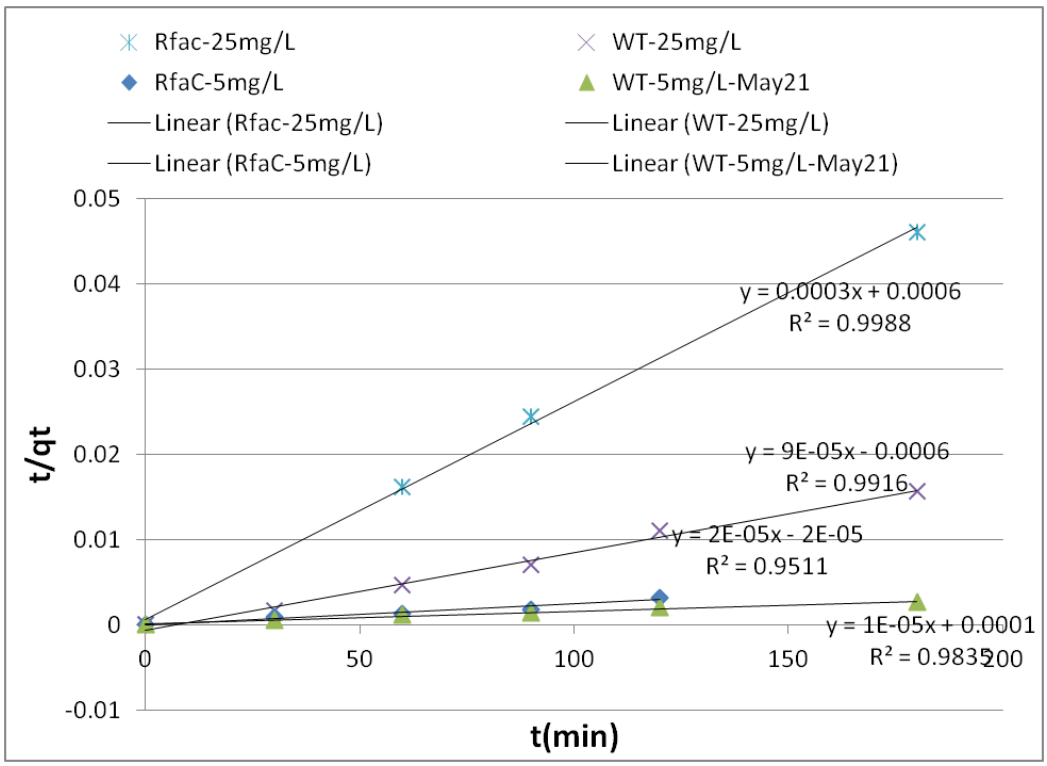

Figure 18. Pseudo second order kinetics for adsorption of *E.coli* cells by GO sheets

Table 4. Constants of pseudo second order kinetics for adsorption of *E.coli* to GO sheets

	q_e (cells/µg GO)	k_2(µg GO/cells/min)
WT-5mg/L GO	1.0E+05	1.0E-06
WT-25mg/L GO	1.1E+04	-1.4E-05
ΔrfaC-5mg/L GO	5.0E+04	-2.0E-05
ΔrfaC-25mg/L GO	3.3E+03	1.5E-04

Chapter 6 The role of surface charge in antibacterial effect of magnetic carbon nanotubes(MCNT) to *E.coli*

Carbon nanotubes (CNTs) have excellent chemical, mechanical and electronic properties and have gained increasing interest in their applications in biosciences such as drug delivery, cell growth, separation of blood cells etc[195]. The applications of CNTs in water purification has been proven to have great potentials and much research was done to maximize its applicability on contaminant removal from water [196-198]. Magnetic CNT (MCNT) or carbon nanoparticles is one of the most outstanding approaches and many researchers had explored the advantages of MCNTs on environmental applications. For instance, Ei-Boubbou et. al. [198] has functionalized silica-coated magnetite nanoparticles with D-mannose and found that it has many advantages on rapid pathogen detection, decontamination and strain differentiation based on various affinities among bacteria strains to the same carbohydrate. The capture efficiencies can reach up to 88% of *E.coli* ORN178 within 45min incubation. Similarly, Huang et. al. [197] used modified magnetic nanoparticles with adding amine functional groups and discovered its significant capture efficiency (97.4%) to bacteria cells. Shan et. al. [199] observed that carboxyl-modified magnetic nanoparticles could have 96.3% capture efficiency for *E.coli* JM109 at PH 3.8.

In this study, three functionalized CNTs were fabricated, which were MCNTs, O-MCNTs, and N-MCNTs, respectively. Briefly, MCNTS were made from commercialized CNTs decorated with magnetite on its outer surface. Then -OH group was added to the outer surface of MCNTs and this material was marked as O-MCNTs. Furthermore, the O-

MCNTs outer surface was chemically covered with -NH_2 functional groups and this material was labelled as N-MCNTs. Maximum bacterial capture efficiencies of the three materials and the effect of chemistry conditions such as ionic strength or bacterial initial concentration were studied. In addition to that, the mechanisms of these materials for removing bacteria from aqueous phase was discussed.

6.1 Materials and Methods

The fabrication process of MCNTs,O-MCNTs and N-MCNTs was demonstrated in Figure 19[200].

E.coli DH5α was used in this study as the test strain. It was originally stored at -80°C refrigerator. Upon using, a tipful of the stored culture was spread onto a LB agar plate, inoculated at 37°C overnight. Then a clear, round colony was picked and transferred into 10 ml LB broth tube and shaken at 200rpm and 37ºC for 18 hours. The overnight grown fresh culture was then centrifuged at 4000 rpm and 4°C for 10min for harvesting purpose. The supernatant was decanted and the cells were resuspended in the same background but bacteria free electrolyte. This centrifugation – decant procedure were repeated 3 times for completely removing growth medium.

The antibacterial test was a suspended type test. Firstly, *E.coli* bacterial concentration was adjusted to ~ 3×10^7 cells/ml with a spectrophotometer (Shimazu 1700)'s reading number of 0.300±0.003 at 220nm. The solution was further diluted 10-fold and 100-fold to the concentration of 3×10^6 and 3×10^5 cells/ml, respectively, for two bacterial initial concentrations. CNTs were then carefully added into tubes each containing 30 ml bacterial solution and mixed on a shaker at shaking speed of 200rpm. After a certain period of contact time (1,10,20,30,40,50 min), the solution tubes were then vertically

fixed on a static rack, and a magnetite was applied underneath for 1 minute. 100 µl supernatant was taken for bacterial enumeration with dropping plate method. Briefly, the 100ul supernatant were diluted accordingly to reach the final bacterial counts on the plate to the range of 30-300 colonies/per plate. 100µl of final solution was spread onto the agar plates and grew 16 hours in 37ºC incubator for colonies reading. Triplicate plates were streaked for every condition. The antibacterial test was conducted at room temperature.

6.2 Results and Conclusions

6.2.1. Bacterial maximum removal rate and equilibrium dosages of MCNTs

The maximum bacterial removal efficiency can reach to 95.9±0.5%, 81.7±1.8% and 94.0±1.2%, for N-MCNT, O-MCNT and MCNT at 10^6cells/ml initial concentration (Figure 20). The dosage for the three materials to get to the maximum bacterial removal rates are 27.5, 36.6 and 61.4 µg/10^5cells for N-MCNT, O-MCNT and MCNT, respectively. It takes only about 10 min to attain equilibrium status for the three materials(data not shown). The short equilibrium period suggests that all MCNTs have high adsorption rate to the bacteria removals.

6.2.2. Isotherm model

Theoretically, the curves fit Langmuir isotherm equation

$$q = \frac{q_m K_A C}{1+K_A C} \qquad (6.1)$$

where

$q =$ mass of species adsorbed/mass of adsorbent (i.e., equilibrium concentration of adsorbable species in solid adsorbent)

C = equilibrium concentration of adsorbable species in solution

q_m = maximum adsorbable value of q

K_A = constant(function of enthalpy of adsorption and temperature)

When the Langmuir isotherm was rearranged in the following form:

$$\frac{1}{q} = \frac{1}{q_m} + \left(\frac{1}{K_A q_m}\right)\frac{1}{C} \qquad (6.2)$$

and we plot the data with $1/q$ vs. $1/C$, then

$$slope = \frac{1}{K_A q_m}$$

$$intercept = \frac{1}{q_m}$$

Figure 21 showed that the data had a good linear relationship fitting to the rearranged Langmuir equation with R^2 of 0.98, 0.97 and 0.97 for N-MCNT and O-MCNT and MCNT, respectively. The values of q_m and K_A of the three materials at 5mM NaCl and conditions were listed in Table 5. For the maximum adsorbable value q_m, the sequence of the three materials are N-MCNT> O-MCNT >MCNT. However, O-MCNT material has the least value of the adsorption rate constant K_A, which is about half of the other two MCNTs and it indicates the slow adsorption rate of cells onto negatively charged nanomaterials.

6.2.3. Adsorption kinetic study

A pseudo second order was used for studying the cells adsorption kinetic behaviour to MCNTs [194]. The pseudo second order equation is based on the assumption that the rate limiting step may be chemical sorption involving valence forces through sharing or exchange of electrons between heavy metal ions and adsorbent.

$$\frac{t}{q_t} = \frac{1}{k_2 q_e^2} + \frac{1}{q_e} t \qquad (6.3)$$

where q_e is the amount of bacteria sorbed at equilibrium, k_2 is the equilibrium rate constant of second order adsorption. This model is more likely to predict the behaviour over the whole range of adsorption.

The adsorption kinetics of *E.coli* on the three materials can be interpreted well with pseudo second order kinetics equation with R^2 value of 1.00, 1.00 and 0.99 for N-MCNT and O-MCNT and MCNT, respectively (Figure 22). The amount of bacteria adsorbed at equilibrium q_e is the highest on N-MCNT among the three materials, which can explain the highest bacterial removal efficiency for N-MCNT material. For adsorption rate k_2, the negatively charged material O- MCNT has the least value of k_2, which implies the slow adsorption rate of cells onto its surface and this is also consistent with the least bacterial cells removal for O-MCNT among the three materials (Table 6).

6.2.4 The effect of ionic strength

N- MCNTs were used to test the effect of ionic strength to the antibacterial rate of MCNTs (Figure 23). The bacterial removal rates of N-MCNT was slightly higher at 154mM (0.9%) NaCl than 5mM NaCl. The q_m,which was calcualted through Langmuir adsorption equation, was also higher at 154mM NaCl (Table 5). Brady-Estevez [201] also found that the removal of virus was increased at higher ionic strength (NaCl) by SWNTs. The suppression of repulsive electrostatic interactions due to ionic strength might be responsible for the increased cells removal efficiency.

6.3 Conclusion

CNT is a prominent material on water treatment with its large surface area, excellent mechanical properties and low cost. The additional magnetic characteristics enabled it to be removed from water at high efficiency and in control. To make the materials more suitable for microbial removing, different functional groups were added to the materials surface and. In our study, N-MCNT material has the highest bacterial removal rate to more than 95% under 10^6 cells/ml initial bacterial concentration condition which is followed by MCNT and O-MCNT. The bacterial removal process fits to langmuir isotherm equation and can be expressed with pseudo second order kinetics equation for all the three materials. This study is an attempt to improve nanomaterials bacterial removal performance in drinking/wastewater water treatment application.

The highest bacterial removal efficiency for N-MCNT and least bacterial removal efficiency for O-MCNT implies the important role of surface charges in attaching, accumulating or removing bacteria from water. Bacteria *E.coli* DH5α was negatively charged on the surface, thus it tends to be adsorbed more onto positively charged surfaces comparing to the other two material surfaces. Similarly, Zardini [202] observed enhanced antibacterial activity to positively charged MWCNTs. Upon the antibacterial mechanism of the MCNTs, some researchers hypothesize that bacterial cell membrane was penetrated through contacting and the permeability across the membrane was increased, reducing metabolic activity were reduced, and thus killed the bacteria. Kim et. al. believed that electrostatic forces between cells and quartz sand instead of hydrophobic force dominated interaction mechanism[71]. Bolster also proposed that surface charge was the primary factor determining the extent of deposition of microorganisms [72]. In the effort of discovering the mechanism on how does the CNT materials antibacterial

effect work, our study suggests that the first step is for bacteria cells attaching to CNTs and surface functional group plays a significant role in determining bacterial attachment efficiency.

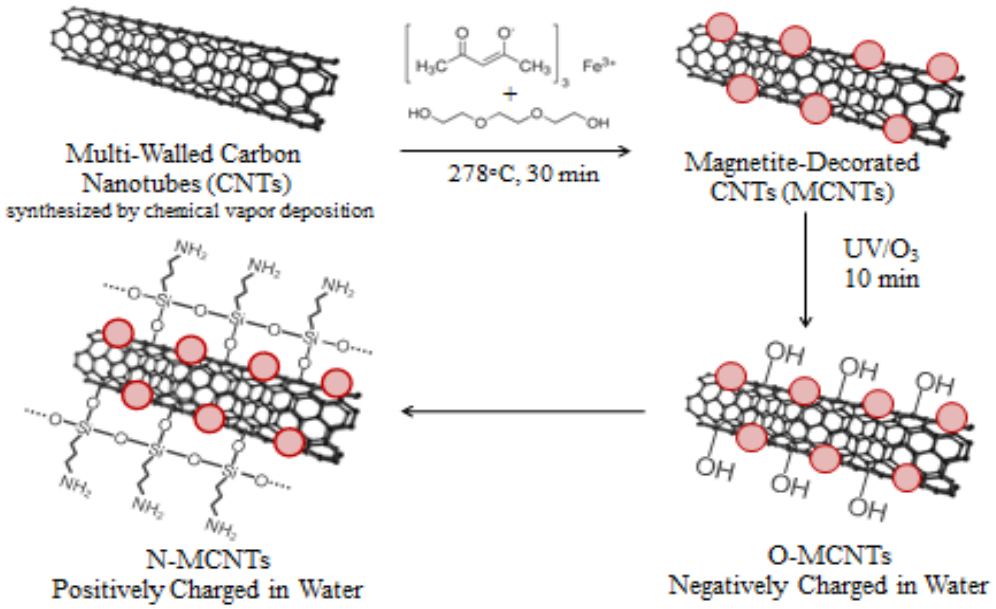

Figure 19. Fabrication of MCNTs, O-MCNTs and N-MCNTs

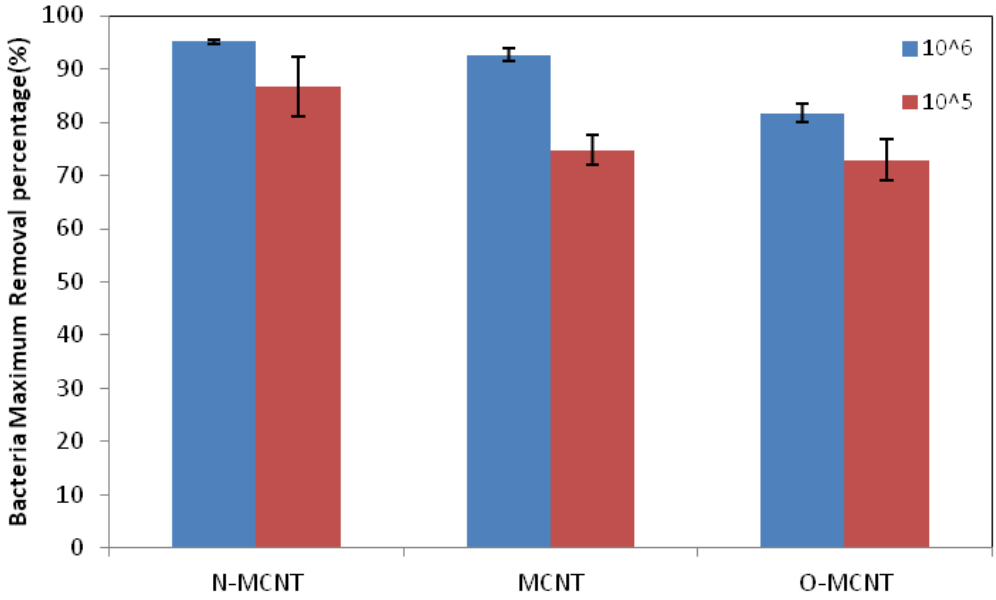

Figure 20. Maximum bacterial capture efficiencies of N-MCNT, MCNT and O-MCNT at two bacterial initial concentration levels(10^5 and 10^6 cells/ml)

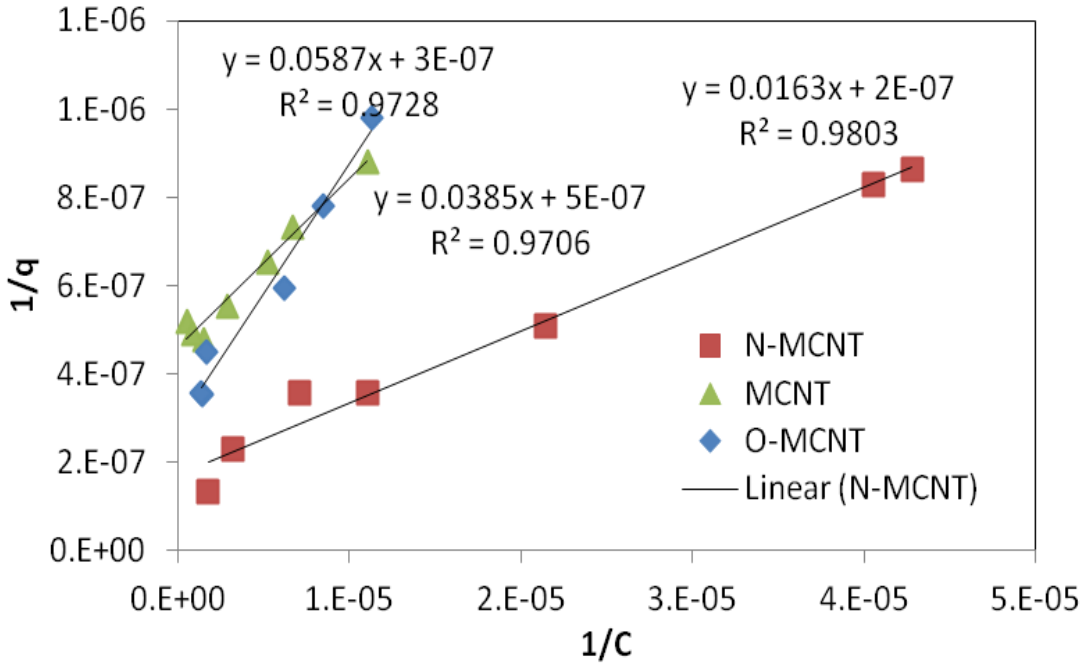

Figure 21. Langmuir isotherm plot for the adsorption of *E.coli* cells onto the three MCNTs Condition: 0.02g MCNTs in 30ml of 10^6 cells/ml bacteria solution at 250rpm for 10mins

Table 5. Constants of Langmuir isotherm models for adsorption of *E.coli* to the three MCNTs

	N-MCNT(5mM)	N-MCNT(154mM)	O-MCNT(5mM)	MCNT(5mM)
q_m	5.00E+06	1.00E+07	3.33E+06	2.00E+06
K_A	1.23E-05	4.78E-06	5.11E-06	1.30E-05
R^2	0.98	0.95	0.97	0.97

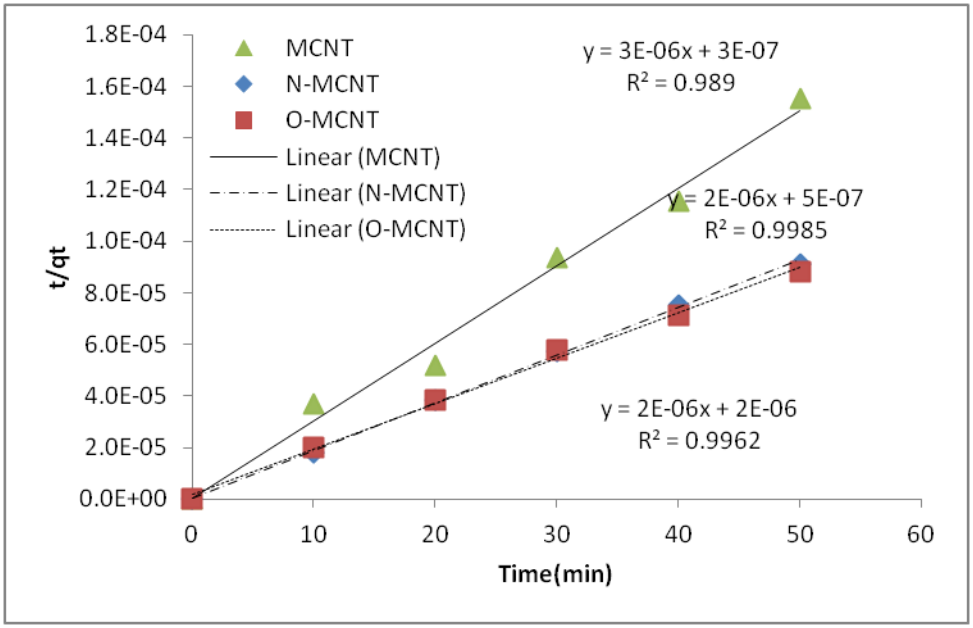

Figure 22. Pseudo second order kinetics for adsorption of *E.coli* cells by MCNTs

Table 6. Constants of pseudo second order kinetics for adsorption of *E.coli* to the three MCNTs

	q_e (cells/µg MCNTs)	k_2(µg MCNTs/cells/min)
N-MCNT	3.44E+05	8.44E-06
O-MCNT	3.33E+05	5.67E-06
MCNT	2.59E+05	1.15E-05

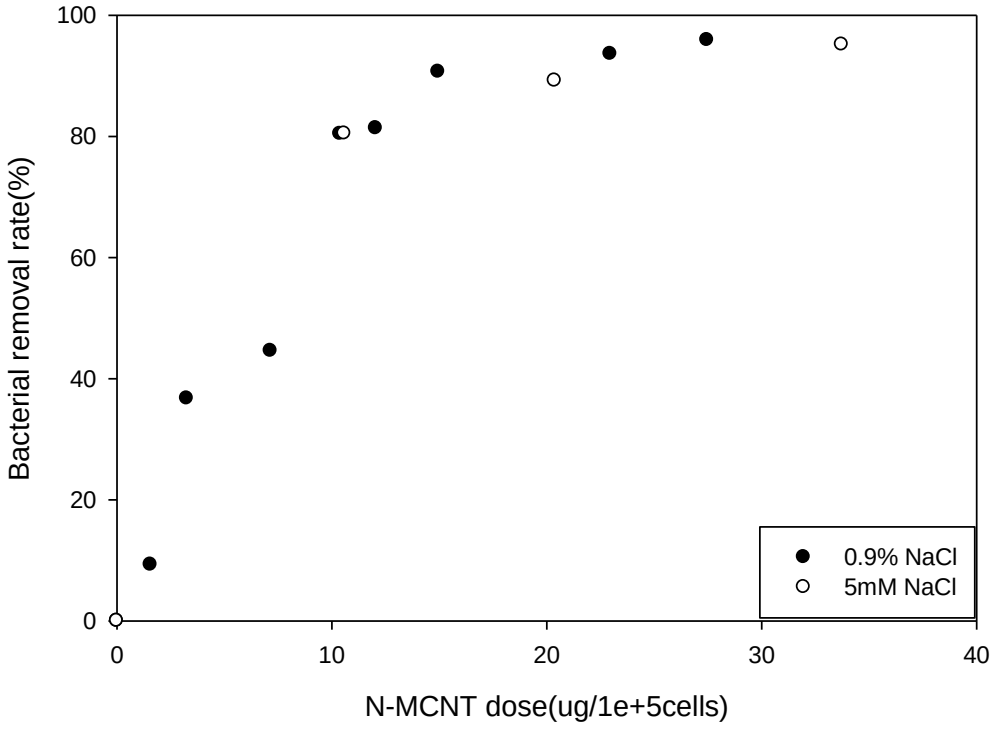

Figure 23. Bacterial removal rates of N-MCNT versus dosage at 154mM (0.9%) NaCl and 5mM NaCl

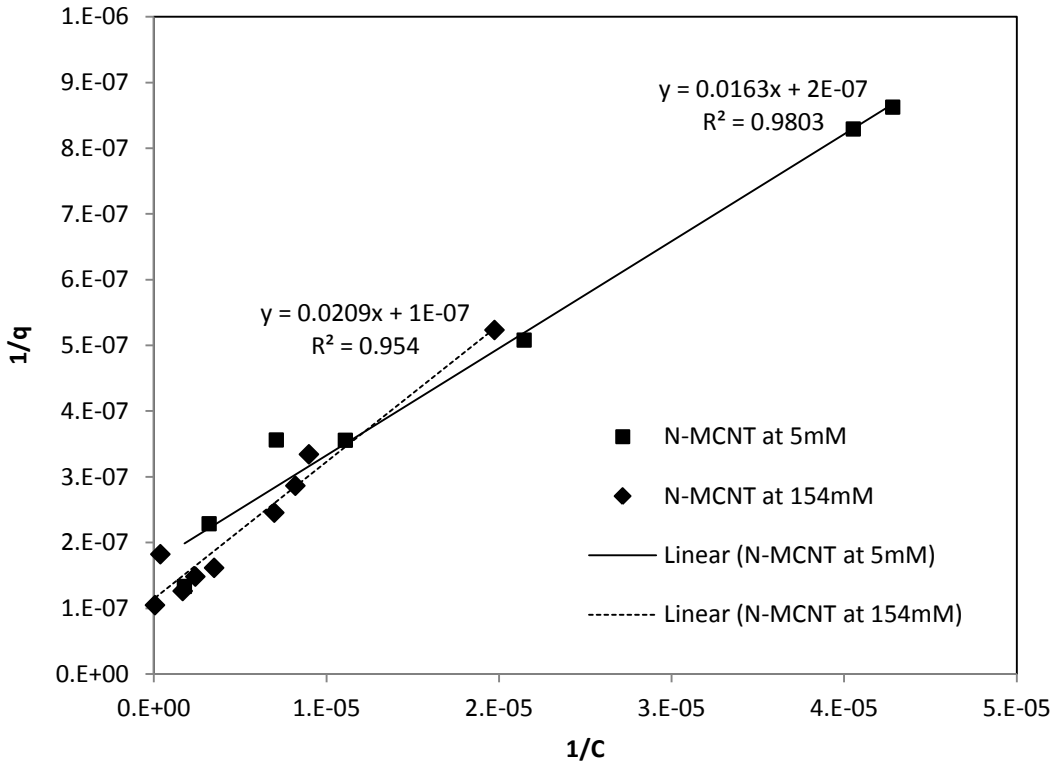

Figure 24. . Langmuir isotherm plot for the adsorption of *E.coli* cells onto N- MCNTs at 154mM (0.9%) NaCl and 5mM NaCl

References

1. Curtis, R. OA Guide to Water Purification.

2. Institute, W. R. A guide to world resources 2000-2001.

3. Interior, U. S. D. o. t.; Survey, U. S. G., Estimated Use of Water in the United States in 2005. **2005**.

4. Craun, G. F.; Brunkard, J. M.; Yoder, J. S.; Roberts, V. A.; Carpenter, J.; Wade, T.; Calderon, R. L.; Roberts, J. M.; Beach, M. J.; Roy, S. L., Causes of Outbreaks Associated with Drinking Water in the United States from 1971 to 2006. *Clinical Microbiology Reviews* **2010,** *23*, (3), 507-528.

5. Macler, B. A.; Merkle, J. C., Current knowledge on groundwater microbial pathogens and their control. *Hydrogeology Journal* **2000,** *8*, (1), 29-40.

6. Michael F. Craun, G. F. C., Rebecca L. Calderon and Michael J. Beach, Waterborne outbreaks reported in the United States. *J Water and Health* **2006,** *04*, 12.

7. Kuznar, Z. A.; Elimelech, M., Cryptosporidium oocyst surface macromolecules significantly hinder oocyst attachment. *Environmental Science & Technology* **2006,** *40*, (6), 1837-1842.

8. Tufenkji, N.; Schinner, T.; Letzner, A.; Liedtke, S.; Castro, F. D.; Eydelnant, I. A., Transport of selected bacterial pathogens in agricultural soil and quartz sand. *Water Research* **2010,** *44*, (4), 1182-1192.

9. Jin, Y.; Zhuang, J., Interactions between viruses and goethite during saturated flow: Effects of solution pH, carbonate, and phosphate. *Journal of Contaminant Hydrology* **2008,** *98*, (1-2), 15-21.

10. Yee, N.; Fein, J. B.; Daughney, C. J., Experimental study of the pH, ionic strength, and reversibility behavior of bacteria-mineral adsorption. *Geochimica Et Cosmochimica Acta* **2000,** *64*, (4), 609-617.

11. Li, J.; Liu, Y.; Yang, C. H., Adhesion and retention of a bacterial phytopathogen Erwinia chrysanthemi in biofilm-coated porous media. *Environmental Science & Technology* **2008,** *42*, (1), 159-165.

12. Prevention, C. f. D. C. a., Outbreak of *Escherichia coli* O157:H7 and Campylobacter among attendees of the Washington County Fair-New York, 1999. *MMWR Morb Mortal Wkly Rep* **1999,** *48*, (36), 3.

13. F J Angulo, S. T., D J Sharp, B J Payne, C Collier, J E Hill, T J Barrett, R M Clark, E E Geldreich, H D Donnell, Jr, and D L Swerdlow, A community waterborne outbreak of *salmonellosis* and the effectiveness of a boil water order. *Am J Public Healt* **1997,** *87*, (4), 5.

14. Yamazaki A, L. J., Hutchins WC, Wang L, Ma J, Ibekwe AM, Yang CH, Commensal Effect of Pectate Lyases Secreted from Dickeya dadantii on Proliferation of *Escherichia coli*

O157:H7 EDL933 on Lettuce Leaves. *APPLIED AND ENVIRONMENTAL MICROBIOLOGY* **2011,** *77*, (1), 156-162.

15. Muniesa, M.; Jofre, J.; Garcia-Aljaro, C.; Blanch, A. R., Occurrence of *Escherichia coli* O157 : H7 and other enterohemorrhagic *Escherichia coli* in the environment. *Environmental Science & Technology* **2006,** *40*, (23), 7141-7149.

16. Rangel, J. M.; Sparling, P. H.; Crowe, C.; Griffin, P. M.; Swerdlow, D. L., Epidemiology of *Escherichia coli* O157 : H7 outbreaks, United States, 1982-2002. *Emerging Infectious Diseases* **2005,** *11*, (4), 603-609.

17. Mead, P. S.; Slutsker, L.; Dietz, V.; McCaig, L. F.; Bresee, J. S.; Shapiro, C.; Griffin, P. M.; Tauxe, R. V., Food-related illness and death in the United States. *Emerging Infectious Diseases* **1999,** *5*, (5), 607-625.

18. Karch, H.; Tarr, P. I.; Blelaszewska, M., Enterohaemorrhagic *Escherichia coli* in human medicine. *International Journal of Medical Microbiology* **2005,** *295*, (6-7), 405-418.

19. CDC http://www.cdc.gov/nczved/divisions/dfbmd/diseases/ecoli_o157h7/

20. Swerdlow DL, W. B., Brady RC, Griffin PM, Tippen S, Donnell HD Jr, Geldreich E, Payne BJ, Meyer A Jr, Wells JG, A waterborne outbreak in Missouri of *Escherichia coli* O157:H7 associated with bloody diarrhea and death. *Ann Intern Med* **1992,** *117*, (10), 8.

21. Sonja J. Olsen, G. M., Thomas Breuer, Malinda Kennedy,Charles Higgins,; Jim Walford, G. M., Kim Fox, William Bibb, and Paul Mead, A Waterborne Outbreak of *Escherichia coli* O157:H7 Infections and Hemolytic Uremic Syndrome: Implications for Rural Water Systems. *Emerging Infectious Diseases* **2002,** *8*, (4), 6.

22. Richards, A., The Walkerton Health Study. *Can Nurse* **2005,** *101*, (5), 16-21.

23. Akashi S, J. K., Tsuji A, Ito H, Hoshi H, Hayakawa T, Ihara J, Abe T, Hatori M, Mori T,, A severe outbreak of haemorrhagic colitis and haemolytic uraemic syndrome associated with *Escherichia coli* O157:H7 in Japan. *Eur J Pediatr* **1994,** *153*, (9), 6.

24. Licence, K.; Oates, K. R.; Synge, B. A.; Reid, T. M. S., An outbreak of E-coli O157 infection with evidence of spread from animals to man through contamination of a private water supply. *Epidemiology and Infect* **2001,** *126*, (1), 135-138.

25. Isaäcson M, C. P., Effler P, Arntzen L, Bomans P, Heenan R., Haemorrhagic colitis epidemic in Africa. *Lancet* **1993,** *342*, (8850), 1.

26. Smith, J. E.; Perdek, J. M., Assessment and management of watershed microbial contaminants. *Critical Reviews in Environmental Science and Technology* **2004,** *34*, (2), 109-139.

27. Centers for Disease Control and Prevention, Outbreak of *Escherichia coli* O157:H7 and Campylobacter Among Attendees of the Washington County Fair - New York, 1999. *Morbidity and Mortality Weekly Report* **1999,** *43*, 803-805.

28. O'Connor, D. *Report of the Walkerton Inquiry*; 2002.

29. Caprioli, A.; Morabito, S.; Brugere, H.; Oswald, E., Enterohaemorrhagic *Escherichia coli*: emerging issues on virulence and modes of transmission. *Veterinary Research* **2005,** *36*, (3), 289-311.

30. Chase-Topping, M. E.; McKendrick, I. J.; Pearce, M. C.; MacDonald, P.; Matthews, L.; Halliday, J.; Allison, L.; Fenlon, D.; Low, J. C.; Gunn, G.; Woolhouse, M. E. J., Risk factors for the presence of high-level shedders of *Escherichia coli* O157 on Scottish farms. *Journal of Clinical Microbiology* **2007,** *45*, (5), 1594-1603.

31. Valcour, J. E.; Michel, P.; McEwen, S. A.; Wilson, J. B., Associations between indicators of livestock farming intensity and incidence of human Shiga toxin-producing *Escherichia coli* infection. *Emerging Infectious Diseases* **2002,** *8*, (3), 252-257.

32. Himathongkham, S.; Bahari, S.; Riemann, H.; Cliver, D., Survival of *Escherichia coli* O157 : H7 and Salmonella typhimurium in cow manure and cow manure slurry. *Fems Microbiology Letters* **1999,** *178*, (2), 251-257.

33. Zhao, T.; Doyle, M. P.; Shere, J.; Garber, L., Prevalence of Enterohemorrhagic Escherichia-Coli O157-H7 in a Survey of Dairy Herds. *Applied and Environmental Microbiology* **1995,** *61*, (4), 1290-1293.

34. Cho, S.; Bender, J. B.; Diez-Gonzalez, F.; Fossler, C. P.; Hedberg, C. W.; Kaneene, J. B.; Ruegg, P. L.; Warnick, L. D.; Wells, S. J., Prevalence and characterization of *Escherichia coli* O157 isolates from Minnesota dairy farms and county fairs. *Journal of Food Protection* **2006,** *69*, (2), 252-259.

35. Faith, N. G.; Shere, J. A.; Brosch, R.; Arnold, K. W.; Ansay, S. E.; Lee, M. S.; Luchansky, J. B.; Kaspar, C. W., Prevalence and clonal nature of *Escherichia coli* O157:H7 on dairy farms in Wisconsin. *Applied and Environmental Microbiology* **1996,** *62*, (5), 1519-1525.

36. Ezawa, A.; Gocho, F.; Kawata, K.; Takahashi, T.; Kikuchi, N., High prevalence of enterohemorrhagic *Escherichia coli* (EHEC) O157 from cattle in selected regions of Japan. *Journal of Veterinary Medical Science* **2004,** *66*, (5), 585-587.

37. Hancock, D. D.; Besser, T. E.; Rice, D. H.; Ebel, E. D.; Herriott, D. E.; Carpenter, L. V., Multiple sources of *Escherichia coli* O157 in feedlots and dairy farms in the northwestern USA. *Preventive Veterinary Medicine* **1998,** *35*, (1), 11-19.

38. Kudva, I. T.; Blanch, K.; Hovde, C. J., Analysis of *Escherichia coli* O157 : H7 survival in ovine or bovine manure and manure slurry. *Applied and Environmental Microbiology* **1998,** *64*, (9), 3166-3174.

39. Lung, A. J.; Lin, C. M.; Kim, J. M.; Marshall, M. R.; Nordstedt, R.; Thompson, N. P.; Wei, C. I., Destruction of *Escherichia coli* O157 : H7 and Salmonella Enteritidis in cow manure composting. *Journal of Food Protection* **2001,** *64*, (9), 1309-1314.

40. Wang, G. D.; Zhao, T.; Doyle, M. P., Fate of enterohemorrhagic *Escherichia coli* O157:H7 in bovine feces. *Applied and Environmental Microbiology* **1996,** *62*, (7), 2567-2570.

41. Gagliardi, J. V.; Karns, J. S., Leaching of *Escherichia coli* O157 : H7 in diverse soils under various agricultural management practices (vol 66, pg 877, 2000). *Applied and Environmental Microbiology* **2000,** *66*, (9), 4172-4172.

42. Elimelech, M., Particle Deposition on Ideal Collectors from Dilute Flowing Suspensions - Mathematical Formulation, Numerical-Solution, and Simulations. *Separations Technology* **1994,** *4*, (4), 186-212.

43. Saiers, J. E.; Xu, S. P.; Liao, Q., Straining of nonspherical colloids in saturated porous media. *Environmental Science & Technology* **2008,** *42*, (3), 771-778.

44. Foppen, J. W.; Van Herwerden, M.; Schijven, J., Measuring and modelling straining of *Escherichia coli* in saturated porous media. *Journal of Contaminant Hydrology* **2007,** *93*, (1-4), 236-254.

45. Scott A. Bradford, S. R. Y., Mehdi Bettahar, Jirka Simunek, Physical factors affecting the transport and fate of colloids in saturated porous media. *Water Resources Research* **2002,** *38*, (12), 1327.

46. Torkzaban, S.; Tazehkand, S. S.; Walker, S. L.; Bradford, S. A., Transport and fate of bacteria in porous media: Coupled effects of chemical conditions and pore space geometry. *Water Resources Research* **2008,** *44*, (4).

47. Vadillo-Rodriguez, V.; Logan, B. E., Localized attraction correlates with bacterial adhesion to glass and metal oxide substrata. *Environmental Science & Technology* **2006,** *40*, (9), 2983-2988.

48. Hoek, E. M. V.; Huang, X. F.; Bhattacharjee, S., Is Surface Roughness a "Scapegoat" or a Primary Factor When Defining Particle-Substrate Interactions? *Langmuir* **2010,** *26*, (4), 2528-2537.

49. Logan, B. E.; Shellenberger, K., Effect of molecular scale roughness of glass beads on colloidal and bacterial deposition. *Environmental Science & Technology* **2002,** *36*, (2), 184-189.

50. Tufenkji, N.; Castro, F. D., Relevance of nontoxigenic strains as surrogates for *Escherichia coli* O157 : H7 in groundwater contamination potential: Role of temperature and cell acclimation time. *Environmental Science & Technology* **2007,** *41*, (12), 4332-4338.

51. Walker, S. L.; Kim, H. N., *Escherichia coli* transport in porous media: Influence of cell strain, solution chemistry, and temperature. *Colloids and Surfaces B-Biointerfaces* **2009,** *71*, (1), 160-167.

52. Guber, A. K.; Shelton, D. R.; Pachepsky, Y. A., Transport and retention of manure-borne coliforms in soil. *Vadose Zone Journal* **2005,** *4*, (3), 828-837.

53. Camesano, T. A.; Logan, B. E., Influence of fluid velocity and cell concentration on the transport of motile and nonmotile bacteria in porous media. *Environmental Science & Technology* **1998,** *32*, (11), 1699-1708.

54. Haznedaroglu, B. Z.; Bolster, C. H.; Walker, S. L., The role of starvation on *Escherichia coli* adhesion and transport in saturated porous media. *Water Research* **2008,** *42*, (6-7), 1547-1554.

55. Li, J.; Liu, Y.; Yang, C. H., Influence of extracellular polymeric substances on Pseudomonas aeruginosa transport and deposition profiles in porous media. *Environmental Science & Technology* **2007,** *41*, (1), 198-205.

56. Xiqing Li, P. Z., C.L. Lin, William P. Johnson, Role of hydrodynamic drag on microsphere deposition and re-entrainment in porous media under unfavorable conditions. *Environ. Sci. Technol.* **2005,** *39*, (11), 4012-4020.

57. Tong, M. P.; Li, X. Q.; Brow, C. N.; Johnson, W. P., Detachment-influenced transport of an adhesion-deficient bacterial strain within water-reactive porous media. *Environmental Science & Technology* **2005,** *39*, (8), 2500-2508.

58. Jewett, D. G.; Hilbert, T. A.; Logan, B. E.; Arnold, R. G.; Bales, R. C., Bacterial Transport in Laboratory Columns and Filters - Influence of Tonic Strength and Ph on Collision Efficiency. *Water Research* **1995,** *29*, (7), 1673-1680.

59. Gannon, J. T.; Manilal, V. B.; Alexander, M., Relationship between Cell-Surface Properties and Transport of Bacteria through Soil. *Applied and Environmental Microbiology* **1991,** *57*, (1), 190-193.

60. Harms, H.; Simoni, S. F.; Bosma, T. N. P.; Zehnder, A. J. B., Bivalent cations increase both the subpopulation of adhering bacteria and their adhesion efficiency in sand columns. *Environmental Science & Technology* **2000,** *34*, (6), 1011-1017.

61. Kim, H. N.; Bradford, S. A.; Walker, S. L., *Escherichia coli* O157:H7 Transport in Saturated Porous Media: Role of Solution Chemistry and Surface Macromolecules. *Environmental Science & Technology* **2009,** *43*, (12), 4340-4347.

62. Foppen, J. W.; Lutterodt, G.; Roling, W. F. M.; Uhlenbrook, S., Towards understanding inter-strain attachment variations of *Escherichia coli* during transport in saturated quartz sand. *Water Research* **2010,** *44*, (4), 1202-1212.

63. Park, S. J.; Kim, S. B., Adhesion of *Escherichia coli* to Iron-Coated Sand in the Presence of Humic Acid: A Column Experiment. *Water Environment Research* **2009,** *81*, (2), 125-130.

64. Foppen, J. W.; Liem, Y.; Schijven, J., Effect of humic acid on the attachment of *Escherichia coli* in columns of goethite-coated sand. *Water Research* **2008,** *42*, (1-2), 211-219.

65. Bolster, C. H.; Haznedaroglu, B. Z.; Walker, S. L., Diversity in Cell Properties and Transport Behavior among 12 Different Environmental *Escherichia coli* Isolates. *Journal of Environmental Quality* **2009,** *38*, (2), 465-472.

66. Morrow, J. B.; Stratton, R.; Yang, H. H.; Smets, B. F.; Grasso, D., Macro- and nanoscale observations of adhesive behavior for several E-coli strains (O157 : H7 and environmental isolates) on mineral surfaces. *Environmental Science & Technology* **2005,** *39*, (17), 6395-6404.

67. Baikun Li, B. E. L., Bacterial adhesion to glass and metal-oxide surfaces. *Colloids and Surfaces B: Biointerfaces* **2004,** *36*, 81-90.

68. Dickson, J. S.; Koohmaraie, M., Cell-Surface Charge Characteristics and Their Relationship to Bacterial Attachment to Meat Surfaces. *Applied and Environmental Microbiology* **1989,** *55*, (4), 832-836.

69. Vanloosdrecht, M. C. M.; Lyklema, J.; Norde, W.; Schraa, G.; Zehnder, A. J. B., Electrophoretic Mobility and Hydrophobicity as a Measure to Predict the Initial Steps of Bacterial Adhesion. *Applied and Environmental Microbiology* **1987,** *53*, (8), 1898-1901.

70. Vanoss, C. J., Acid-Base Interfacial Interactions in Aqueous-Media. *Colloids and Surfaces a-Physicochemical and Engineering Aspects* **1993,** *78*, 1-49.

71. Kim, S. B.; Park, S. J., Influence of (bi)carbonate on bacterial interaction with quartz and metal oxide-coated surfaces. *Colloids and Surfaces B-Biointerfaces* **2010,** *76*, (1), 57-62.

72. Bolster, C. H.; Walker, S. L.; Cook, K. L., Comparison of *Escherichia coli* and Campylobacter jejuni transport in saturated porous media. *Journal of Environmental Quality* **2006,** *35*, (4), 1018-1025.

73. Camper, A. K.; Hayes, J. T.; Sturman, P. J.; Jones, W. L.; Cunningham, A. B., Effects of Motility and Adsorption Rate Coefficient on Transport of Bacteria through Saturated Porous-Media. *Applied and Environmental Microbiology* **1993,** *59*, (10), 3455-3462.

74. Valerie Williams, M. F., *Pseudomonas fluorescens* Adhesion and Transport through Porous Media Are Affected by Lipopolysaccharide Composition. *Applied and Environmental Microbiology* **1996**, 100-104.

75. Logan, B. E.; Burks, G. A.; Velegol, S. B.; Paramonova, E.; Lindenmuth, B. E.; Feick, J. D., Macroscopic and nanoscale measurements of the adhesion of bacteria with varying outer layer surface composition. *Langmuir* **2003,** *19*, (6), 2366-2371.

76. Harms, H.; Jucker, B. A.; Zehnder, A. J. B., Quantification of polymer interactions in bacterial adhesion. *Environmental Science & Technology* **1998,** *32*, (19), 2909-2915.

77. Lower, S. K., Directed natural forces of affinity between a bacterium and mineral. *American Journal of Science* **2005,** *305*, (6-8), 752-765.

78. Bradford, S. A.; Kim, H. N.; Walker, S. L., Macromolecule mediated transport and retention of *Escherichia coli* O157:H7 in saturated porous media. *Water Research* **2010,** *44*, (4), 1082-1093.

79. Hyunjung N. Kim, Y. H., IIkeun Lee, Scott A. Bradford and Sharon, L , Walker, Surface Characteristics and Adhesion Behavior of *Escherichia coli* O157:H7: Role of Extracellular Macromolecules. *Biomacromolecules* **2009,** *10*, 2556-2564.

80. Tsuneda, S.; Aikawa, H.; Hayashi, H.; Yuasa, A.; Hirata, A., Extracellular polymeric substances responsible for bacterial adhesion onto solid surface. *Fems Microbiology Letters* **2003,** *223*, (2), 287-292.

81. Biggs, C. A.; Eboigbodin, K. E., Characterization of the extracellular polymeric substances produced by *Escherichia coli* using infrared spectroscopic, proteomic, and aggregation studies. *Biomacromolecules* **2008,** *9*, (2), 686-695.

82. Matthysse, A. G.; Deora, R.; Mishra, M.; Torres, A. G., Polysaccharides cellulose, poly-beta-1,6-N-acetyl-D-glucosamine, and colanic acid are required for optimal binding of *Escherichia coli* O157 : H7 strains to alfalfa sprouts and K-12 strains to plastic but not for binding to epithelial cells. *Applied and Environmental Microbiology* **2008,** *74*, (8), 2384-2390.

83. Geoghegan, M.; Andrews, J. S.; Biggs, C. A.; Eboigbodin, K. E.; Elliott, D. R.; Rolfe, S.; Scholes, J.; Ojeda, J. J.; Romero-Gonzalez, M. E.; Edyvean, R. G. J.; Swanson, L.; Rutkaite, R.; Fernando, R.; Pen, Y.; Zhang, Z. Y.; Banwart, S. A., The polymer physics and chemistry of microbial cell attachment and adhesion. *Faraday Discussions* **2008,** *139*, 85-103.

84. Tong, M. P.; Long, G. Y.; Zhu, P. T.; Shen, Y., Influence of Extracellular Polymeric Substances (EPS) on Deposition Kinetics of Bacteria. *Environmental Science & Technology* **2009,** *43*, (7), 2308-2314.

85. Gomez-Suarez, C.; Pasma, J.; van der Borden, A. J.; Wingender, J.; Flemming, H. C.; Busscher, H. J.; van der Mei, H. C., Influence of extracellular polymeric substances on deposition and redeposition of Pseudomonas aeruginosa to surfaces. *Microbiology-Sgm* **2002,** *148*, 1161-1169.

86. Elimelech, M.; Walker, S. L.; Redman, J. A., Role of cell surface lipopolysaccharides in *Escherichia coli* K12 adhesion and transport. *Langmuir* **2004,** *20*, (18), 7736-7746.

87. Giron, J. A.; Rendon, M. A.; Saldana, Z.; Erdem, A. L.; Monteiro-Neto, V.; Vazquez, A.; Kaper, J. B.; Puente, J. L., Commensal and pathogenic *Escherichia coli* use a common pilus adherence factor for epithelial cell colonization. *Proceedings of the National Academy of Sciences of the United States of America* **2007,** *104*, (25), 10637-10642.

88. Chen, J.; Pawar, D. M.; Rossman, M. L., Role of curli fimbriae in mediating the cells of enterohaemorrhagic *Escherichia coli* to attach to abiotic surfaces. *Journal of Applied Microbiology* **2005,** *99*, (2), 418-425.

89. McClaine, J. W.; Ford, R. M., Characterizing the adhesion of motile and nonmotile *Escherichia coli* to a glass surface using a parallel-plate flow chamber. *Biotechnology and Bioengineering* **2002,** *78*, (2), 179-189.

90. Smets., H.-h. Y. B. F., Antecedent Growth Conditions Alter Retention of Environmental *Escherichia coli* Isolates in Transiently Wetted Porous Media. *Environ. Sci. Technol.* **2008,** *42*, 7.

91. Tufenkji, N., Role of Oxygen Tension on the Transport and Retention of Two Pathogenic Bacteria in Saturated Porous Media. *Environ. Sci. Technol.* **2008,** *42*, 6.

92. Ryu, J.-H., Larry R. Beuchat, Biofilm Formation by *Escherichia coli* O157:H7 on Stainless Steel: Effect of Exopolysaccharide and Curli Production on Its Resistance to Chlorine. *AEM* **2005**, 8.

93. Michael B. Salerno, S. R., Chisomaga Nwachukwu, Haithem Shelbi, Darrell Velegol, Bruce E. Logan, Differences between Chemisorbed and Physisobed Biomolecules on Particles Deposition to Hydrophobic Surfaces. *Environ. Sci. Technol.* **2005,** *39*, (17), 7.

94. Kotra, L. P.; Golemi, D.; Amro, N. A.; Liu, G. Y.; Mobashery, S., Dynamics of the lipopolysaccharide assembly on the surface of *Escherichia coli*. *Journal of the American Chemical Society* **1999,** *121*, (38), 8707-8711.

95. Abu-Lail, N. I.; Camesano, T. A., Role of lipopolysaccharides in the adhesion, retention, and transport of *Escherichia coli* JM109. *Environmental Science & Technology* **2003,** *37*, (10), 2173-2183.

96. Caroff, M., Karibian, D.,, Structure of bacterial lipopolysaccharides. *Carbohydr. Res.* **2003,** *41*, 13.

97. Sharon L. Walker, J. A. R., and Menachem Elimelech, Role of Cell Surface Lipopolysaccharides in *Escherichia coli* K12 Adhesion and Transport. *Langmuir* **2004,** *20*, 7736-7746.

98. Ong, Y. L.; Razatos, A.; Georgiou, G.; Sharma, M. M., Adhesion forces between E-coli bacteria and biomaterial surfaces. *Langmuir* **1999,** *15*, (8), 2719-2725.

99. D.E. Fontes, A. L. M., G.M.Hornberger, J.S. Herman, Physical and chemical factors influencing transport of microorganisms through porous media. *Applied and Environmental Microbiology* **1991,** *57*, (9), 9.

100. Hailiang Dong, T. C. O., Mary F. Deflaun, Mark E.Fuller, Timothy D. Streger, Randi K. Rothmel, Brian J. Mailoux, Relative dominance of physical versus chemcial effects on the transport of adhesion-deficient bacteria in intact cores from South Oyster, Virginia. *Environ. Sci. Technol.* **2002,** *36*, (5), 10.

101. Ruben Kretzschmar, M. B., Daniel Grolimund, and Menachem Elimelech, Mobile subsurface colloids and their role in contaminant transport. *Advances in Agronomy* **1999,** *66*, 73.

102. Gang Chen, H. Z., Bacterial deposition in porous medium as impacted by solution chemistry. *Research in Microbiology* **2004,** *155*, 8.

103. Tufenkji, N.; Elimelech, M., Correlation equation for predicting single-collector efficiency in physicochemical filtration in saturated porous media. *Environmental Science & Technology* **2004,** *38*, (2), 529-536.

104. Hermansson, M., The DLVO theory in microbial adhesion. *Colloids and Surfaces B-Biointerfaces* **1999,** *14*, (1-4), 105-119.

105. Hermansson, M., The DLVO theory in microbial adhesion. *Colloids and Surfaces B: Biointerfaces* **1999,** *14*, 105-119.

106. Yao, K. M.; Habibian, M. M.; Omelia, C. R., Water and waste water filtration - concepts and applications. *Environmental Science & Technology* **1971,** *5*, (11), 1105-1112.

107. Camesano, T. A.; Abu-Lail, N. I., Role of ionic strength on the relationship of biopolymer conformation, DLVO contributions, and steric interactions to bioadhesion of Pseudomonas putida KT2442. *Biomacromolecules* **2003,** *4*, (4), 1000-1012.

108. Bayoudh, S.; Othmane, A.; Mora, L.; Ben Ouada, H., Assessing bacterial adhesion using DLVO and XDLVO theories and the jet impingement technique. *Colloids and Surfaces B-Biointerfaces* **2009,** *73*, (1), 1-9.

109. Farahat, M.; Hirajima, T.; Sasaki, K.; Doi, K., Adhesion of *Escherichia coli* onto quartz, hematite and corundum: Extended DLVO theory and flotation behavior. *Colloids and Surfaces B-Biointerfaces* **2009,** *74*, (1), 140-149.

110. Yea-Ling Ong, A. r., George Georgiou, and Mukul M. Sharma, Adhesion Forces between *E. coli* Bacteria and Biomaterial Surfaces. *Langmuir* **1999,** *15*, 2719-2725.

111. van Oss, C. J., Acid-Base Interfacial Interactions in Aqueous-Media. *Colloids and Surfaces a-Physicochemical and Engineering Aspects* **1993,** *78*, 1-49.

112. Israelachvili, J. N., *Intermolecular and surface forces*. 2nd ed.; Academic Press: London ; San Diego, 1991; p xxi, 450.

113. Degennes, P. G., Polymers at an Interface - a Simplified View. *Advances in Colloid and Interface Science* **1987,** *27*, (3-4), 189-209.

114. Appenzeller, B. M. R.; Duval, Y. B.; Thomas, F.; Block, J. C., Influence of phosphate on bacterial adhesion onto iron oxyhydroxide in drinking water. *Environmental Science & Technology* **2002,** *36*, (4), 646-652.

115. Park, S. J.; Lee, C. G.; Kim, S. B., The role of phosphate in bacterial interaction with iron-coated surfaces. *Colloids and Surfaces B-Biointerfaces* **2009,** *68*, (1), 79-82.

116. Nelson, N. O.; Mikkelsen, R. L., Polyethersulfone membrane filters for sampling soil water from in situ soils and intact soil columns for phosphate analysis. *Communications in Soil Science and Plant Analysis* **2006,** *37*, (3-4), 377-388.

117. Wang, Z. Y.; Kelly, J. M.; Kovar, J. L., In situ dynamics of phosphorus in the rhizosphere solution of five species. *Journal of Environmental Quality* **2004,** *33*, (4), 1387-1392.

118. Wang, Z. Y.; Wen, S. F.; Li, A. F., Analysis of Phosphate in Rhizosphere Soil Solution Samples Using Capillary Electrophoresis. *Chinese Journal of Analytical Chemistry* **2010,** *38*, (1), 87-90.

119. Rajan, S. S. S., Comparison of phosphate fertilizers for pasture and their effect on soil solution phosphate. *Communications in Soil Science and Plant Analysis* **2002,** *33*, (13-14), 2227-2245.

120. Bierman, P. M.; Rosen, C. J.; Bloom, P. R.; Nater, E. A., Soil Solution Chemistry of Sewage-Sludge Incinerator Ash and Phosphate Fertilizer Amended Soil. *Journal of Environmental Quality* **1995,** *24*, (2), 279-285.

121. Gilley, J. E.; Eghball, B.; Marx, D. B., Nutrient concentrations of runoff during the year following manure application. *Transactions of the Asabe* **2007,** *50*, (6), 1987-1999.

122. Zhuang, J.; Jin, Y., Interactions between viruses and goethite during saturated flow: Effects of solution pH, carbonate, and phosphate. *Journal of Contaminant Hydrology* **2008,** *98*, (1-2), 15-21.

123. Blanford, W. J.; Brusseau, M. L.; Yeh, T. C. J.; Gerba, C. P.; Harvey, R., Influence of water chemistry and travel distance on bacteriophage PRD-1 transport in a sandy aquifer. *Water Research* **2005,** *39*, (11), 2345-2357.

124. Walczak, J. J.; Bardy, S. L.; Feriancikova, L.; Xu, S., Influence of Tetracycline Resistance on the Transport of Manure-derived *Escherichia coli* in Saturated Porous Media. *Water Research* **2011,** *45*, (4), 1681-1690.

125. Brown, D. G.; Jaffe, P. R., Effects of nonionic surfactants on bacterial transport through porous media. *Environmental Science & Technology* **2001,** *35*, (19), 3877-3883.

126. Xu, S. P.; Gao, B.; Saiers, J. E., Straining of colloidal particles in saturated porous media. *Water Resources Research* **2006,** *42*, (12), W12S16, doi:10.1029/2006WR004948.

127. Walker, S. L.; Redman, J. A.; Elimelech, M., Influence of growth phase on bacterial deposition: Interaction mechanisms in packed-bed column and radial stagnation point flow systems. *Environmental Science & Technology* **2005,** *39*, (17), 6405-6411.

128. Kretzschmar, R.; Barmettler, K.; Grolimund, D.; Yan, Y. D.; Borkovec, M.; Sticher, H., Experimental determination of colloid deposition rates and collision efficiencies in natural porous media. *Water Resources Research* **1997,** *33*, (5), 1129-1137.

129. Castro, F. D.; Tufenkji, N., Relevance of nontoxigenic strains as surrogates for *Escherichia coli* O157 : H7 in groundwater contamination potential: Role of temperature and cell acclimation time. *Environmental Science & Technology* **2007,** *41*, (12), 4332-4338.

130. Camesano, T. A.; Logan, B. E., Probing bacterial electrosteric interactions using atomic force microscopy. *Environmental Science & Technology* **2000,** *34*, (16), 3354-3362.

131. Tong, M. P.; Camesano, T. A.; Johnson, W. P., Spatial variation in deposition rate coefficients of an adhesion-deficient bacterial strain in quartz sand. *Environmental Science & Technology* **2005,** *39*, (10), 3679-3687.

132. Bayoudh, S.; Othmane, A.; Bettaieb, F.; Bakhrouf, A.; Ben Ouada, H.; Ponsonnet, L., Quantification of the adhesion free energy between bacteria and hydrophobic and hydrophilic substrata. *Materials Science & Engineering C-Biomimetic and Supramolecular Systems* **2006,** *26*, (2-3), 300-305.

133. Redman, J. A.; Walker, S. L.; Elimelech, M., Bacterial adhesion and transport in porous media: Role of the secondary energy minimum. *Environmental Science & Technology* **2004,** *38*, (6), 1777-1785.

134. Huang, X. F.; Bhattacharjee, S.; Hoek, E. M. V., Is Surface Roughness a "Scapegoat" or a Primary Factor When Defining Particle-Substrate Interactions? *Langmuir* **2010,** *26*, (4), 2528-2537.

135. Butt, H. J.; Cappella, B.; Kappl, M., Force measurements with the atomic force microscope: Technique, interpretation and applications. *Surface Science Reports* **2005,** *59*, (1-6), 1-152.

136. Strauss, J.; Burnham, N. A.; Camesano, T. A., Atomic force microscopy study of the role of LPS O-antigen on adhesion of*E. coli*. *Journal of Molecular Recognition* **2009,** *22*, (5), 347-355.

137. Neidhardt, F. C., *Escherichia coli* and salmonella typhimurium. In 1996; p 1.

138. Oshea, S. J.; Welland, M. E.; Rayment, T., An Atomic-Force Microscope Study of Grafted Polymers on Mica. *Langmuir* **1993,** *9*, (7), 1826-1835.

139. Walker, S. L.; Redman, J. A.; Elimelech, M., Role of cell surface lipopolysaccharides in *Escherichia coli* K12 adhesion and transport. *Langmuir* **2004,** *20*, (18), 7736-7746.

140. Liu, Y.; Yang, C. H.; Li, J., Influence of extracellular polymeric substances on Pseudomonas aeruginosa transport and deposition profiles in porous media. *Environmental Science & Technology* **2007,** *41*, (1), 198-205.

141. Morel, F.; Hering, J. G., *Principles and applications of aquatic chemistry*. Wiley: New York, 1993; p xv, 588.

142. Hahn, M. W.; Abadzic, D.; O'Melia, C. R., Aquasols: On the role of secondary minima. *Environmental Science & Technology* **2004,** *38*, (22), 5915-5924.

143. Riley LW, R. R., Helgerson SD, McGee HB, Wells JG, Davis BR, Hebert RJ, Olcott ES, Johnson LM, Hargrett NT, Blake PA, Cohen ML., Hemorrhagic colitis associated with a rare *Escherichia coli* serotype. *N Engl J Med.* **1983,** *308*, (12), 681-685.

144. CDC, Questions & Answers: Sickness caused by *E. coli*; Centers for Disease Control and Prevention: Atlanta, GA. **2006**.

145. Licence, K.; Oates, K. R.; Synge, B. A.; Reid, T. M. S., An outbreak of E-coli O157 infection with evidence of spread from animals to man through contamination of a private water supply. *Epidemiology and Infection* **2001,** *126*, (1), 135-138.

146. Johnson, J. Y. M.; Thomas, J. E.; Graham, T. A.; Townshend, I.; Byrne, J.; Selinger, L. B.; Gannon, V. P. J., Prevalence of *Escherichia coli* O157 : H7 and Salmonella spp. in surface waters of southern Alberta and its relation to manure sources. *Canadian Journal of Microbiology* **2003,** *49*, (5), 326-335.

147. Ferguson, C. M.; Charles, K.; Deere, D. A., Quantification of Microbial Sources in Drinking-Water Catchments. *Critical Reviews in Environmental Science and Technology* **2009,** *39*, (1), 1-40.

148. Gagliardi, J. V.; Karns, J. S., Leaching of *Escherichia coli* O157 : H7 in diverse soils under various agricultural management practices. *Applied and Environmental Microbiology* **2000,** *66*, (3), 877-883.

149. Pennington, H., *Escherichia coli* O157. *Lancet* **2010,** *376*, (9750), 1428-1435.

150. Abong'o, B. O.; Momba, M. N. B., Prevalence and potential link between *E. coli* O157 : H7 isolated from drinking water, meat and vegetables and stools of diarrhoeic confirmed and non-confirmed HIV/AIDS patients in the Amathole District - South Africa. *Journal of Applied Microbiology* **2008,** *105*, (2), 424-431.

151. Islam, M.; Doyle, M. P.; Phatak, S. C.; Millner, P.; Jiang, X. P., Persistence of enterohemorrhagic *Escherichia coli* O157 : H7 in soil and on leaf lettuce and parsley grown in fields treated with contaminated manure composts or irrigation water. *Journal of Food Protection* **2004,** *67*, (7), 1365-1370.

152. Avery, L. M.; Killham, K.; Jones, D. L., Survival of E-coli O157 : H7 in organic wastes destined for land application. *Journal of Applied Microbiology* **2005,** *98*, (4), 814-822.

153. Haznedaroglu, B. Z.; Kim, H. N.; Bradford, S. A.; Walker, S. L., Relative transport behavior of *Escherichia coli* O157:H7 and *Salmonella enterica* serovar pullorum in packed bed column systems: Influence of solution chemistry and cell concentration. *Environmental Science & Technology* **2009,** *43*, (6), 1838-1844.

154. Kim, H. N.; Hong, Y.; Lee, I.; Bradford, S. A.; Walker, S. L., Surface characteristics and adhesion behavior of *Escherichia coli* O157:H7: role of extracellular macromolecules. *Biomacromolecules* **2009,** *10*, (9), 2556-64.

155. Kim, H. N.; Walker, S. L.; Bradford, S. A., Macromolecule mediated transport and retention of *Escherichia coli* O157:H7 in saturated porous media. *Water Research* **2010,** *44*, (4), 1082-1093.

156. G. Seltmann, O. H., the bacterial cell wall. **2002**.

157. Penagonda, V.; Hilton, A. C.; Chen, G., Impact of Lipopolysaccharide Extraction on Bacterial Adhesion and Transport. *Journal of Adhesion Science and Technology* **2008,** *22*, (10-11), 1073-1088.

158. Theresa Lindhout, P. C. Y. L., Dyanne Brewer, and Joseph S. Lam, Truncation in the core oligosaccharide of lipopolysaccharide affects flagella-mediated motility in Pseudomonas aeruginosa PAO1 via modulation of cell surface attachment. *microbiology* **2009,** *155*, 3449-3460.

159. Abu-Lail, N. I.; Camesano, T. A., The effect of solvent polarity on the molecular surface properties and adhesion of *Escherichia coli*. *Colloids and Surfaces B-Biointerfaces* **2006,** *51*, (1), 62-70.

160. Strauss, J.; Burnham, N. A.; Camesano, T. A., Atomic force microscopy study of the role of LPS O-antigen on adhesion of *E. coli*. *Journal of Molecular Recognition* **2009,** *22*, (5), 347-355.

161. Currie, C. G.; Poxton, I. R., The lipopolysaccharide core type of *Escherichia coli* O157 : H7 and other non-O157 verotoxin-producing *E. coli*. *Fems Immunology and Medical Microbiology* **1999,** *24*, (1), 57-62.

162. Chart, H.; Perry, N. T.; Jenkins, C., The expression of an R3 lipopolysacchadde-core by pathotypes of *Escherichia coli*. *Journal of Applied Microbiology* **2004,** *96*, (5), 982-986.

163. Kastowsky, M.; Gutberlet, T.; Bradaczek, H., Molecular Modeling of the 3-Dimensional Structure and Conformational Flexibility of Bacterial Lipopolysaccharide. *Journal of Bacteriology* **1992,** *174*, (14), 4798-4806.

164. Burks, G. A.; Velegol, S. B.; Paramonova, E.; Lindenmuth, B. E.; Feick, J. D.; Logan, B. E., Macroscopic and Nanoscale Measurements of the Adhesion of Bacteria with Varying Outer Layer Surface Composition. *Langmuir* **2003,** *19*, (6), 2366-2371.

165. Lu, Q.; Wang, J.; Faghihnejad, A.; Zeng, H.; Liu, Y., Understanding the molecular interactions of lipopolysaccharides during *E. coli* initial adhesion with a surface forces apparatus. *Soft Matter* **2011,** *7*, 9366-9379.

166. Abu-Lail, N. I.; Camesano, T. A., Role of lipopolysaccharides in the adhesion, retention, and transport of *Escherichia coli* JM109. *Environmental Science & Technology* **2003,** *37*, (10), 2173-83.

167. Liu, Y.; Li, J., Role of Pseudomonas aeruginosa biofilm in the initial adhesion, growth and detachment of *Escherichia coli* in porous media. *Environmental Science & Technology* **2008,** *42*, (2), 443-9.

168. Won, J.; Kim, J. W.; Kang, S.; Choi, H., Transport and adhesion of *Escherichia coli* JM109 in soil aquifer treatment (SAT): One-dimensional column study. *Environmental Monitoring and Assessment* **2007,** *129*, (1-3), 9-18.

169. Chen, G.; Strevett, K. A., Impact of Bacterial Extracellular Polymers on lindane Transport. *Environmental Engineering Science* **2001,** *18*, (3), 13.

170. Li, B.; Logan, B. E., Bacterial adhesion to glass and metal-oxide surfaces. *Colloids and Surfaces B: Biointerfaces* **2004,** *36*, 81-90.

171. Ma, J.; Ibekwe, A.; Yi, X.; Wang, H.; A., Y.; Crowley, D.; Yang, C., Persistence of *Escherichia coli* O157:H7 and Its Mutants in Soils. *PLoS ONE* **2011,** *6*, (8), e23191.

172. Enne, V. I.; Delsol, A. A.; Roe, J. M.; Bennett, P. M., Evidence of Antibiotic Resistance Gene Silencing in *Escherichia coli*. *Antimicrobial Agents and Chemotherapy* **2006,** *50*, (9), 3003-3010.

173. Liu, Y.; Li, J.; Yang, C. H., Influence of extracellular polymeric substances on *Pseudomonas aeruginosa* transport and deposition profiles in porous media. *Environmental Science & Technology* **2007,** *41*, (1), 198-205.

174. O'Brien, R. W., White, Lee R., Electrophoretic mobility of a spherical colloidal particle. *J. Chem. Soc., Faraday Trans. 2* **1978,** *74*, 1607-1626.

175. Sheng, H.; Lim, J. Y.; Watkins, M. K.; Minnich, S. A.; Hovde, C. J., Characterization of an *Escherichia coli* O157:H7 O-antigen deletion mutant and effect of the deletion on bacterial persistence in the mouse intestine and colonization at the bovine terminal rectal mucosa. *Appl Environ Microbiol* **2008,** *74*, (16), 5015-22.

176. Dodds, K. L.; Perry, M. B.; Mcdonald, I. J., Alterations in Lipopolysaccharide Produced by Chemostat-Grown Escherichia-Coli O157-H7 as a Function of Growth-Rate and Growth-Limiting Nutrient. *Can J Microbiol* **1987,** *33*, (5), 452-458.

177. Tsai, C. M.; Frasch, C. E., A sensitive silver stain for detecting lipopolysaccharides in polyacrylamide gels. *Anal Biochem* **1982,** *119*, (1), 115-9.

178. Lytle, D. A.; Rice, E. W.; Johnson, C. H.; Fox, K. R., Electrophoretic Mobilities of *Escherichia coli* O157:H7 and Wild-Type *Escherichia coli* Strains. *Applied and Environmental Microbiology* **1999,** *65*, (7), 3222-3225.

179. Chheda, P.; Grasso, D.; van Oss, C. J., Impact of ozone on stability of montmorillonite suspensions. *Journal of Colloid and Interface Science* **1992,** *153*, (1), 226-236.

180. Benefield, C. B.; Howard, P. J. A.; Howard, D. M., The estimation of dehydrogenase activity in soil. *Soil Biology and Biochemistry* **1977,** *9*, (1), 67-70.

181. Grasso, D.; Subramaniam, K.; Butkus, M.; Strevett, K.; Bergendahl, J., A review of non-DLVO interactions in environmental colloidal systems. *Re/views in Environmental Science& Bio/Technology* **2002,** *1*, 17-38.

182. Albinger, O.; Biesemeyer, B. K.; Arnold, R. G.; Logan, B. E., Effect of bacterial heterogeneity on adhesion to uniform collectors by monoclonal populations. *FEMS Microbiology Letters* **1994,** *124*, (3), 321-326.

183. Liu, S.; Zeng, T. H.; Hofmann, M.; Burcombe, E.; Wei, J.; Jiang, R.; Kong, J.; Chen, Y., Antibacterial Activity of Graphite, Graphite Oxide, Graphene Oxide, and Reduced Graphene Oxide: Membrane and Oxidative Stress. *ACS Nano 5*, (9), 6971-6980.

184. Hu, W.; Peng, C.; Luo, W.; Lv, M.; Li, X.; Li, D.; Huang, Q.; Fan, C., Graphene-Based Antibacterial Paper. *ACS Nano 4*, (7), 4317-4323.

185. Fisher, C.; Rider, A. E.; Han;, Z. J.; Kumar, S.; Levchenko, I.; Ostrikov, K. K., Applications and Nanotoxicity of Carbon Nanotubes and Graphene in Biomedicine. *Journal of Nanomaterials* **2012**, 1-19.

186. Feriancikova, L.; Xu, S., Deposition and remobilization of graphene oxide within saturated sand packs. *Journal of Hazardous Materials 235â€“236*, (0), 194-200.

187. Dumé, B. Graphene oxide encourages cells to grow.

188. Akhavan, O.; Ghaderi, E., Toxicity of Graphene and Graphene Oxide Nanowalls Against Bacteria. *ACS Nano 4*, (10), 5731-5736.

189. Perry, M. B.; MacLean, L.; Griffith, D. W., Structure of the O-chain polysaccharide of the phenol-phase soluble lipopolysaccharide of *Escherichia coli* 0:157:H7. *Biochem Cell Biol* **1986,** *64*, (1), 21-8.

190. Akashi, S.; Joh, K.; Tsuji, A.; Ito, H.; Hoshi, H.; Hayakawa, T.; Ihara, J.; Abe, T.; Hatori, M.; Mori, T., A severe outbreak of haemorrhagic colitis and haemolytic uraemic syndrome associated with *Escherichia coli* O157:H7 in Japan. *Eur J Pediatr* **1994,** *153*, (9), 650-655.

191. CDC, Outbreak of *Escherichia coli* O157:H7 and *Campylobacter* among attendees of the Washington County Fair-New York, 1999. *MMWR Morb Mortal Wkly Rep* **1999,** *48*, (36), 803-805.

192. B.Z. Haznedaroglu, H. N. K., S.A.Bradford, S.L. Walker, Relative Transport Behavior of *Escherichia coli* O157:H7 and *Salmonella enterica Serovar Pullorum* in Packed Bed Column Systems: Influence of Solution Chemistry and Cell Concentration. *Environ. Sci. Technol.* **2009,** *43*, (6), 1838-1844.

193. Walker, S. L.; Redman, J. A., Bacterial transport and deposition in porous media: Role of cell surface lipopolysaccharides (LPS). *Abstracts of Papers of the American Chemical Society* **2004,** *228*, U606-U606.

194. Ho, Y. S.; McKay, G., Sorption of dye from aqueous solution by peat. *Chemical Engineering Journal* **1998,** *70*, (2), 115-124.

195. Dima, D.; Murarescu, M.; Andrei, G., Dispersion of carbon nanotubes coated with iron (iii) oxide into polymer composite under oscillating magnetic field. *Digest J. of Nanom. and Biostruct.* **2010,** *5*, (4), 5.

196. Kang, S.; Herzberg, M.; Rodrigues, D. F.; Elimelech, M., Antibacterial Effects of Carbon Nanotubes: Size Does Matter! *Langmuir* **2008,** *24*, (13), 6409.

197. Huang, Y.-F.; Wang, Y.-F.; Yan, X.-P., Amine-Functionalized Magnetic Nanoparticles for Rapid Capture and Removal of Bacterial Pathogens. *Environmental Science & Technology* **2010,** *44*, (20), 7908-7913.

198. El-Boubbou, K.; Gruden, C.; Huang, X., Magnetic Glyco-nanoparticles:â€‰ A Unique Tool for Rapid Pathogen Detection, Decontamination, and Strain Differentiation. *Journal of the American Chemical Society* **2007,** *129*, (44), 13392-13393.

199. Shan, Y.; Chen, K.; Yu, X.; Gao, L., Preparation and characterization of biocompatible magnetic carbon nanotubes. *Applied Surface Science 257*, (2), 362-366.

200. Wang, H.; Lin, K.-Y.; Jing, B.; Krylova, G.; Sigmon, G. E.; McGinn, P.; Zhu, Y.; Na, C., Removal of oil droplets from contaminated water using magnetic carbon nanotubes. *Water Research 47*, (12), 4198-4205.

201. Brady-EstÃ©vez, A. S.; Nguyen, T. H.; Gutierrez, L.; Elimelech, M., Impact of solution chemistry on viral removal by a single-walled carbon nanotube filter. *Water Research 44*, (13), 3773-3780.

202. Zardini, H. Z.; Amiri, A.; Shanbedi, M.; Maghrebi, M.; Baniadam, M., Enhanced antibacterial activity of amino acids-functionalized multi walled carbon nanotubes by a simple method. *Colloids and Surfaces B: Biointerfaces 92*, (0), 196-202.

CURRICULUM VITAE

LIXIA WANG Ph.D.

EDUCATION

2007 - 2013 Ph.D., Department of Civil Engineering & Mechanics,
University of Wisconsin-Milwaukee
Dissertation: "The role of solution chemistry and cell surface properties in mediating bacterial transport and retention in porous media and interaction with nanomaterials."

2001 - 2004 M.S., Environmental Engineering,
Beijing University of Chemical Technology, Beijing, China
Thesis: "Optimized treatment process of sanitary landfill leachate with integrated biological and chemical methods."

1997 - 2001 B.S., Environmental Engineering,
Beijing University of Chemical Technology, Beijing, China.
Thesis: "Treatment of chromate ($Cr_2O_7^{2-}$) wastewater with modified zeolite."

RESEARCH EXPERIENCE

Research Assistant
University of Wisconsin – Milwaukee(UWM), Milwaukee, WI *2007 - 2011*

Research Assistant
Beijing University of Chemical Technology, Beijing *2000 - 2004*

ENGINEERING EXPERIENCE

Engineer, Project Manager
Center for Water Engineering, Beijing Hydrological Research Institute, Beijing 2004 - 2007

TEACHING EXPERIENCE

Teaching Assistant
University of Wisconsin – Milwaukee, Milwaukee, WI *2011 – 2012*
Civ. Eng. 280- Computer Based Engineering Analysis

HONORS AND AWARDS

- UWM Distinguished Dissertation Fellowship, 2012-2013
- UWM Chancellor's Awards, 2007-2013

- UWM's Graduate School Research Travel Award, 2011
- First place at the ASM International Milwaukee Chapter 53rd Annual H.R. Bergmann Memorial Seminar Student Poster Competition, 2011

PUBLICATIONS

- **Wang, L.,** Yamazaki, A., Yang, C., Xu, S., Li, J., Influence of lipopolysaccharides (LPS) on the Transport of *Escherichia coli* O157:H7 within Saturated Quartz Sand. *In preparation.*
- Feriancikova, L., Bardy, S., **Wang, L.,** Li, J., Xu, S., Effects of Outer Membrane Protein TolC on the Transport of *Escherichia coli* within Saturated Quartz Sands. *Environmental Science & Technology,* doi: 10.1021/es400292x.
- **Wang, L.,** Yamazaki, A., Yang, C., Xu, S., Li, J., Drinking Water Sustainability and Safety: A Laboratory Study of *Escherichia coli* O157:H7 Contamination in Groundwater. *In review.*
- **Wang, L.,** Xu, S., Li, J., 2011, Influence of Phosphate on the Transport of *Escherichia coli* O157:H7 in Saturated Quartz Sand, *Environmental Science & Technology*, 45 (22), 9566-9573, doi: 10.1021/es201132s.
- Walczak, J., **Wang, L.,** Feriancikova, L., Li, J., Xu, S., 2011, Influence of desiccation on the transport of *Escherichia coli* through saturated sand packs, *Water, Air & Soil Pollution*, doi: 10.1007/s11270-011-0950-2.
- Walczak, J., **Wang**, **L.,** Bardy, S., Feriancikova, L., Li, J., Xu, S., 2011, The effects of starvation on the transport of *Escherichia coli* in saturated porous media are dependent on pH and ionic strength, *Colloids and Surfaces B: Biointerfaces*, doi: 10.1016/j.colsurfb.2011.10.010.
- Yamazaki, A., Li, J., Hutchins, W. C., **Wang, L.,** Ma, J., Ibekwe, A.M., Yang, CH, 2011, Commensal effect of pectate lyases secreted from Dickeya dadantii on the poliferation of *Escherichia coli* O157:H7 EDL933 on lettuce leaves, *Applied and Environmental Microbiology*, 77(1):156-162.
- **Wang, L.,** Pang, Y., Li, X., 2004, Treatment of landfill leachate with constructed wetland: A review, *Techniques and Equipment for Environmental Pollution Control*, 6(4), 61-65

CONFERENCE PRESENTATIONS

- **Wang, L.**, Liu, Y., Li, J., Understanding the impact of biofilm and biofilm EPS on the fate of *Escherichia coli* in saturated porous media. International Water Association Biofilm Conference, Shanghai, China, Oct. 2011.
- **Wang, L.,** Yamazaki, A., Yang, C., Xu, S., Li, J., A laboratory study of *Escherichia coli* O157:H7 contamination in groundwater (Keynote presentation).

International Conference on Drinking Water Safety, Security and Sustainability, Hangzhou, China, Oct. 2011.

- **Wang, L.,** Yamazaki, A., Yang, C., Xu, S., Li, J., Role of lipopolysaccharide (LPS) in *Escherichia coli* O157:H7 transport in saturated porous media. 85th Annual Conference of the Colloid and Surface Science, Montreal, Canada, June 2011.

SEMINARS

- **Wang, L.**, Liu, Y., Li, J., Impact of biofilm and biofilm EPS on the fate of *Escherichia coli* in saturated porous media. The ASM International Milwaukee Chapter 53rd Annual H.R. Bergmann Memorial Seminar, May 2011.
- **Wang, L.,** Yamazaki, A., Yang, C., Xu, S., Li, J., Role of lipopolysaccharide(LPS) in *Escherichia coli* O157:H7 transport in saturated porous media. UWM CEAS Seminar and UWM CEAS Poster Competition, April 2011.